Immune transcriptomic differences in paediatric patients with SARS-CoV-2 compared to other lower respiratory tract infections

Negusse Tadesse Kitaba[1], Lesley Workman[2], Cheryl Cohen[3,4], Diana Baralle[1,5,6], Ellen Kong[7], Maresa Botha[2], Marina Johnson[8,9], David Goldblatt[8,9], Mark P Nicol[10], John W Holloway[1,6]# and Heather J Zar[2]#

#These authors contributed equally: Heather J Zar & John W. Holloway.
Corresponding author: Heather J Zar heather.zar@uct.ac.za

[1]Human Development and Health, Faculty of Medicine, University of Southampton, Southampton, UK
[2]Department of Paediatrics and Child Health, Red Cross War Memorial Children's Hospital and SA-MRC Unit on Child & Adolescent Health, University of Cape Town, Cape Town, South Africa
[3]Center for Respiratory disease and Meningitis, National Institute for Communicable Diseases, a division of the National Health Laboratory Service, 1 Modderfontein Road Sandringham, South Africa
[4]School of Public Health, University of the Witwatersrand, Johanneburg, South Africa
[5]National Health, Service (NHS) Foundation Trust Southampton, UK
[6]NIHR Southampton Biomedical Research Centre, University Hospitals Southampton, Southampton, UK
[7]National Heart and Lung Institute, Imperial College London, London, UK
[8]Great Ormond Street Institute of Child Health University College London, UK
[9]National Heart and Lung Institute, Imperial College London, London, UK
[10]The University of Western Australia: Perth, Australia

Graphical abstract

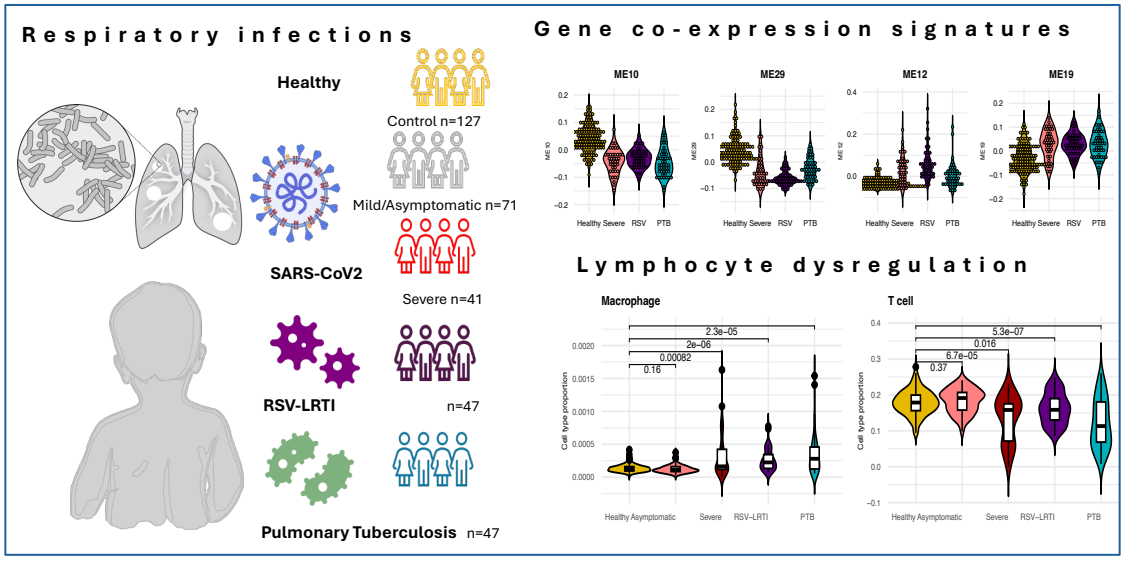

Abstract

The clinical severity of SARS-CoV-2 infection in children varies, with asymptomatic or mild illness predominating and a minority developing severe disease. Understanding the immunological responses that underlie severity of disease may guide future development of preventive or therapeutic interventions. This study compared whole blood transcriptomes of healthy children (N=127), children with mild/asymptomatic SARS-CoV-2 infection (N=71) and children hospitalised with severe SARS-COV-2 (N=41), lower respiratory tract illness (LRTI) or LRTI due to Respiratory Syncytial Virus (RSV-LRTI) (N=47) or Pulmonary Tuberculosis (PTB) (N=47). We identified >5000 differentially expressed genes including: *OLFM4, IFI27, CBX7, IGF2BP3, OTOF* for severe SARS-CoV-2; *IFI27, OTOF, SIGLEC1, IFI44L* and *USP18* for RSV-LRTI, and *MMP8, LTF, IGF2BP3, GPR84, CD177, C1QC* and *DEFA4* for PTB, at false discovery rate (FDR) <0.05. Pathway analysis identified enrichment for neutrophil degranulation, interferon gamma signalling, overexpression of ribosomal proteins and depletion of immune response in severe SARS-CoV-2 compared to healthy (SAR-COV-2 uninfected) children. Weighted Gene Co-expression Network Analysis (*WGCNA*) identified 10 correlated gene modules shared between LRTI showing similar underlying response mechanisms. Cellular decomposition analysis identified the depletion of 22 cell types in severe SARS-CoV-2, 16 for RSV-LRTI and 21 for PTB compared to healthy SARS-CoV-2 uninfected control children. We identified 82 genes important for discriminating asymptomatic/mild from severe SARS-CoV-2 including *CBX7, TRAF1, ZNF324* and *CASS4*; 93 healthy from severe SARS-CoV-2 including *RORC, CBX7, NR3C2, MID2* and *ADAMTS2*; 110 genes for RSV-LRTI and 95 for PTB children which can be used for future therapeutic targets.

Keywords: Respiratory infection, Covid-19, PTB, RSV-LRTI, WGCNA, Child

Introduction

Lower respiratory tract illness (LRTI) is a major cause of hospitalisation and mortality globally in children, with the burden heavily skewed to low- and medium-income countries (LMICs). RSV predominates as a cause of severe LRTI and hospitalisation. Pulmonary tuberculosis (PTB) has also increasingly been recognised as an important cause of acute LRTI in children in countries in which TB is endemic[1]. During the SARS-COV-2 pandemic, SARS-CoV-2 emerged as a cause of LRTI in children.

The clinical manifestation of COVID-19 in children varies widely from mild or asymptomatic illness to severe LRTI[2], although severe disease is rare. Immunologically, the hallmarks of COVID-19 include dysregulation of type I IFN activity, hyperinflammation, lymphopenia, heterogeneous adaptive immunity, dysregulated myeloid response and lymphocyte impairment[3,4]. COVID-19 severity is also associated with different levels of neutralizing antibodies[5,6]. While the blood transcriptomic response to SARS-CoV-2 infection has been described in adults[7,8,9], few studies have investigated responses to SARS-CoV-2 in infants and children[10,11] and little is known about differences in host gene expression between children asymptomatic with SARS-CoV-2 infection and those hospitalized with severe COVID-19 or other LRTI such as Respiratory Syncytial Virus (RSV-LRTI) or pulmonary tuberculosis (PTB)[12,13,14,15].

A multi-omics approach has previously shown utility in characterising the complexity and severity of Covid-19[16]. Weighted Gene Co-expression Networks Analysis (WGCNA) is a widely implemented approach to identify co-regulated genes and potential hub-genes for druggable targets[17]. The aim of this study was to compare host RNA gene expression in healthy children compared to those with asymptomatic or mild SARS-CoV-2 infection, as well as to those

hospitalised with COVID-19, RSV-LRTI or PTB and to utilise WGCNA to identify underlying immune responses associated with disease.

Methods

This was a prospective study conducted during the SARS-COV-2 pandemic that investigated patterns of whole blood gene expression in HIV-negative children enrolled in a South African birth cohort study, the Drakenstein Child Health study (DCHS), and those hospitalised with SARS-COV-2 (severe COVID-19), RSV-LRTI or PTB.

Participants

Healthy controls or previous SARS-CoV-2 mild or asymptomatic infection: Participants were from the Drakenstein Child Health Study, a prospective population-based birth cohort study of children in a low- and middle-income, peri-urban community outside Cape Town, South Africa[18]. In the DCHS, during the SARS-CoV-2 pandemic, a convenience sample of a subset of children (N=201) was included in intensive surveillance for SARS-CoV-2 infection with blood sampling every 3 months from 15-May-2020 through 15-Sept-2022, with blood and nasopharyngeal swabs collected, irrespective of symptoms.

In addition, continuous surveillance for illness or hospitalisation was undertaken, and blood and nasal sampling repeated at any intercurrent illness. Serum samples were stored and batched for measurement of IgG to Spike antigen (CoV-2-S-IgG) by ELISA as previously described[19]. In the current study, samples from children during wave 1 were used; subjects seronegative for SARS-CoV-2 were defined as healthy controls, and those seropositive for SARS-CoV-2 were considered mild/asymptomatic infection as no child reported symptomatic illness or was hospitalised.

Children with LRTI

COVID-19 or RSV-LRTI: Children with acute LRTI hospitalised at Red Cross Childrens Hospital were identified through the National Syndromic Surveillance for pneumonia in South Africa programme (PSP) at Red Cross War Memorial Children's Hospital, in Cape Town, South Africa. Sequential children hospitalised with LRTI were enrolled and a nasal swab for PCR detection of SARS-CoV2, RSV and other pathogens was taken for testing at National Institute of Communicable Disease as previously described[20]. Children who were positive for SARS-CoV-2 and negative for other pathogens were considered to have severe COVID-19 (N=41); those positive for RSV were included as RSV-LRTI (N=51).

PTB: Children enrolled in a TB diagnostic study (N=47) at Red Cross Children's Hospital, microbiologically confirmed (by mycobacterial liquid culture or Xpert MTB/RIF) and negative for SARS-CoV-2 and RSV, were included in this study. Serum and PAXgene samples were collected at the time of illness (Severe COVID-19, RSV-LRTI, PTB) were used for this study[20].

Whole blood PAXgene samples were stored at -80˚C, randomized prior to shipment, with RNA extraction and sequencing undertaken at the Genomics Shared Resource (GSR), Roswell Park Comprehensive Cancer Centre, Buffalo NY, USA.

Sequencing and processing RNAseq data

Raw reads were processed with the bcbio-nextgen pipeline. Reads quality were assessed using FastQC[21] and MultiQC[22]. Sequencing reads were aligned to the human transcriptome reference using STAR[23]. Quantification of gene expression was carried out using Salmon[24] with default settings. Read counts were normalized using CPM (counts per million) from edgeR[25] with the TMM (Trimmed Mean of the M-values) method which accounts for both sequencing depth and

gene length[26]. Sample outliers were detected using Robust Principal Component Analysis (rPCA) with PcaHubert and PcaGrid functions[27]; samples detected by both methods were excluded from downstream analysis.

Identification of differentially expressed genes (DEGs)

Amongst 198 children in DCHS, 64% were seronegative (N=127) and regarded as healthy controls. Those were compared to hospitalised children with COVID-19 (N=41), RSV-LRT (N=47) or PTB (N=47). SARS-CoV-2 seropositive during wave 1 (N=71), who did not report any respiratory symptoms or hospitalization over this period, were regarded as having had mild or asymptomatic infection.

The R-package limma[28] was used to identify differentially-expressed genes adjusting for children's sex and age. Multiple testing correction was performed using the Benjamini-Hochberg (BH) procedure for False Discovery Rate (FDR) < 0.05. The biological function of gene lists were identified via gene set and pathway enrichment analyses using toppGene[29].

Weighted Gene Co-expression Network Analysis (*WGCNA*)

Signed weighted gene co-expression network analyses were conducted using WGCNA[30]. The gene module/clusters represent genes with highly correlated expression patterns, where the first principal component of the gene expression profile (Eigengene) is used to summarise the overall expression of each module. The module eigengenes identified by WGCNA were correlated with Severe COVID-19, PTB and RSV-LRTI. The module associations were visualised as a correlation barplot using the lares R package[31]. Protein-Protein Interaction (PPI) network were identified with GeneMANIA[32] and network properties for hub genes were analysed and visualized using Cytoscape[33]. Significantly associated modules were further characterized for functional

112 enrichment using toppGene[29]. Non-redundant biological process terms were generated and
113 visualized using rrvgo package[34].

114 Cell type proportion estimation

115 Cell type proportion differences between groups were estimated and assessed using xCell 2.0[35]
116 using the Immune Compendium[36] and immunoprofiling[37] reference datasets. The t-test was used
117 to determine the difference between groups (asymptomatic vs hospitalized SARS-CoV-2 , control
118 vs RSV-LRTI and control vs PTB).

119 Severity predictors

120 Gene biomarkers to predict SARS-CoV-2 severity, RSV-LRTI or PTB were selected using the
121 Boruta[38] R package[39] with default settings.

122 Gene and target drug look-up

123 In order to identify the druggability of differentially expressed genes, the look-up target score
124 generated by DrugnomeAI[40] was utilised (accessed on 19 March 2025). All statistical analyses
125 were conducted in R version 4.5.1.

126

Results

Participant characteristics.

This analysis includes 333 children: 71 with previous mild/asymptomatic SARS-CoV-2, 127 seronegative, healthy, and 135 children hospitalised with LRTI (41 with SARS-COV-2, 47 with RSV-LRTI and 47 with PTB or pulmonary TB). The characteristics of each group are shown in Table 1. As there was a significant age difference between DCHS children and those with LRTI, age was included as a covariate in regression analyses.

Table 1 Comparison of participants' characteristics for healthy controls and children with respiratory tract infections

Variable	**Healthy SARS-CoV-2 seronegative**	**Mild/asymptomatic SARS-CoV-2 infection**		**Severe COVID-19**		**RSV-LRTI**		**PTB**	
	N = 127	**N = 71**	**p-value**[2]	N = 41	**p-value**[2]	N = 47	**p-value**[2]	N = 47	**p-value**[2]
Gender Male N (%)	65 (51%)	28 (39%)	0.11	24 (59%)	0.4	28 (60%)	0.3	27 (57%)	0.5
Age (months) Median (Q1, Q3)	81 (71, 87)	83 (72, 90)	0.4	11 (3, 45)	<0.001	7 (2, 22)	<0.001	8 (4, 40)	<0.001

Healthy: DCHS children seronegative for SARS-CoV-2 in wave 1of the Covid-19 pandemic; **Mild/asymptomatic**: DCHS children seropositive for SARS-CoV-2 in wave 1; **Severe COVID-19**: Children admitted with COVID-19 lower respiratory tract infection (LRTI) and not co-infected; **RSV-LRTI**: children admitted with Respiratory Syncytial Virus LRTI; **PTB**: children with pulmonary tuberculosis infection.

Differential gene expression analysis

To identify differentially expressed genes and enriched GO terms in children with LRTI, seronegative DCHS participants from wave 1 (healthy controls) were compared to each LRTI

group separately (COVID-19, RSV-LRTI, PTB). The summary statistics and gene lists for TWAS at FDR <0.05 are provided in Supplementary Table S1. The biological gene ontology enrichment is also provided in Supplementary Table S2.

COVID-19 disease

The transcriptional response in healthy controls was compared to hospitalised children with COVID-19. There were 118 up-regulated and 160 down-regulated differentially expressed genes (DEGs) between healthy control and severe SARS-CoV-2 cases (FDR < 0.05 and log2 fold change >1), as shown in Figure 1A. Top DEGs included: *IFI27, MMP8, OLFM4, CEACAM8, LTF, IGF2BP3, DEFA4, ADAMTS2* and *CBX7*. Pathways identified as enriched include regulation of immune system and lymphocyte activation (Figure 2A).

RSV-LRTI

DGE analysis identified 210 upregulated and 195 downregulated genes at FDR < 0.05 and log2 fold change >1 and differentially expressed between healthy controls and children hospitalized with RSV-LRTI; top DEGs included *IFI27, OTOF, SIGLEC1, IFI44L, USP18, TCN2, CD177, HERC6, C1QC* and *EPHB2*. For all summary statistics see RSV-LRTI in Table S1 and the volcano plot shown in Figure 1B. Pathways significantly enriched included regulation of immune system translation, interferon mediated signalling, viral life cycle and viral processing (Figure 2B).

Pulmonary Tuberculosis

Children with PTB had identified 203 upregulated and 1843 downregulated genes differentially expressed genes (FDR < 0.05 and log2 fold change >1) compared to healthy controls. Top genes identified include *MMP8, LTF, IGF2BP3, GPR84, CD177, C1QC, DEFA4* and *OLFM4* (see

Figure 1 and Supplementary table S1). The pathways identified as enriched include defence response to bacteria, and innate immune response (see PTB in Figure 2C).

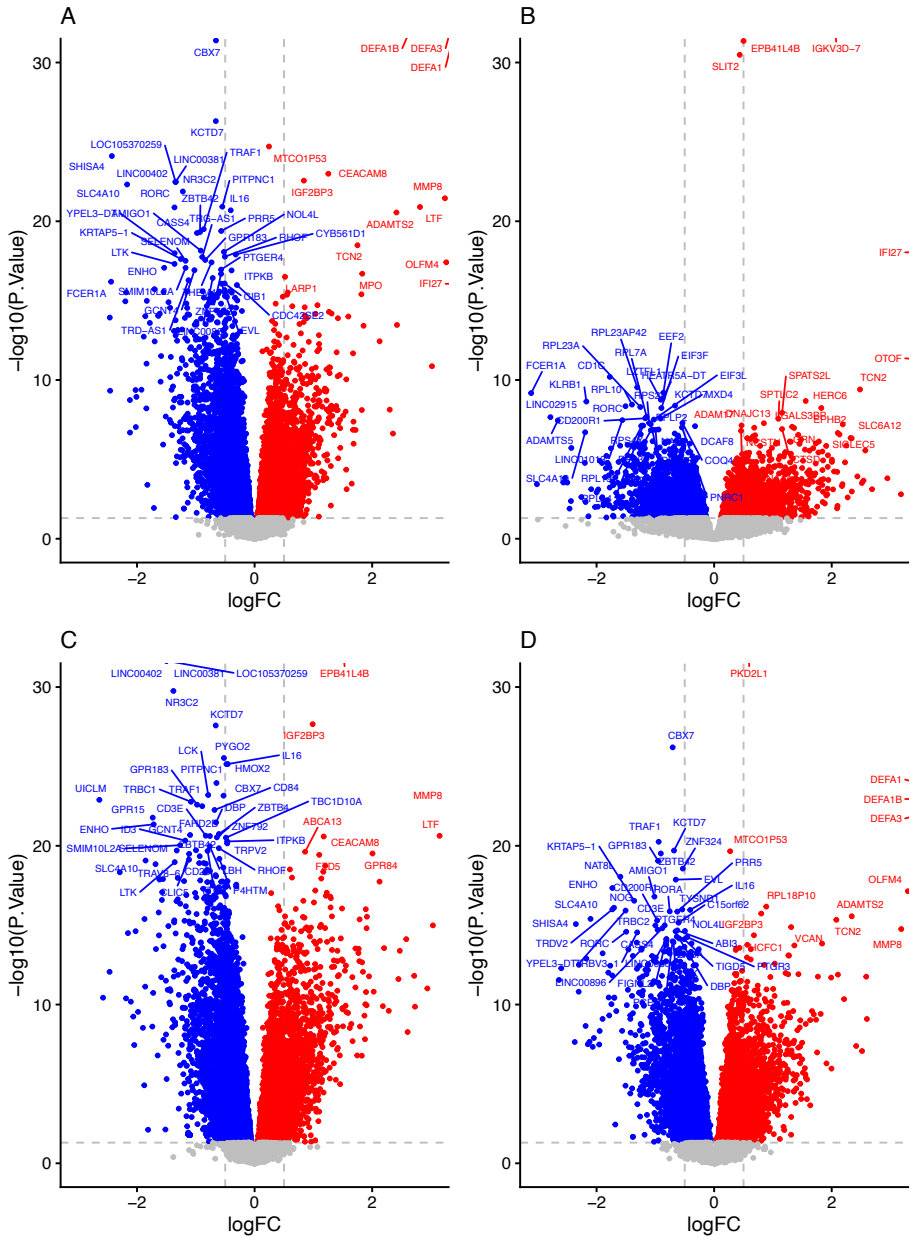

Figure 1 TWAS Volcano plot. A) Severe COVID-19, B) RSV-LRTI, C) PTB D) COVID-19 Severity. Red - upregulated, Blue - down regulated (P value <0.05, log2 Fold Change > 0).

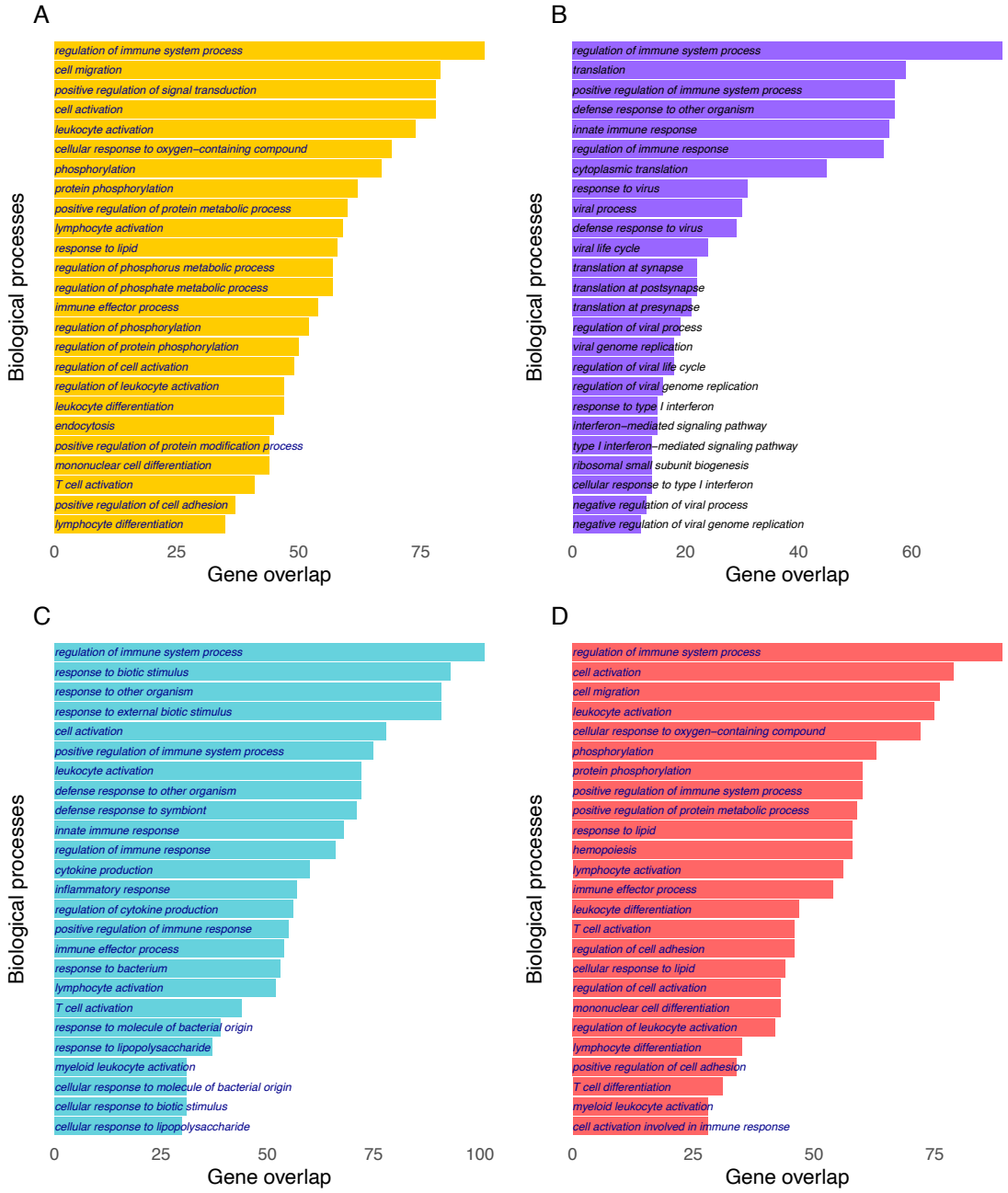

Figure 2 Gene ontology term for biological process for top 500 genes. A) Severe COVID-19 B) RSV-LRTI C) PTB D) COVID-19 severity.

Severity of SARS-CoV-2 infection

In order to determine transcriptional responses that distinguish mild/asymptomatic SARS-CoV-2 infection from severe COVID-19, children hospitalised with COVID-19 were compared with seropositive DCHS children. We identified 163 upregulated and 183 down downregulated genes at FDR < 0.05 and log2 fold change >1 see supplementary table S1. The pathways identified as enriched include regulation of immune system, hemopoieses and lymphocyte activation (see Figure 2D and supplementary table S2).

Weighted Gene Co-expression Networks Analysis of LRTI

The WGCNA analysis identified 46 significant modules including 22 with severe COVID-19 , 22 with RSV-LRTI and 20 with PTB when compared with healthy controls ($p<0.05$). Modules 10, 29, 22, 28 and 15 were downregulated and modules 32, 7, 19, 26 and 12 upregulated across LRTIs. The distribution of Eigengenes vs LRTI is shown in Figure 3A and Supplementary Table S3. The distribution of the relationship between the modules is represented as a dendrogram (Supplementary Figure 1) and genes per module are shown in Supplementary Table S3. The correlation of modules with COVID-19 , RSV-LRTI and PTB are shown in Figure 3B. Thirty modules showing correlation across LRTIs ($r >0.25$) were identified, of which 10 modules were correlated with all LRTI, 6 were in common between COVID-19 and RSV-LRTI, and 6 between COVID-19 and PTB (see Table 2 and Supplementary Fig 3). There were 4 modules specific to RSV-LRTI and 2 were specific to PTB.

The gene list in each module was used to generate a network using GeneMANIA with 10 additional interactors for biological processes in Cytoscape. Network analyses were conducted to characterise the network properties including identifying hub genes based on degree of connectivity. The top five hub genes for modules are shown in Table 2. The network connectivity degree distribution for

each module is provided in Supplementary Table S4. The Cytoscape session is also provided as Supplementary file 1.

The GO terms enrichment for modules which showed Pearson correlation of $r > 0.25$ with specific LRTI is in Supplementary Table S5. Further, redundant gene ontology was removed based on similarity matrix of GO terms using rrvgo R package. For biological process visualisation for all other modules see Supplementary Figure 4.

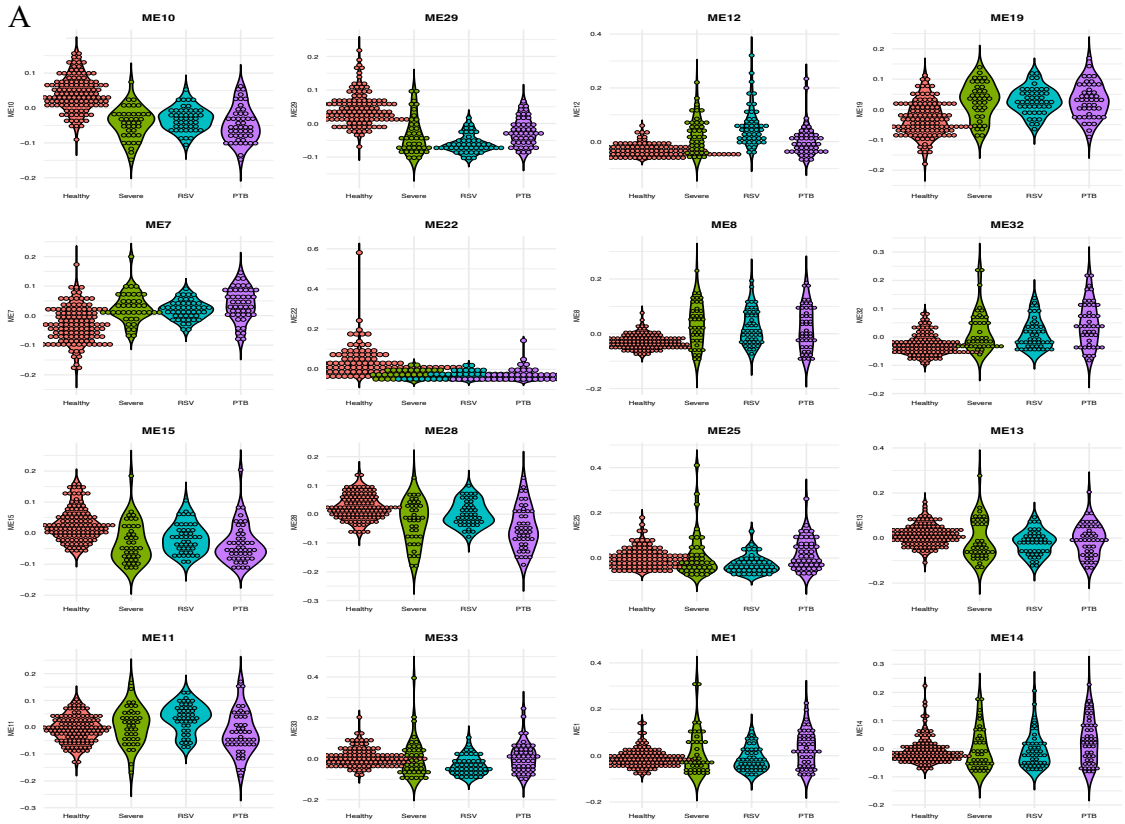

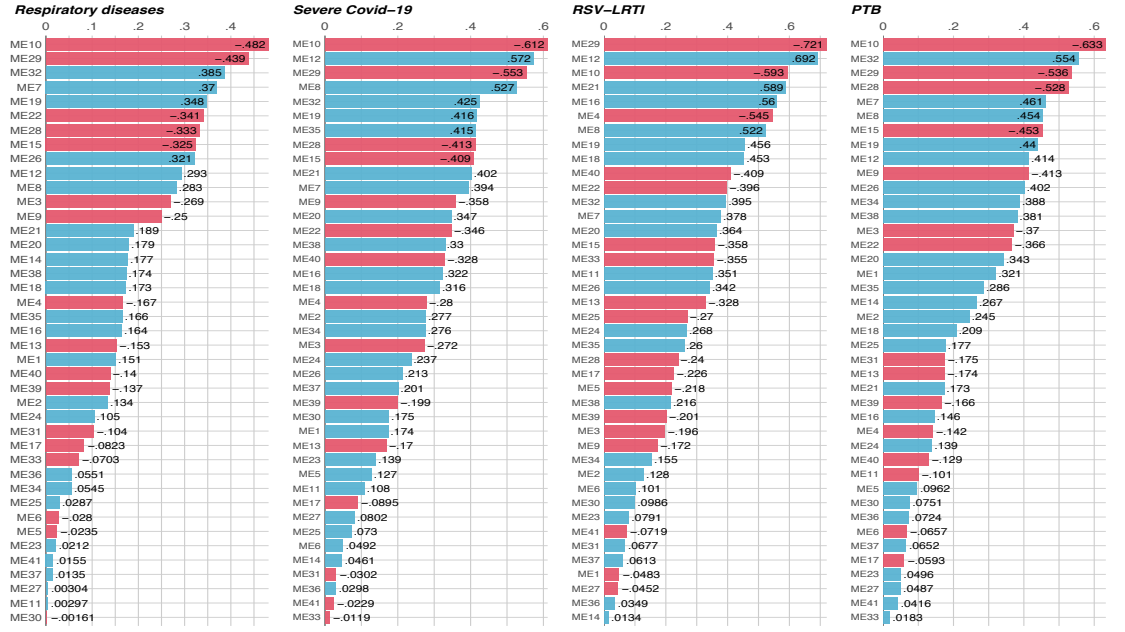

Figure 3. WGCNA analysis for respiratory infections and module correlation. A) Distribution of significant modules per respiratory infection (x-axis module eigengene vs y-axis respiratory infection), B) Correlation of Eigengene with respiratory infection.

205 Table 2 WGCNA modules correlated with respiratory infections at Pearson correlation r >0.25 and p< 0.05.

Name	Total	Element	Top gene ontology	Top five hub genes
COVID19 PTB RSV-LRTI	10	ME7	Olfactory receptor activity and telomere maintenance	*OPHN1, PARD6A, ACADS, PMM1* and *VPS72*
		ME15	Adaptive immune response and granzyme-mediated programmed cell death	*TBX21, CCL5, GZMA, IL2RB* and *SH2D2A*
		ME29	Negative regulation of apoptosis	*AOC3, AMPD2, SGK1, DPEP2* and *TIGD3*
		ME22	Macrophage differentiation and cellular response to oxygen level	*CCR3, PIK3R6, CLC, PTGDR2* and *P2RY2*
		ME32	Eukaryotic translation initiation factor 4F complex and lyphocyte count	*STX18, PARP4, RASSF1, BLCAP* and *SAV1*
		ME10	Cytosolic transport and *TNFR2*	*TRIM28, MAPK3, P4HTM, ACTR1B* and *CNNM3*
		ME19	Viral transcription, aerobic respiration	*POLR2G, POLR2J, PSMB3, COX8A* and *NEDD8*
		ME12	Regulation of cell cycle	*CDK1, CCNB1, PLK1, MCM2* and *CDC6*
		ME8	B cell activation	*CD79A, BLNK, VPREB3, FCRLA* and *MS4A1*
		ME28	Adaptive immune response and T cell activation	*CD3E, LCK, CD3D, FYN* and *CD2*
COVID19 RSV-LRTI	6	ME18	Regulation of viral process and response to type I interferon	*STAT2, IRF9, STAT1, ISG15* and *IFIT3*
		ME16	RNA processes	*ABCE1, XPO1, MYC, IARS1* and *DHX15*
		ME4	Ribosomal biogenesis and leukocyte migration	*RGL2, TSEN34, MYC, SIRT7* and *FAM53C*
		ME21	Chromatin remodelling and hematopoietic stem cell differentiation	*MYC, PRPF8, TRIM28, TP53* and *FUS*
		ME24	Adaptive immune response and positive regulation of type I hypersensitivity	*HSP90B1, HSPA5, STT3A, PPIB* and *RPN1*
		ME40	Oxidative phosphorylation (mitochondrial respiratory chain complex)	*NDUFS4, NDUFS3, NDUFA9, COX6B1* and *NDUFV2*
COVID19 PTB	6	ME35	Urea metabolic process	*IL1R2, PYGL, ITPKC, MTARC1* and *SDC4*
		ME3	Ribosomal biogenesis and viral gene expression	*RPL6, RPL37, RPS5, RPL35* and *RPL9*
		ME2	Active transmembrane transport	*STAC2, CDH3, PHLDB1, HAO1* and *SLC26A4*
		ME34	Antibacterial humoral response and regulation of cytokine production	*ELANE, CEACAM8, AZU1, CTSG* and *CEBPE*
		ME9	T cell differentiation and adaptive immune response	*ITK, LCK, CD3E, CD3D* and *CD3G*
		ME38	Positive regulation of carbohydrate metabolic process	*PIK3R1, INSR, IRS2, GRB10* and *ZBTB16*
PTB RSV-LRTI	2	ME26	Defence response to another organism, interferon-gamma and cell killing	*TAP1, STAT1, PSMB8, GBP1* and *PSMB9*
		ME20	Lipid catabolic process and Regulation of immune repones	*HEXB, CD14, FCER1G, GRN* and *LY96*
RSV-LRTI	4	ME25	Blood coagulation and haemostasis	*ITGB5, VCL, GP1BA, ITGB3* and *PF4*
		ME13	Antigen presenting -positive regulation of leukocyte mediated cytotoxicity	*UBC, ARPC1B, ARPC3, ARPC1A* and *GNAI2*
		ME11	rRNA processes and Mitochondrial gene expression	*PSMD14, CCT2, RFC4, CCT4* and *PRIM1*
		ME33	Autophagosome and viral process	*UBC, ULK1, MAPK14, RAB5B* and *TSG101*
PTB	2	ME1	Immune response regulation and Neutrophil degranulation	*HDAC1, PPP4R1, IFNGR2, ATP6V1B2* and *PRKCD*
		ME14	Regulation of defence response	*MYD88, CASP1, IRF9, IRF2* and *GBP2*

206

Cell population differences associated with LRTI

To determine cell type composition differences in peripheral blood between healthy controls and hospitalised subjects with LRTI due to different pathogens, blood cell type proportions were estimated with xCell2 2.0 generated with the ImmuneCompendium.xCell2Ref reference panel. Significant cell type composition differences were identified between healthy controls and hospitalised LRTI groups: 23 for severe COVID-19, 16 for RSV-LRTI and 21 for PTB ($p < 0.05$) (see Fig 4). To determine cell type composition difference between LRTIs we conducted t-tests as shown in Figure 5B. There was no difference in cell composition between healthy controls and those with mild/asymptomatic COVID-19. When the different hospitalised LRTI groups were compared with each other, several differences in cell composition were observed ($p < 0.05$). These included T cells (lower in severe COVID-19 vs PTB), non-classical monocytes (severe COVID-19 vs RSV-LRTI and RSV-LRTI and PTB) and myeloid cells (RSV-LRTI vs PTB). PTB also showed depletion of central memory CD8+ T Cells and overexpression of granulocytes compared to RSV-LRTI (see Supplementary Fig 5).

Seven cell types showed differences with healthy controls across all LRTIs including: Macrophages, transitional memory CD8+ T cells (CD8+ Ttm, T cells, Central memory CD8+ alpha-beta T cells, basophils, myeloid cells and naive thymus-derived CD8+ alpha-beta T cells. Neutrophils and class switched memory B cells showed significant changes for RSV-LRTI and PTB compared to the healthy controls but not for severe COVID-19. Disease specific unique cell type proportion changes were identified for severe COVID-19 as shown in Figure 5. The details are provided in Supplementary Table S6 and Supplementary Fig 6.

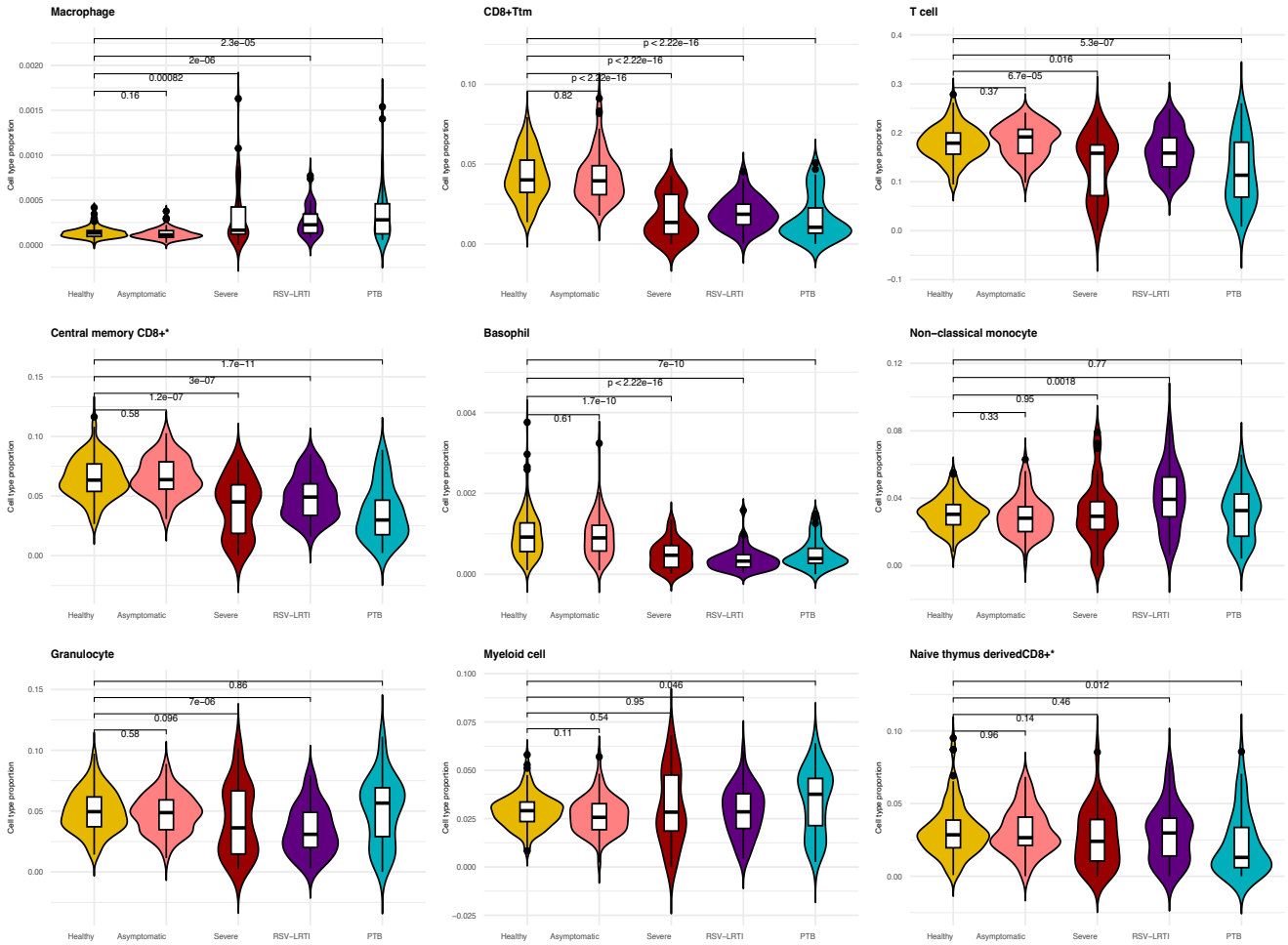

Figure 4 Differences in the proportions of immune cells in respiratory infections comparing healthy controls vs different LRTI groups. It shows the comparison of the five top cell types for LRTI and cell types uniquely different for RSV-LRTI and PTB.

Predictors of severe LRTI

To identify genes that represent biomarkers for each hospitalised LRTI, the normalized counts of the top 1000 significantly differentially expressed genes with respect to healthy controls were used and machine learning algorithms applied to identify the most informative genes. Ninety-three genes were identified as biomarkers for severe (hospitalised) COVID-19, 110 for RSV-LRTI and 95 for PTB as shown in Figure 5 and Supplementary Table S7.

Some genes were able to discriminate specific LRTIs from healthy controls including Severe COVID-19 (23), RSV-LRTI (74), PTB (37) and asymptomatic COVID-19 from severe COVID-19 (COVID-19 severity) (N=25) as shown in the Supplementary Figure 8. There were 10 genes that discriminated healthy controls from any LRTI including *IL16, LTK, IGIP, IGF2BP3, CBX7, KCTD7, FCER1A, TRAF1, RORC* and *SLC4A10*. See details of shared predictor genes amongst the LRTI groups in Supplementary Table S7.

Drug target lookup for genes associated with LRTI

To determine potentially therapeutic targets from DEGs associated with each LRTI, a look-up was undertaken for overlap with known druggability score generated by drugnomeAI. We identified 689, 159 and 849 genes for COVID-19, RSV-LRTI and PTB respectively with Tclin (approved drug targets) drugnomeAI score >90, as shown in Supplementary Table S8. For availability of drug and new therapeutic options we examined our predictors for availability of drugs as shown in Supplementary Table S9.

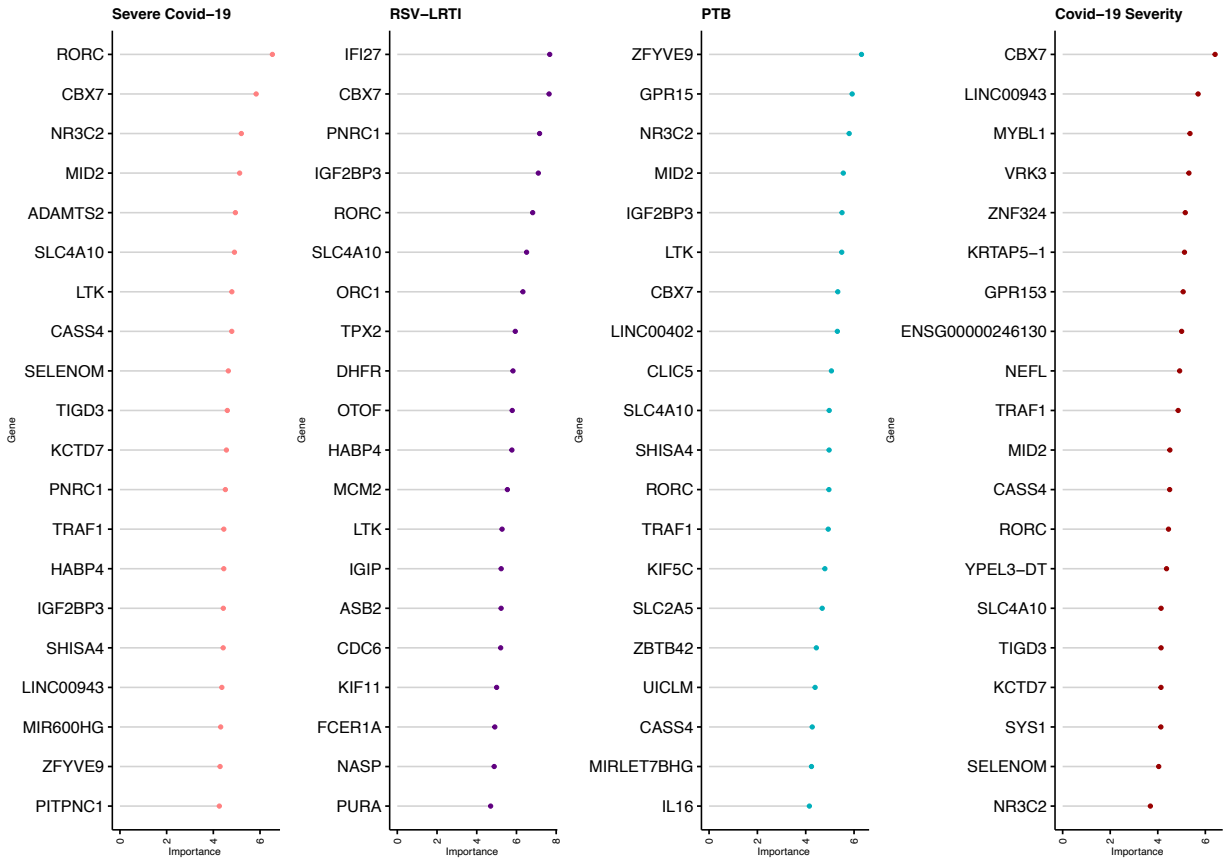

Figure 5 Top 20 gene severity predictors of LRTI for different etiologies based on mean importance. See shared predictors in Supplementary Fig 7.

Discussion

The transcriptional landscape of peripheral blood in response to viral and bacterial infections exhibits age-dependent variation, with implications for disease severity and immune regulation. In adults, SARS-CoV-2 infection has been studied extensively and elicits a robust transcriptional response characterized by upregulation of neutrophil activation markers, inflammatory cytokines, and interferon-stimulated genes (ISGs), alongside suppression of adaptive immune pathways and lymphocyte-associated transcripts [41,42]. Children infected with SARS-CoV-2 typically exhibit mild or asymptomatic disease, with transcriptomic profiles showing restrained inflammatory responses and lower expression of viral entry receptors such as *ACE2* and *TMPRSS2*[43]. However studies of the transcriptional responses to SARS-CoV-2 infection in children are extremely limited, focussing mainly on adolescents[44]. In this study, for the first time, we report genome-wide assessment of transcriptional responses of children hospitalized with one of three LRTIs (COVID-19, RSV-LRTI, PTB), compared to healthy children in a birth cohort from a low- and middle-income African setting. We identify 4500 genes related to hospitalized COVID-19 and known signature genes for RSV-LRTI and for PTB. Unique and shared pathways and gene modules were characterised between LRTIs, along with unique signatures for each of the LRTIs.

COVID-19 related genes were enriched for immune system, neutrophil degranulation and interferon gamma signalling as previously reported in other studies in adults. Neutrophil degranulation has been previously correlated with COVID severity[45] and excess neutrophil degranulation is associated with tissue damage[46]. The top upregulated genes included known genes responsible for immune responses, such as Interferon alpha-inducible protein 27 (*IFI27*) which is known to be an early predictor for COVID-19 outcome[47]. Many studies have shown reduced

ribosomal protein expression and immune suppression associated with persistence of COVID-19 infection[48]. Massoni *et al*[3] have discussed immune dysregulation and exhaustion as a hallmark of COVID-19 where adaptive immune responses are highly heterogeneous. Thus, at an early phase of infection, type I IFN activity as an anti-viral response is important in the development of both adaptive and innate immunity.

RSV-LRTI upregulated genes include *OTOF*[49]**,** *SIGLEC1*[50,51], *USP18*[52] and *ISG15* [53]. These genes were enriched for pathways including response to other organisms, regulation of viral life cycle, translational and interferon gamma signalling.

For PTB, we identified genes including *MMP8* and *MMP9* which are known to be associated with TB disease, by degradation of extracellular matrices[54,55,56]. *DEFA1, DEFA1B, DEFA3* and *DEFA4* are a known cluster of genes in the PTB defence response pathway. The expression of *LTF* is also known to be an important biomarker for PTB disease[57,58]. PTB specific markers such as *NCR3, CR2 CD28, IL10RA* and *GPR183* are functionally related to immune response, where *NCR3* stimulates NK cytotoxicity and *CR2* is involved in lymphocyte activation. These findings may contribute to understanding host responses in children in PTB and to strengthening diagnostic possibilities.

Using *WGCNA* co-expression analysis, we identified four RSV-LRTI specific modules: ME11 (translation and aerobic respiration), ME13 (antigen processing and T-cell mediated cytotoxicity), ME25 (coagulation and positive regulation of leukocyte) and ME33 (autophagy, viral processing and negative regulation of ferroptosis). A further two modules were specific to PTB: ME1 (immune response regulating signalling pathway and leukocyte differentiation) and ME14 (regulation of immune and defence response and cytokine production) (see Supplementary Fig 4).

While no modules were identified as specific to COVID-19, 22 modules were shared between COVID-19 and one or more LRTI, reflecting the seriousness of SARS-CoV-2 infection.

Ten shared modules were identified across all LRTIs (Table 2) including module 10, which is associated with endosomes[59] and contains the hub gene *TNFR2*, known to be linked with immune dysregulation in severe COVID-19[60]. In addition, module 10 contains many key hub genes known to be associated with COVID-19 severity including *TRIM28* (265 degree), *P4HTM* (245), *ACTR1B* (244), *CNNM3* (243), and *VPS51* (238). *TRIM28* is known to regulate SARS-CoV-2 entry by targeting *ACE2*[61], suppressing antiviral immunity[62] and is linked with COVID-19 severity[63]. *P4HTM* is known to play a role in adaptation to hypoxia and energy response and is linked with hypoventilation[64].

Other shared modules include: Module 22 the hub gene *CCR3* (C-C motif chemokine receptor 3) regulates cell migration and inflammatory responses by acting as a receptor for various CC chemokines such as eotaxin, and is a susceptibility gene for severe COVID-19 [65]. Module 28 was related to adaptive immune response and T-cell activation; with hub genes including *CD3E* involved in T-cell signalling to detect and clear pathogens. Module 7 was enriched for sensory perception such as olfactory dysfunction, a known symptom in COVID-19 [66]. Module 15 was related to T-cell differentiation and adaptive immunity where hub gene *TBX21* is a transcription factor that modulates innate immunity by regulating the expression of *TLR2*[67]. *GZMA* and *GZMB* play a role in immune response during respiratory infection[68]. *IFNG* is involved in clearing viral infection[69].

A further six modules were shared between COVID-19 and PTB including module 34 which was enriched for antimicrobial humoral responses (*DEFA1, DEFA3, RNASE3, BPI, PGLYRP1, CAMP, AZU1, ELANE* and *LTF*) and neutrophil degranulation[70] in the Reactome database (*DEFA1,*

ORM1, ORM2, RNASE3, ATP8B4, STBD1, BPI, PGLYRP1, TCN1, MS4A3, ABCA13, CLEC5A, CAMP, AZU1, CPNE3, CEACAM8, ELANE, CEACAM6, CRISP3, LTF, PLD1, MMP8, CHIT1, LCN2, OLR1 and *SLC2A).* The hub gene *ELANE* encodes a serine protease secreted by neutrophils that is known to regulate the function of natural killer cells, monocytes and granulocytes and is essential for neutrophils in fighting infections[71,72]. Neutrophil activation is characteristic of severe COVID-19[73] and shared with other inflammatory states[74]. Module 26, identified as shared between PTB and RSV-LRTI , includes the hub gene *TAP1* which is known for its antiviral activity through Type I interferon production[75]. Other hub genes include *STAT, PSMB8, GBP1, PSMB9, HLA-E , GBP5 , HLA-F , GBP2, IRF9, APOL3* and *CASP1* which are also known be associated with COVID-*19*[76]. The detailed enrichment for GO terms are provided in Supplementary Table S5 and Supplementary Fig 4.

Cell proportion estimation showed that in children hospitalised with COVID-19 there was depletion of macrophages and monocytes compared to healthy controls. In contrast, in children hospitalised with RSV-LRTI, increased proportions of regulatory T-cells and macrophages, and a depletion of T-cells and class switched memory B-cells were observed. Similarly, for PTB, there was an increase in macrophages, monocytes and neutrophils, and a depletion of T-cells and CD8+ alpha-beta T-cells, and cytotoxic NK cells (Fig 4). The depletion of T and B cells is a key feature of COVID-19 severity[77]. T-cell immunity is essential to control PTB[78].

We identified 247 genes that predicted the severity of LRTI. Ten were common among LRTIs. *IL16* is involved in pro-inflammatory responses to activate T-cells and the production of cytokines[79]. Five genes could discriminate hospitalised children with LRTI including: *PITPNC1*, *TPX2*, *LARP1*, *HABP4* and *SMIM10L2A*. *PITPNC1* is known for pulmonary function and asthma[80]. Five genes, including *PAFAH2, LINC02915, CLSPN, EIF4G1* and *IFI27,* were

predictors of both COVID-19 and RSV-LRTI hospitalization. *PAFAH2* is known to be associated with pulmonary micro-thromboses linked with LRTI severity[81,82]. The top COVID-19 predictor, *RORC,* is a key regulator of cellular differentiation, immunity and glucose metabolism. *CBX7* is part of the Polycomb complex required for transcriptional repression of many genes and cancer progression[83] and is functionally linked with lymphocyte, monocyte and neutrophil counts. *ZFVE9* is known to be predictive of active TB[84]. The *ADAMTS2* is metalloprotease that processes extracellular matrix is implicated in tissue damage[85] and is a marker for COVID-19 severity across disease conditions[86].

Assessing the potential druggability of differentially expressed genes can help in prioritizing drug targets. Amongst the DEGs for LRTIs, known approved drug targets (TClin) were identified including: *KCND3, CACNA1E, GABRG2, CHRNA5, KCND1* and *ADRB2* for severe COVID-19; *GABRG2, KCND1, CA12, CACNA1A, IMPDH2* and *PDE1B* for RSV-LRTI; *CACNA1E, GABRG2, KCNK3, CHRNA5* and *CHRNB2* for PTB as shown in Supplementary Table S8.

Interestingly, the top predictors of severity were not previously identified as drug targets, including CBX*7, MYBL1, VRK3, ZNF324, KRTAP5-1* and *GPR153.* In the top PTB predictors, *NR3C2* and *GPR15* have high scores for Tclin but the top predictors, *MID2* and *ZFYVE9,* have not previously been identified as drug targets showing opportunity for drug target prioritization for this population. For RSV-LRTI, except for *RORC,* most top predictors (*IFI27, CBX7, PNRC1* and *IGF2BP3)* have not previously been targeted for drug development (Supplementary Table S9).

One of the strengths of our study is the assessment of hospitalised children with one of the three major LRTIs in children in LMICs and comparison with healthy children using datasets generated from a similar genetic background. Many known signature-genes identified for COVID-19 (*IFI27, OLFM4*), RSV-LRTI (*SIGLEC1, ISG15, IFI44)* and PTB (*MMP8, MMP9, DEFA1, DEFA1B,*

DEFA3 and *DEFA4*) are known to be associated with progressive severity[87], showing the reproducibility of our findings. A limitation is that the DCHS children were older than children with LRTI, but we used age as a covariate to overcome this confounding effect.

From our transcriptomic analysis of children with LRTIs due to three different aetiologies, we have identified novel data providing key immune response related genes associated with severity for children hospitalised with COVID-19, RSV-LRTI and PTB in African children. These genes can be used for baseline characterization, as predictive markers for respiratory infection severity and as potential therapeutic targets.

Data availability

Supplementary data and summary statistics for transcriptome wide association analyses are available from: DOI https://doi.org/10.5258/SOTON/D3587.

An anonymised, de-identified version with data can be made available on request. All requests should be directed to Prof Heather Zar, DCHS Study Principal Investigator.

Code availability

The custom code used to generate graphics is available at GitHub repository: https://github.com/negusse2025/respiratory_infections.git.

Acknowledgements

Funding, participants/ families and staff. The some of the graphic illustrations for graphic abstract were accessed from NIH BIOART, including TB (https://bioart.niaid.nih.gov/bioart/527), child (https://bioart.niaid.nih.gov/bioart/75) and SARS-CoV-2 (https://bioart.niaid.nih.gov/bioart/464).

Funding

HJZ reports grants from UK NIHR (GEC111), Wellcome Biomedical resources grant (221372/Z/20/Z), Wellcome Trust Centre for Infectious Disease Research in Africa (CIDRI), Bill & Melinda Gates Foundation USA, (OPP1017641, OPP1017579) and NIH H3 Africa (U54HG009824, U01AI110466]). HZ is supported by the SA-MRC. NTK is supported by the National Institute for Health and Care Research through the NIHR Southampton Biomedical Research Centre. Additionally, both NTK and JHW received supported from University of Southampton's Global Partnership Award University of Southampton.

Author information

H.J.Z., M.P.K., M.B., N.T.K., D.B. and J.W.H. contributed to conceptualisation.

N.T.K., L.W, H.J.Z. and J.W.H. performed data curation.

N.T.K., E.K. and J.W.H. carried out formal analysis.

N.T.K., M.J, E.K, M.B, D.G, M.P.K. and J.W.H. provided methodology.

H.J.Z performed project administration. N.T.K., H.J.Z. and J.W.H. performed writing—original draft. N.T.K., C.C., D.B., E.K., L.W., M.B., M.J., M.P.K., H.J.Z. and J.W.H. contributed to writing—review, editing and final approval.

References

1. Mazur, N. I., Caballero, M. T. & Nunes, M. C. Severe respiratory syncytial virus infection in children: burden, management, and emerging therapies. *The Lancet* **404**, 1143–1156 (2024).
2. De Souza, T. H., Nadal, J. A., Nogueira, R. J. N., Pereira, R. M. & Brandão, M. B. Clinical manifestations of children with COVID-19: A systematic review. *Pediatr. Pulmonol.* **55**, 1892–1899 (2020).
3. Mazzoni, A., Salvati, L., Maggi, L., Annunziato, F. & Cosmi, L. Hallmarks of immune response in COVID-19: Exploring dysregulation and exhaustion. *Semin. Immunol.* **55**, 101508 (2021).
4. Sun, Y.-K. *et al.* Severe pediatric COVID-19: a review from the clinical and immunopathophysiological perspectives. *World J. Pediatr.* **20**, 307–324 (2024).
5. Soares-Schanoski, A. *et al.* Asymptomatic SARS-CoV-2 Infection Is Associated With Higher Levels of Serum IL-17C, Matrix Metalloproteinase 10 and Fibroblast Growth Factors Than Mild Symptomatic COVID-19. *Front. Immunol.* **13**, 821730 (2022).
6. Khoury, D. S. *et al.* Neutralizing antibody levels are highly predictive of immune protection from symptomatic SARS-CoV-2 infection. *Nat. Med.* **27**, 1205–1211 (2021).
7. Legebeke, J. *et al.* Evaluating the Immune Response in Treatment-Naive Hospitalised Patients With Influenza and COVID-19. *Front. Immunol.* **13**, 853265 (2022).
8. Bibert, S. *et al.* Transcriptomic Signature Differences Between SARS-CoV-2 and Influenza Virus Infected Patients. *Front. Immunol.* **12**, 666163 (2021).
9. Penrice-Randal, R. *et al.* Blood gene expression predicts intensive care unit admission in hospitalised patients with COVID-19. *Front. Immunol.* **13**, 988685 (2022).
10. Loy, C. J. *et al.* Nucleic acid biomarkers of immune response and cell and tissue damage in children with COVID-19 and MIS-C. *Cell Rep. Med.* **4**, 101034 (2023).

11. Patnaik, S. *et al.* RNAseq-based transcriptomics of treatment-naïve multi-inflammatory syndrome in children (MIS-C) demonstrates predominant activation of matrisome, innate and humoral immune pathways. *Rheumatol. Int.* **44**, 1445–1454 (2023).

12. Yang, Z. *et al.* Recent progress in tuberculosis diagnosis: insights into blood-based biomarkers and emerging technologies. *Front. Cell. Infect. Microbiol.* **15**, 1567592 (2025).

13. Theuretzbacher, U., Jumde, R. P., Hennessy, A., Cohn, J. & Piddock, L. J. V. Global health perspectives on antibacterial drug discovery and the preclinical pipeline. *Nat. Rev. Microbiol.* https://doi.org/10.1038/s41579-025-01167-w (2025) doi:10.1038/s41579-025-01167-w.

14. Farhat, M. *et al.* Drug-resistant tuberculosis: a persistent global health concern. *Nat. Rev. Microbiol.* **22**, 617–635 (2024).

15. Fossati, A. *et al.* Plasma proteomics for novel biomarker discovery in childhood tuberculosis. Preprint at https://doi.org/10.1101/2024.12.05.24318340 (2024).

16. Gygi, J. P. *et al.* Integrated longitudinal multiomics study identifies immune programs associated with acute COVID-19 severity and mortality. *J. Clin. Invest.* **134**, e176640 (2024).

17. Zhang, B. & Horvath, S. A General Framework for Weighted Gene Co-Expression Network Analysis. *Stat. Appl. Genet. Mol. Biol.* **4**, (2005).

18. Investigating the early-life determinants of illness in Africa: the Drakenstein Child Health Study.

19. Benede, N. *et al.* Distinct T cell polyfunctional profile in SARS-CoV-2 seronegative children associated with endemic human coronavirus cross-reactivity. *iScience* **27**, 108728 (2024).

20. Zar, H. J. *et al.* Natural immunity and protection against variants in South African children through five COVID-19 waves: A prospective study. *Int. J. Infect. Dis.* **150**, 107300 (2025).

21. Simon, Andrew. FastQC: A Quality Control Tool for High Throughput Sequence Data [Online]. *2010* **Available online at: http://www.bioinformatics.babraham.ac.uk/projects/fastqc/**,.

22. Ewels, P., Magnusson, M., Lundin, S. & Käller, M. MultiQC: Summarize analysis results for multiple tools and samples in a single report. *Bioinformatics* **32**, 3047–3048 (2016).

23. Dobin, A. *et al.* STAR: ultrafast universal RNA-seq aligner. *Bioinformatics* **29**, 15–21 (2013).

24. Patro, R., Duggal, G., Love, M. I., Irizarry, R. A. & Kingsford, C. Salmon: fast and bias-aware quantification of transcript expression using dual-phase inference. *Nat. Methods* **14**, 417–419 (2017).

25. Robinson, M. D., McCarthy, D. J. & Smyth, G. K. edgeR: A Bioconductor package for differential expression analysis of digital gene expression data. *Bioinformatics* **26**, 139–140 (2009).

26. Robinson, M. D. & Oshlack, A. A scaling normalization method for differential expression analysis of RNA-seq data. *Genome Biol.* **11**, R25 (2010).

27. Chen, X., Zhang, B., Wang, T., Bonni, A. & Zhao, G. Robust principal component analysis for accurate outlier sample detection in RNA-Seq data. *BMC Bioinformatics* **21**, 269 (2020).

28. Ritchie, M. E. *et al.* limma powers differential expression analyses for RNA-sequencing and microarray studies. *Nucleic Acids Res.* **43**, e47 (2015).

29. Chen, J., Bardes, E. E., Aronow, B. J. & Jegga, A. G. ToppGene Suite for gene list enrichment analysis and candidate gene prioritization. *Nucleic Acids Res.* **37**, W305–W311 (2009).

30. Horvath, P. L. and S. WGCNA: an R package for weighted correlation network analysis. *Oncol. Rep.* **11**, 515–522 (2004).

31. Lares, B. lares: Lean Analytics and Robust Exploration Sidekick. *2025* 2025.

32. Warde-Farley, D. *et al.* The GeneMANIA prediction server: biological network integration for gene prioritization and predicting gene function. *Nucleic Acids Res.* **38**, W214–W220 (2010).

33. Christmas, C., Rowan; Avila-Campillo, Iliana; Bolouri, Hamid; Schwikowski, Benno; Anderson, Mark; Kelley, Ryan; Landys, Nerius; Workman, Chris; Ideker, Trey; Cerami, Ethan; Sheridan, Rob; Bader, Gary D. ;. Sander. Cytoscape: a software environment for integrated models of biomolecular interaction networks. *Am. Assoc. Cancer Res. Educ. Book* 12–16 (2005) doi:10.1101/gr.1239303.metabolite.

34. Sayols, S. rrvgo: a Bioconductor package for interpreting lists of Gene Ontology terms. *Open Access*.

35. Angel, A., Naom, L., Nabet-Levy, S. & Aran, D. xCell 2.0: Robust Algorithm for cell type Proportion Estimation Predicts Response to Immune Checkpoint Blockade. Preprint at https://doi.org/10.1101/2024.09.06.611424 (2024).

36. Godec, J. *et al.* Compendium of Immune Signatures Identifies Conserved and Species-Specific Biology in Response to Inflammation. *Immunity* **44**, 194–206 (2016).

37. Tarke, A. *et al.* Comprehensive analysis of T cell immunodominance and immunoprevalence of SARS-CoV-2 epitopes in COVID-19 cases. *Cell Rep. Med.* **2**, 100204 (2021).

38. Kursa, M. B., Jankowski, A. & Rudnicki, W. R. Boruta – A System for Feature Selection. *Fundam. Informaticae* **101**, 271–285 (2010).

504 39. Andy Liaw and Matthew Wiener. Classification and Regression by randomForest. *R News*
505 **2**, 18–22 (2002).
506 40. Raies, A. *et al.* DrugnomeAI is an ensemble machine-learning framework for predicting
507 druggability of candidate drug targets. *Commun. Biol.* **5**, 1291 (2022).
508 41. Schulte-Schrepping, J. *et al.* Severe COVID-19 Is Marked by a Dysregulated Myeloid Cell
509 Compartment. *Cell* **182**, 1419-1440.e23 (2020).
510 42. Legebeke, J. *et al.* Evaluating the Immune Response in Treatment-Naive Hospitalised
511 Patients With Influenza and COVID-19. *Front. Immunol.* **13**, 853265 (2022).
512 43. Pierce, C. A. *et al.* Immune responses to SARS-CoV-2 infection in hospitalized pediatric
513 and adult patients. *Sci. Transl. Med.* **12**, eabd5487 (2020).
514 44. Bando, S. Y. *et al.* Blood leukocyte transcriptional modules and differentially expressed
515 genes associated with disease severity and age in COVID-19 patients. *Sci. Rep.* **13**, 898 (2023).
516 45. Muralidharan, A., Wyatt, T. A. & Reid, S. P. SARS-CoV-2 Dysregulates Neutrophil
517 Degranulation and Reduces Lymphocyte Counts. *Biomedicines* **10**, 382 (2022).
518 46. Herro, R. & Grimes, H. L. The diverse roles of neutrophils from protection to pathogenesis.
519 *Nat. Immunol.* **25**, 2209–2219 (2024).
520 47. Shojaei, M. *et al.* IFI27 transcription is an early predictor for COVID-19 outcomes, a multi-
521 cohort observational study. *Front. Immunol.* **13**, 1060438 (2023).
522 48. Yang, B. *et al.* Clinical and molecular characteristics of COVID-19 patients with persistent
523 SARS-CoV-2 infection. *Nat. Commun.* **12**, 3501 (2021).
524 49. Ding, H. *et al.* Membrane Protein OTOF Is a Type I Interferon-Induced Entry Inhibitor of
525 HIV-1 in Macrophages. *mBio* **13**, e01738-22 (2022).

526 50. Jans, J. *et al.* Siglec-1 inhibits RSV-induced interferon gamma production by adult T cells
527 in contrast to newborn T cells. *Eur. J. Immunol.* **48**, 621–631 (2018).
528 51. Herzog, S., Fragkou, P. C., Arneth, B. M., Mkhlof, S. & Skevaki, C. Myeloid
529 CD169/Siglec1: An immunoregulatory biomarker in viral disease. *Front. Med.* **9**, 979373
530 (2022).
531 52. Hou, J. *et al.* USP18 positively regulates innate antiviral immunity by promoting K63-
532 linked polyubiquitination of MAVS. *Nat. Commun.* **12**, 2970 (2021).
533 53. González-Sanz, R. *et al.* ISG15 Is Upregulated in Respiratory Syncytial Virus Infection
534 and Reduces Virus Growth through Protein ISGylation. *J. Virol.* **90**, 3428–3438 (2016).
535 54. Ong, C. W. M. *et al.* Neutrophil-Derived MMP-8 Drives AMPK-Dependent Matrix
536 Destruction in Human Pulmonary Tuberculosis. *PLOS Pathog.* **11**, e1004917 (2015).
537 55. Ugarte-Gil, C. A. *et al.* Induced Sputum MMP-1, -3 & -8 Concentrations during Treatment
538 of Tuberculosis. *PLoS ONE* **8**, e61333 (2013).
539 56. Sathyamoorthy, T. *et al.* Membrane Type 1 Matrix Metalloproteinase Regulates Monocyte
540 Migration and Collagen Destruction in Tuberculosis. *J. Immunol.* **195**, 882–891 (2015).
541 57. Shao, M. *et al.* Screening of potential biomarkers for distinguishing between latent and
542 active tuberculosis in children using bioinformatics analysis. *Medicine (Baltimore)* **100**, e23207
543 (2021).
544 58. Datta, A., Gupta, D., Waryani, D. & C, G. P. D. Decoding differentially expressed genes
545 to identify potential immunity associated biomarkers in Tuberculosis: An integrative
546 bioinformatics approach. *Biochem. Biophys. Rep.* **40**, 101870 (2024).
547 59. Vale-Costa, S. & Amorim, M. Recycling Endosomes and Viral Infection. *Viruses* **8**, 64
548 (2016).

549 60. Ahmad, S. *et al.* The role of TNFR2+ Tregs in COVID-19: An overview and a potential
550 therapeutic strategy. *Life Sci.* **286**, 120063 (2021).
551 61. Wang, Y. *et al.* TRIM28 regulates SARS-CoV-2 cell entry by targeting ACE2. *Cell. Signal.*
552 **85**, 110064 (2021).
553 62. Ren, J. *et al.* TRIM28-mediated nucleocapsid protein SUMOylation enhances SARS-CoV-
554 2 virulence. *Nat. Commun.* **15**, 244 (2024).
555 63. Tavakoli, R. *et al.* Comparing the expression levels of tripartite motif containing 28 in mild
556 and severe COVID-19 infection. *Virol. J.* **19**, 156 (2022).
557 64. Hay, E. *et al.* Biallelic P4HTM variants associated with HIDEA syndrome and
558 mitochondrial respiratory chain complex I deficiency. *Eur. J. Hum. Genet.* **29**, 1536–1541
559 (2021).
560 65. Sun, Z., Pan, L., Tian, A. & Chen, P. Critically-ill COVID-19 susceptibility gene CCR3
561 shows natural selection in sub-Saharan Africans. *Infect. Genet. Evol.* **121**, 105594 (2024).
562 66. Othman, B. A. *et al.* Olfactory dysfunction as a post-infectious symptom of SARS-CoV-2
563 infection. *Ann. Med. Surg.* **75**, (2022).
564 67. Woo, C. H., Shin, S. G., Koh, S. H. & Lim, J. H. TBX 21 participates in innate immune
565 response by regulating Toll-like receptor 2 expression in *S treptococcus pneumoniae*
566 infections. *Mol. Oral Microbiol.* **29**, 233–243 (2014).
567 68. Loebbermann, J. *et al.* Regulatory T cells expressing granzyme B play a critical role in
568 controlling lung inflammation during acute viral infection. *Mucosal Immunol.* **5**, 161–172
569 (2012).
570 69. Eichinger, K. M. *et al.* Alveolar macrophages support interferon gamma-mediated viral
571 clearance in RSV-infected neonatal mice. *Respir. Res.* **16**, 122 (2015).

572 70. Zhang, F. *et al.* Neutrophil diversity and function in health and disease. *Signal Transduct.*
573 *Target. Ther.* **9**, 343 (2024).
574 71. Jia, W., Mao, Y., Luo, Q., Wu, J. & Guan, Q. Targeting neutrophil elastase is a promising
575 direction for future cancer treatment. *Discov. Oncol.* **15**, 167 (2024).
576 72. Tralau, T., Meyer-Hoffert, U., Schröder, J. & Wiedow, O. Human leukocyte elastase and
577 cathepsin G are specific inhibitors of C5a-dependent neutrophil enzyme release and chemotaxis.
578 *Exp. Dermatol.* **13**, 316–325 (2004).
579 73. Wang, X., Sanborn, M. A., Dai, Y. & Rehman, J. Temporal transcriptomic analysis using
580 TrendCatcher identifies early and persistent neutrophil activation in severe COVID-19. *JCI*
581 *Insight* **7**, e157255 (2022).
582 74. Schimke, L. F. *et al.* Severe COVID-19 Shares a Common Neutrophil Activation Signature
583 with Other Acute Inflammatory States. *Cells* **11**, 847 (2022).
584 75. Zhao, J. *et al.* Broadly Antiviral Activities of TAP1 through Activating the TBK1-IRF3-
585 Mediated Type I Interferon Production. *Int. J. Mol. Sci.* **22**, 4668 (2021).
586 76. Schmidt, N. *et al.* The SARS-CoV-2 RNA–protein interactome in infected human cells.
587 *Nat. Microbiol.* **6**, 339–353 (2020).
588 77. Ahern, D. J. *et al.* A blood atlas of COVID-19 defines hallmarks of disease severity and
589 specificity. *Cell* **185**, 916-938.e58 (2022).
590 78. Ogongo, P. *et al.* Tissue-resident-like CD4+ T cells secreting IL-17 control Mycobacterium
591 tuberculosis in the human lung. *J. Clin. Invest.* **131**, e142014 (2021).
592 79. Mathy, N. L. *et al.* Interleukin-16 stimulates the expression and production of pro-
593 inØammatory cytokines by human monocytes. (2000).

80. Yucesoy, B. *et al.* Genome-Wide Association Study Identifies Novel Loci Associated With Diisocyanate-Induced Occupational Asthma. *Toxicol. Sci.* **146**, 192–201 (2015).

81. Theoharides, T. C., Antonopoulou, S. & Demopoulos, C. A. Coronavirus 2019, Microthromboses, and Platelet Activating Factor. *Clin. Ther.* **42**, 1850–1852 (2020).

82. Demopoulos, C., Antonopoulou, S. & Theoharides, T. C. COVID -19, microthromboses, inflammation, and platelet activating factor. *BioFactors* **46**, 927–933 (2020).

83. Pallante, P., Forzati, F., Federico, A., Arra, C. & Fusco, A. Polycomb protein family member CBX7 plays a critical role in cancer progression.

84. Duffy, F. J. *et al.* Use of a Contained *Mycobacterium tuberculosis* Mouse Infection Model to Predict Active Disease and Containment in Humans. *J. Infect. Dis.* **225**, 1832–1840 (2022).

85. Loy, C. J. *et al.* Nucleic acid biomarkers of immune response and cell and tissue damage in children with COVID-19 and MIS-C. *Cell Rep. Med.* **4**, 101034 (2023).

86. Singh, M. S., Arun, P. P. S. & Ansari, M. A. Unveiling common markers in COVID-19: ADAMTS2, PCSK9, and OLAH emerged as key differential gene expression profiles in PBMCs across diverse disease conditions. *AIMS Mol. Sci.* **11**, 189–205 (2024).

87. Armignacco, R. *et al.* Whole blood transcriptome signature predicts severe forms of COVID-19: Results from the COVIDeF cohort study. *Funct. Integr. Genomics* **24**, 107 (2024).

Supplementary data

Supplementary Fig 1 Module dendrogram

Supplementary Fig 2 Distribution of genes per module

Supplementary Fig 3 Venn diagram shared modules between respiratory infections

Supplementary Fig 4 REVIGO biological process for correlated modules with LRTI

Supplementary Fig 5 Blood composition comparisons between LRTI

Supplementary Fig 6 Shared cell types

Supplementary Fig 7 Shared severity predictors for LRTI

Supplementary table S1 Respiratory infection TWAS FDR< 0.05

Supplementary table S2 Respiratory infection TWAS enrichment

Supplementary table S3 WGCNA module genes and eigengene

Supplementary table S4 Network degree distribution for module correlated to LRTI

Supplementary table S5 Enrichment for module correlated to LRTI

Supplementary Table S6 Cell type proportions

Supplementary table S7 severity predictors

Supplementary table S8 Drug target look-up

Supplementary table S9 Severity predictors and target prioritization

Supplementary file Modules_Network_analysis.cys.

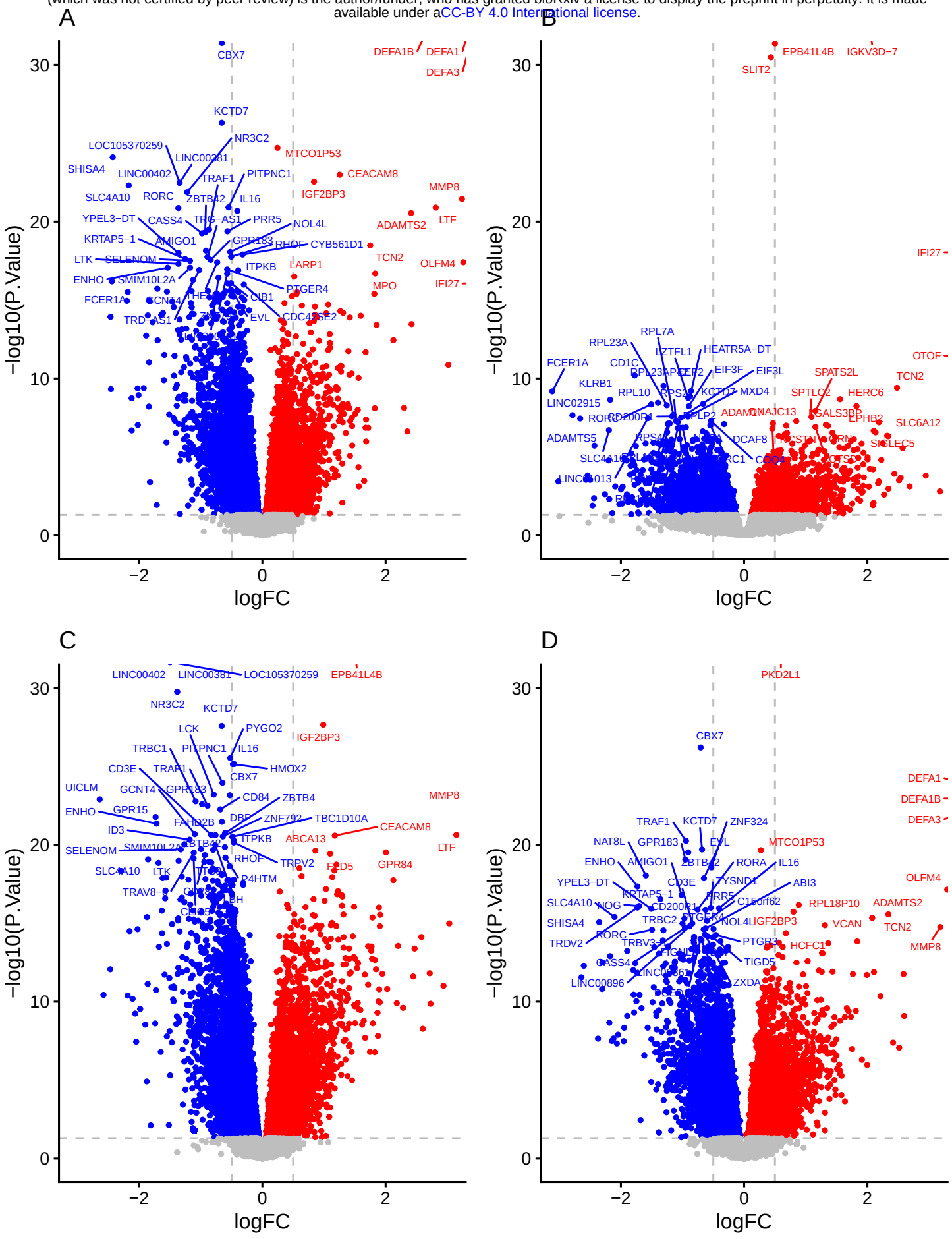

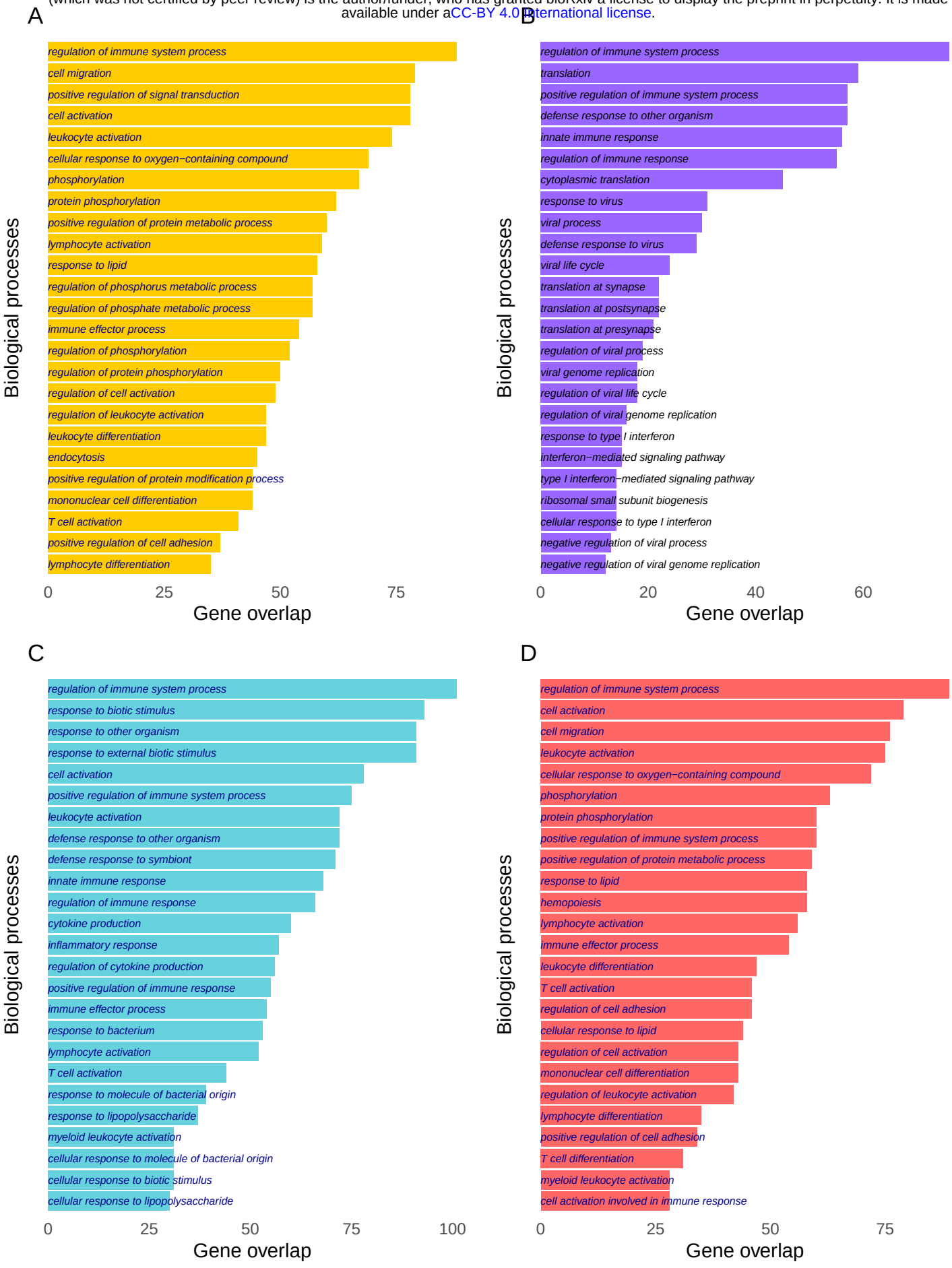

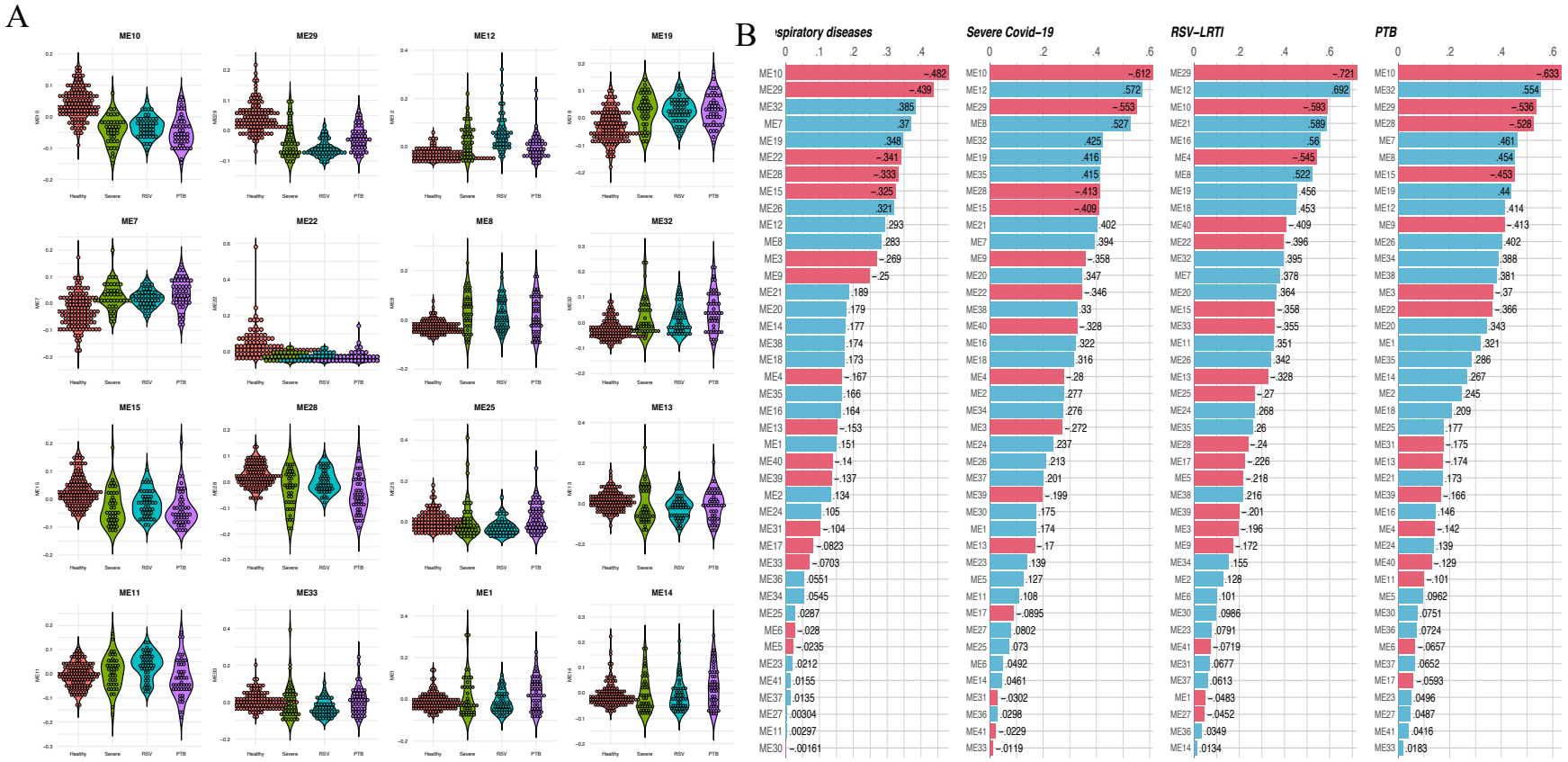
A
ME10
ME29
ME12
ME19
ME7
ME22
ME8
ME32
ME15
ME28
ME25
ME13
ME11
ME33
ME1
ME14
Healthy
Severe
RSV
PTB
B
spiratory diseases
Severe Covid−19
RSV−LRTI
PTB
ME10 −.482
ME29 −.439
ME32 .385
ME7 .37
ME19 .348
ME22 −.341
ME28 −.333
ME15 −.325
ME26 .321
ME12 .293
ME8 .283
ME3 −.269
ME9 −.25
ME21 .189
ME20 .179
ME14 .177
ME38 .174
ME18 .173
ME4 −.167
ME35 .166
ME16 .164
ME13 −.153
ME1 .151
ME40 −.14
ME39 −.137
ME2 .134
ME24 .105
ME31 −.104
ME17 −.0823
ME33 −.0703
ME36 .0551
ME34 .0545
ME25 .0287
ME6 −.028
ME5 −.0235
ME23 .0212
ME41 .0155
ME37 .0135
ME27 .00304
ME11 .00297
ME30 −.00161
ME10 −.612
ME12 .572
ME29 −.553
ME8 .527
ME32 .425
ME19 .416
ME35 .415
ME28 −.413
ME15 −.409
ME21 .402
ME7 .394
ME9 −.358
ME20 .347
ME22 −.346
ME38 .33
ME40 −.328
ME16 .322
ME18 .316
ME4 −.28
ME2 .277
ME34 .276
ME3 −.272
ME24 .237
ME26 .213
ME37 .201
ME39 −.199
ME30 .175
ME1 .174
ME13 −.17
ME23 .139
ME5 .127
ME11 .108
ME17 −.0895
ME27 .0802
ME25 .073
ME6 .0492
ME14 .0461
ME31 −.0302
ME36 .0298
ME41 −.0229
ME33 −.0119
ME29 −.721
ME12 .692
ME10 −.593
ME21 .589
ME16 .56
ME4 −.545
ME8 .522
ME19 .456
ME18 .453
ME40 −.409
ME22 −.396
ME32 .395
ME7 .378
ME20 .364
ME15 −.358
ME33 −.355
ME11 .351
ME26 .342
ME13 −.328
ME25 −.27
ME24 .268
ME35 .26
ME28 −.24
ME17 −.226
ME5 −.218
ME38 .216
ME39 −.201
ME3 −.196
ME9 −.172
ME34 .155
ME2 .128
ME6 .101
ME30 .0986
ME23 .0791
ME41 −.0719
ME31 .0677
ME37 .0613
ME1 −.0483
ME27 −.0452
ME36 .0349
ME14 .0134
ME10 −.633
ME32 .554
ME29 −.536
ME28 −.528
ME7 .461
ME8 .454
ME15 −.453
ME19 .44
ME12 .414
ME9 −.413
ME26 .402
ME34 .388
ME38 .381
ME3 −.37
ME22 −.366
ME20 .343
ME1 .321
ME35 .286
ME14 .267
ME2 .245
ME18 .209
ME25 .177
ME31 −.175
ME13 −.174
ME21 .173
ME39 −.166
ME16 .146
ME4 −.142
ME24 .139
ME40 −.129
ME11 −.101
ME5 .0962
ME30 .0751
ME36 .0724
ME6 −.0657
ME37 .0652
ME17 −.0593
ME23 .0496
ME27 .0487
ME41 .0416
ME33 .0183

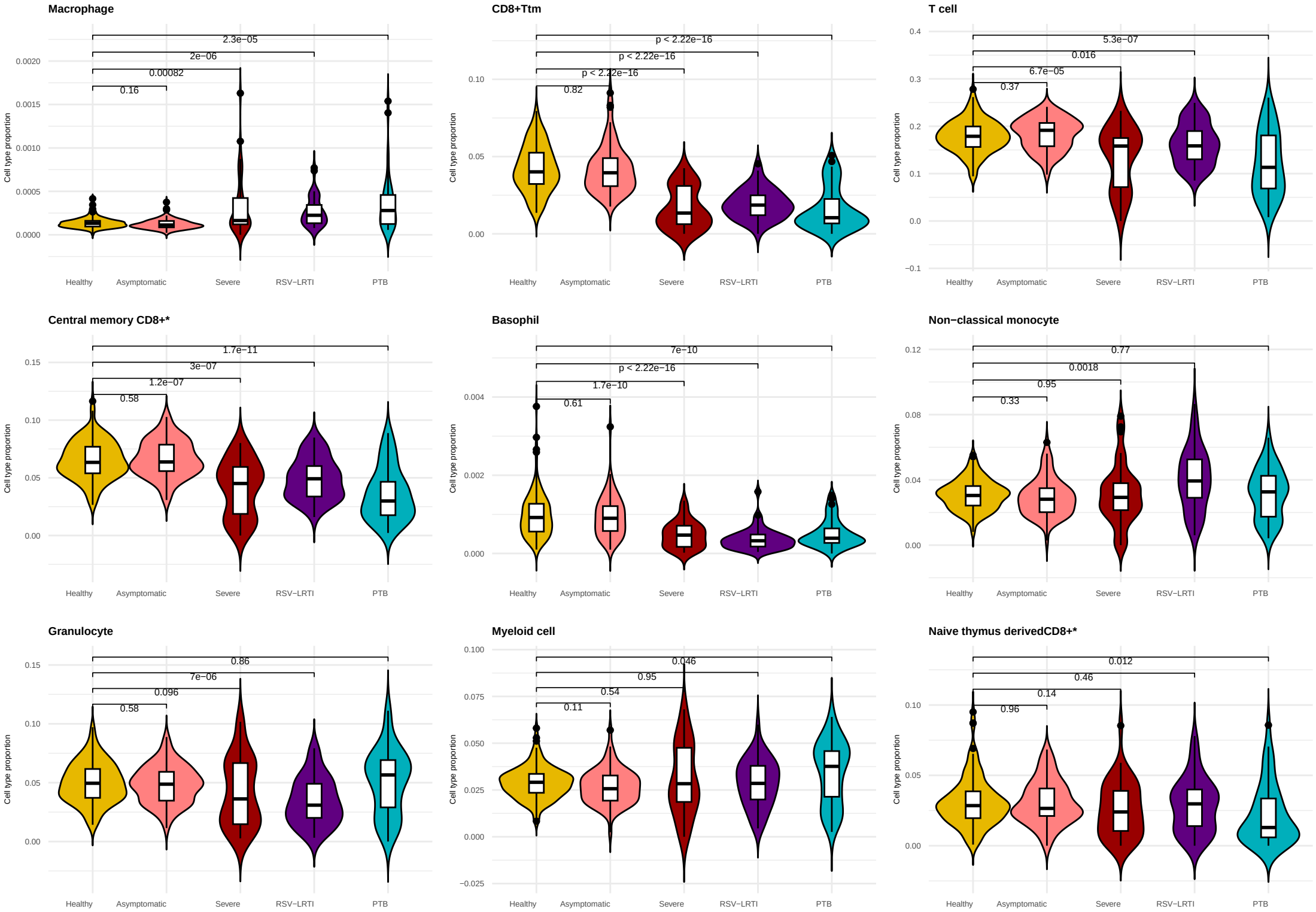
Macrophage
2.3e−05
2e−06
0.00082
0.16
CD8+Ttm
p < 2.22e−16
p < 2.22e−16
p < 2.22e−16
0.82
T cell
5.3e−07
0.016
6.7e−05
0.37
Central memory CD8+*
1.7e−11
3e−07
1.2e−07
0.58
Basophil
7e−10
p < 2.22e−16
1.7e−10
0.61
Non−classical monocyte
0.77
0.0018
0.95
0.33
Granulocyte
0.86
7e−06
0.096
0.58
Myeloid cell
0.046
0.95
0.54
0.11
Naive thymus derivedCD8+*
0.012
0.46
0.14
0.96
Cell type proportion
Healthy
Asymptomatic
Severe
RSV−LRTI
PTB

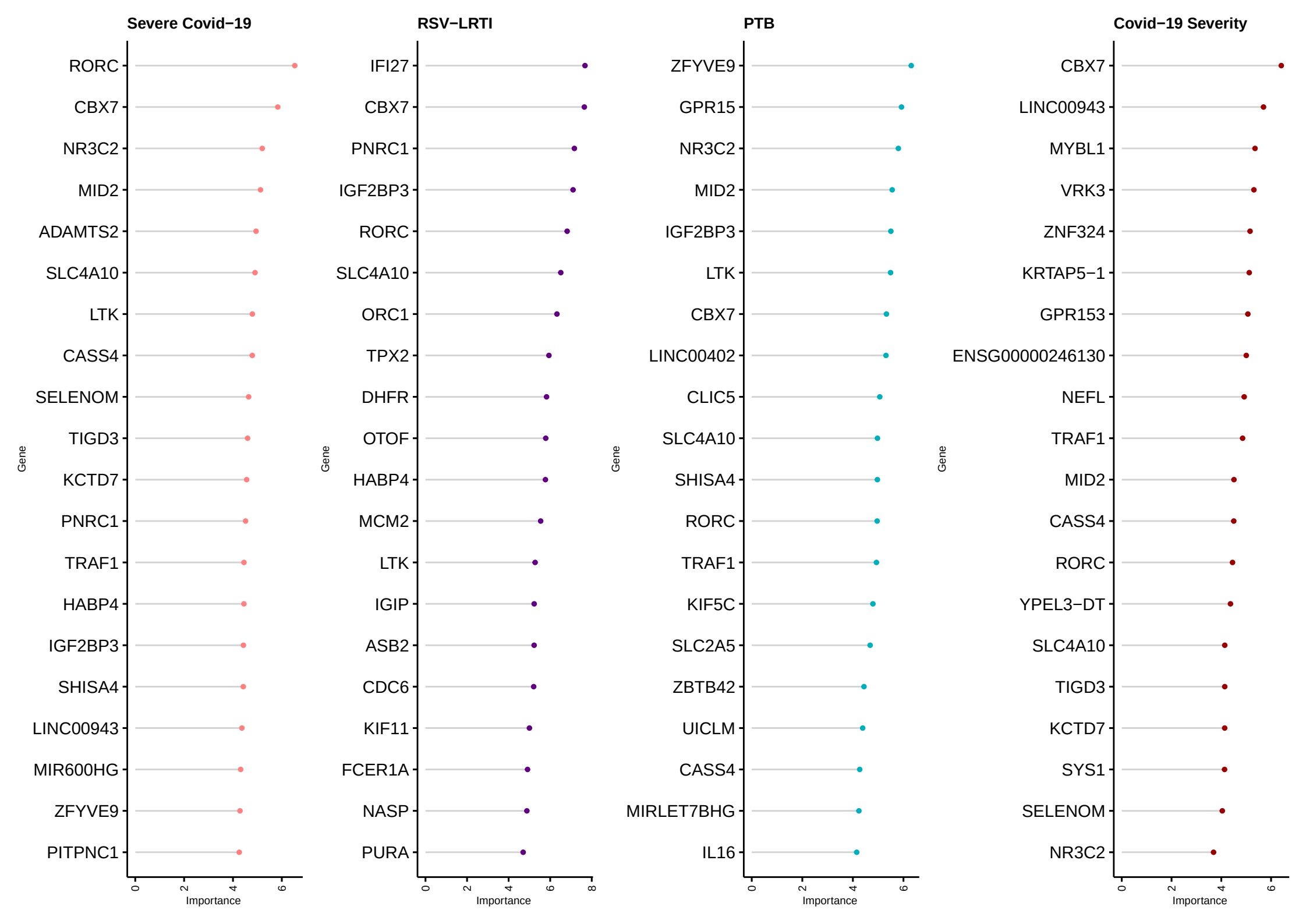
Severe Covid−19
RORC
CBX7
NR3C2
MID2
ADAMTS2
SLC4A10
LTK
CASS4
SELENOM
TIGD3
KCTD7
PNRC1
TRAF1
HABP4
IGF2BP3
SHISA4
LINC00943
MIR600HG
ZFYVE9
PITPNC1
Gene
0
2
4
6
Importance
RSV−LRTI
IFI27
CBX7
PNRC1
IGF2BP3
RORC
SLC4A10
ORC1
TPX2
DHFR
OTOF
HABP4
MCM2
LTK
IGIP
ASB2
CDC6
KIF11
FCER1A
NASP
PURA
Gene
0
2
4
6
8
Importance
PTB
ZFYVE9
GPR15
NR3C2
MID2
IGF2BP3
LTK
CBX7
LINC00402
CLIC5
SLC4A10
SHISA4
RORC
TRAF1
KIF5C
SLC2A5
ZBTB42
UICLM
CASS4
MIRLET7BHG
IL16
Gene
0
2
4
6
Importance
Covid−19 Severity
CBX7
LINC00943
MYBL1
VRK3
ZNF324
KRTAP5−1
GPR153
ENSG00000246130
NEFL
TRAF1
MID2
CASS4
RORC
YPEL3−DT
SLC4A10
TIGD3
KCTD7
SYS1
SELENOM
NR3C2
Gene
0
2
4
6
Importance

Respiratory infections

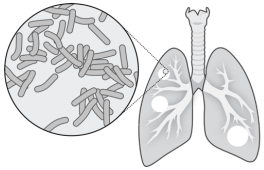

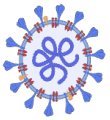

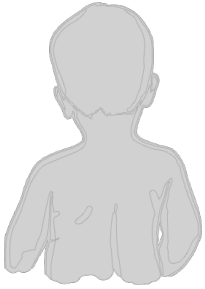

Healthy

Control n=127

Mild/Asymptomatic n=71

SARS-CoV2

Severe n=41

RSV-LRTI

n=47

Pulmonary Tuberculosis n=47

Gene co-expression signatures

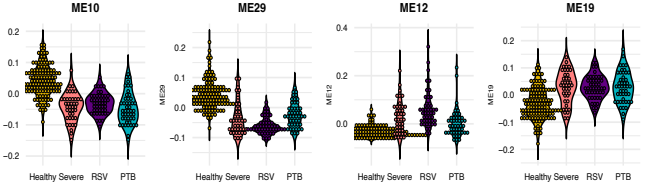

Lymphocyte dysregulation

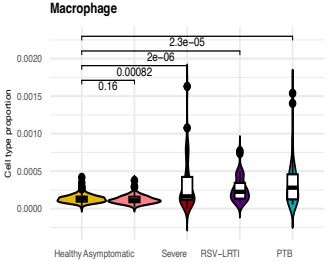

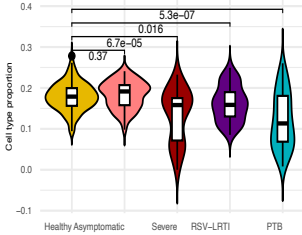

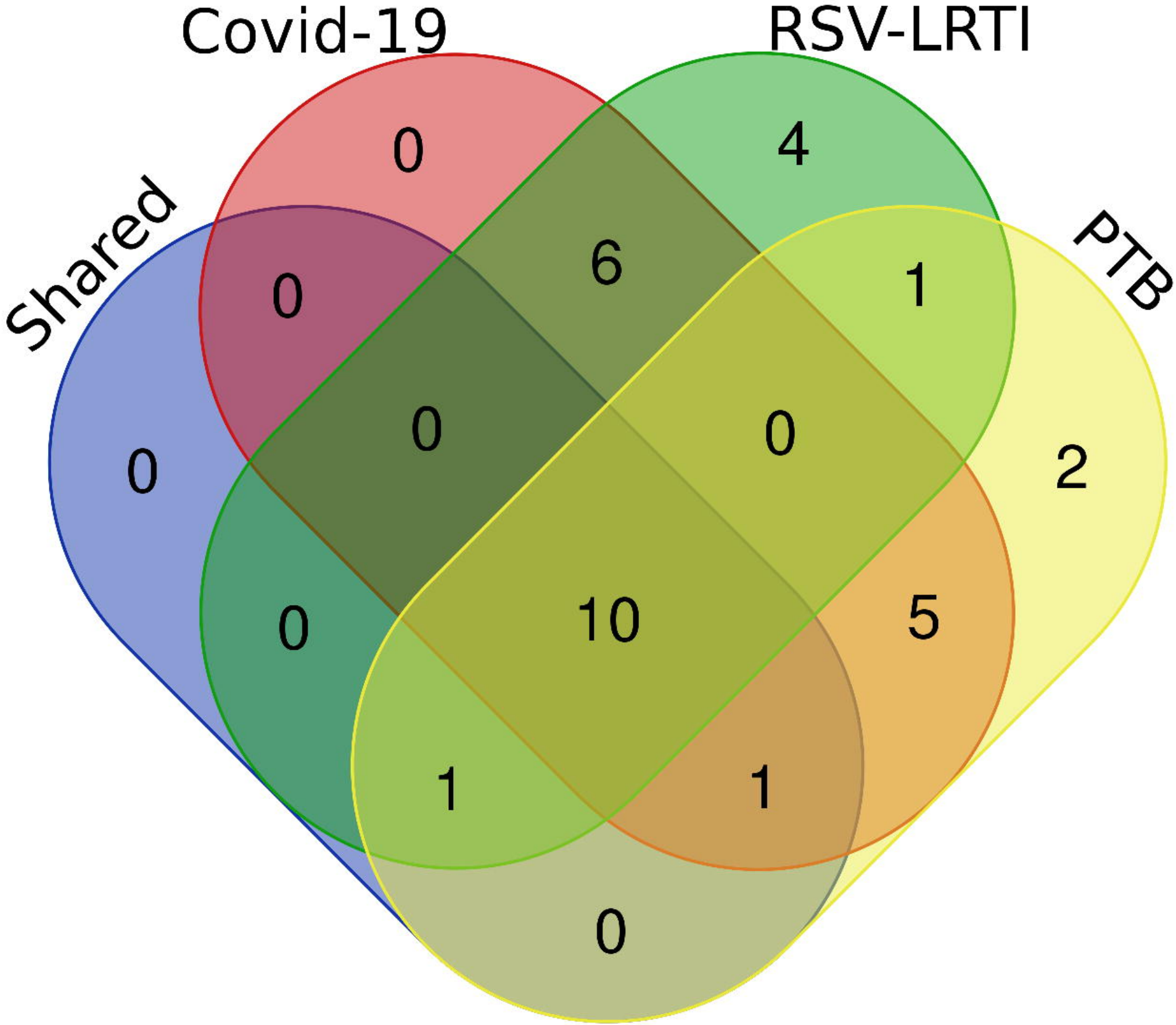
Covid-19
RSV-LRTI
Shared
PTB
0
4
0
6
1
0
0
0
2
0
10
5
1
1
0

ME1

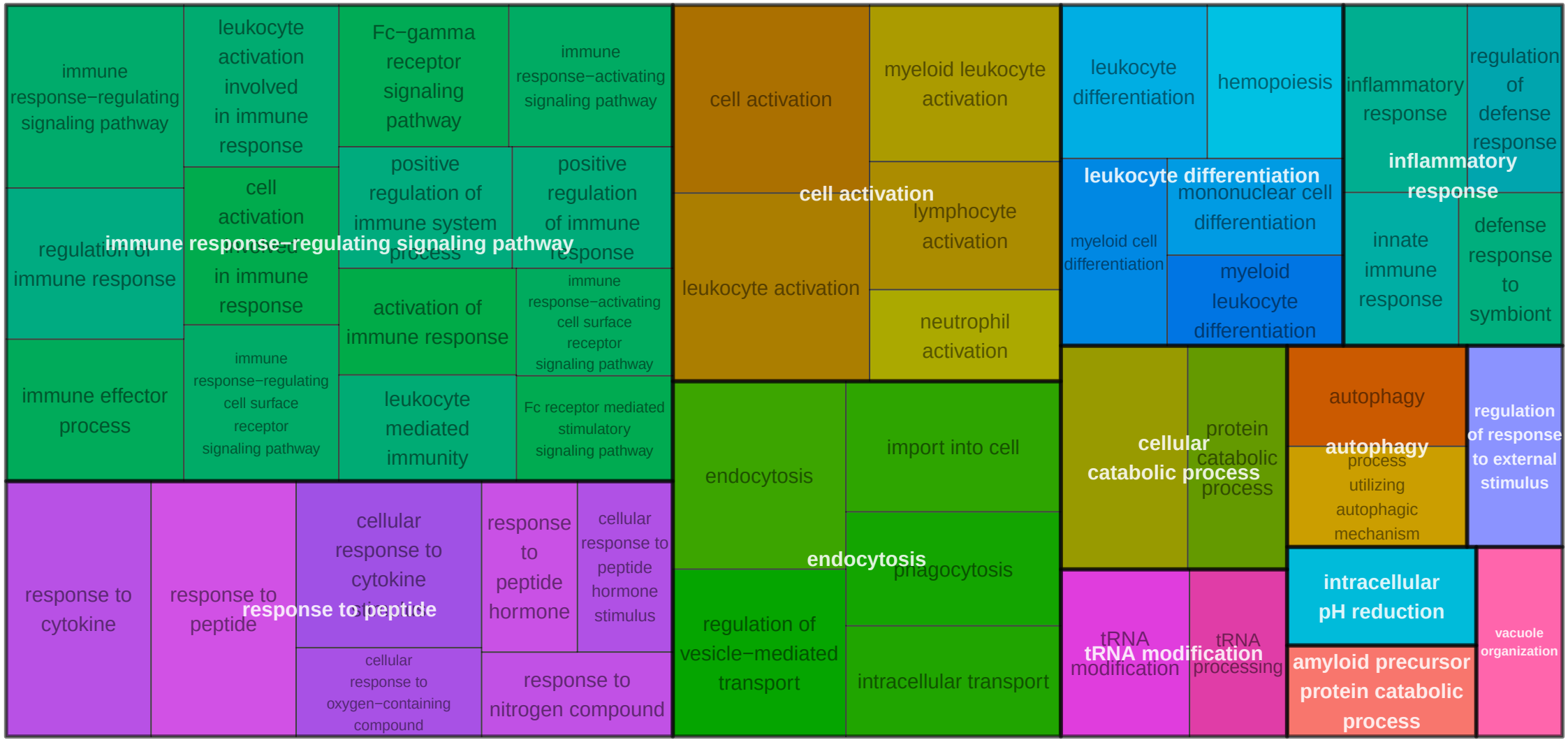
immune response−regulating signaling pathway
leukocyte activation involved in immune response
Fc−gamma receptor signaling pathway
immune response−activating signaling pathway
regulation of immune response
cell activation involved in immune response
positive regulation of immune system process
positive regulation of immune response
immune effector process
immune response−regulating cell surface receptor signaling pathway
activation of immune response
immune response−activating cell surface receptor signaling pathway
leukocyte mediated immunity
Fc receptor mediated stimulatory signaling pathway
cell activation
myeloid leukocyte activation
leukocyte activation
lymphocyte activation
neutrophil activation
leukocyte differentiation
hemopoiesis
myeloid cell differentiation
mononuclear cell differentiation
myeloid leukocyte differentiation
inflammatory response
regulation of defense response
innate immune response
defense response to symbiont
endocytosis
import into cell
phagocytosis
regulation of vesicle−mediated transport
intracellular transport
cellular catabolic process
protein catabolic process
autophagy
process utilizing autophagic mechanism
regulation of response to external stimulus
response to cytokine
response to peptide
cellular response to cytokine stimulus
response to peptide hormone
cellular response to peptide hormone stimulus
cellular response to oxygen−containing compound
response to nitrogen compound
tRNA modification
tRNA processing
intracellular pH reduction
amyloid precursor protein catabolic process
vacuole organization

ME10

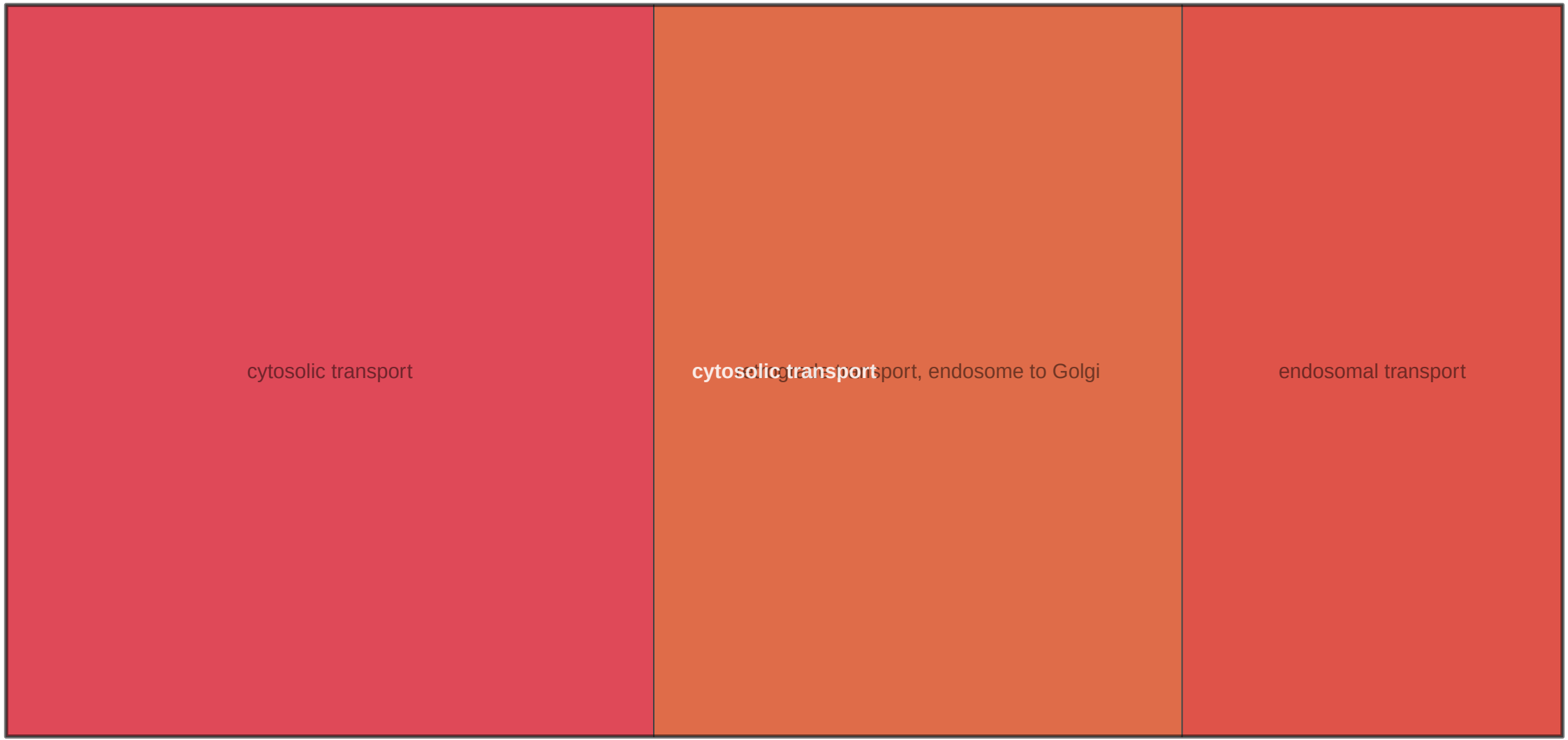
cytosolic transport
cytosolic transport
endosomal transport

ME11

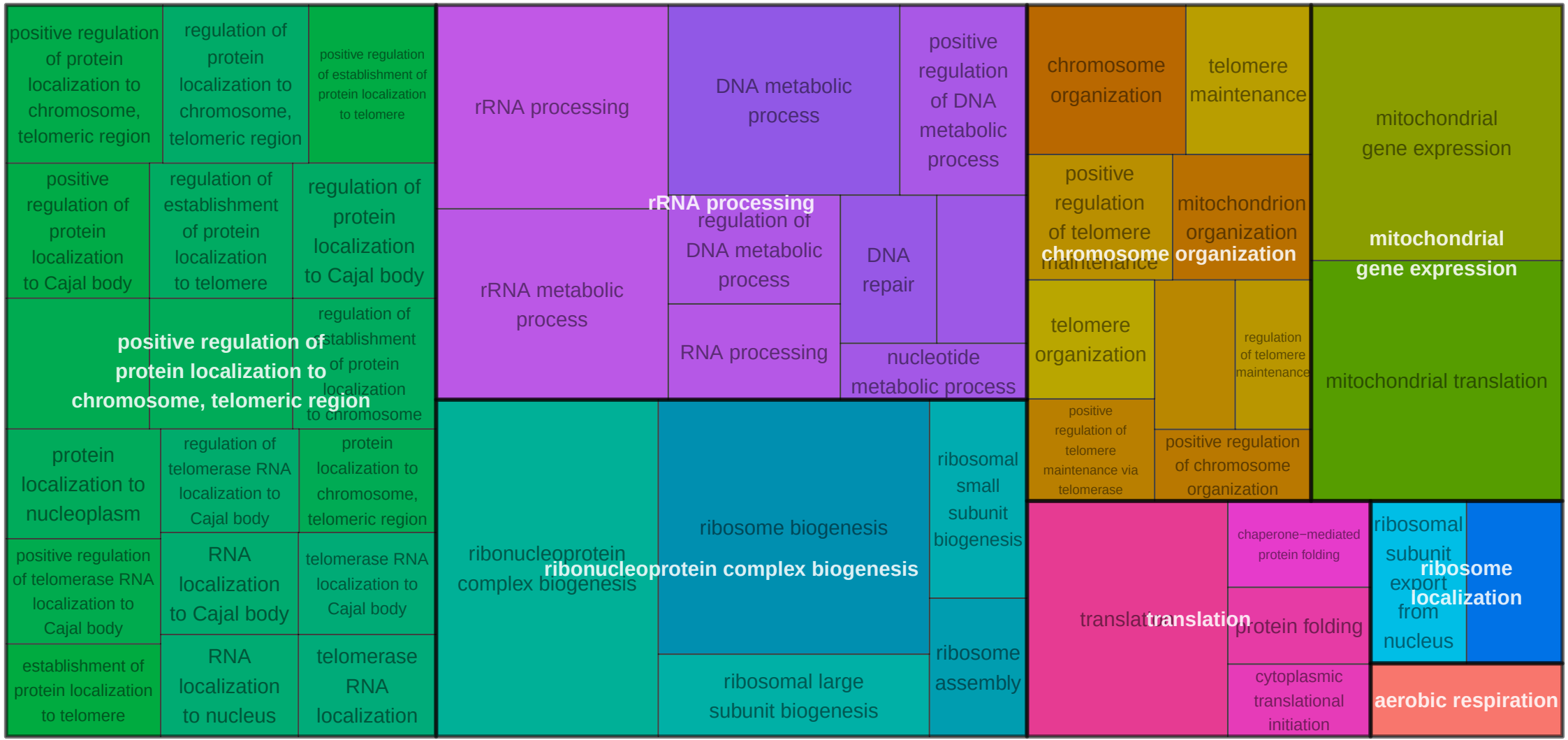
positive regulation of protein localization to chromosome, telomeric region
regulation of protein localization to chromosome, telomeric region
positive regulation of establishment of protein localization to telomere
positive regulation of protein localization to Cajal body
regulation of establishment of protein localization to telomere
regulation of protein localization to Cajal body
positive regulation of protein localization to chromosome, telomeric region
regulation of establishment of protein localization to chromosome
protein localization to nucleoplasm
regulation of telomerase RNA localization to Cajal body
protein localization to chromosome, telomeric region
positive regulation of telomerase RNA localization to Cajal body
RNA localization to Cajal body
telomerase RNA localization to Cajal body
establishment of protein localization to telomere
RNA localization to nucleus
telomerase RNA localization
rRNA processing
DNA metabolic process
positive regulation of DNA metabolic process
rRNA processing
rRNA metabolic process
regulation of DNA metabolic process
DNA repair
RNA processing
nucleotide metabolic process
ribonucleoprotein complex biogenesis
ribosome biogenesis
ribosomal small subunit biogenesis
ribonucleoprotein complex biogenesis
ribosomal large subunit biogenesis
ribosome assembly
chromosome organization
telomere maintenance
positive regulation of telomere maintenance
mitochondrion organization
chromosome organization
telomere organization
regulation of telomere maintenance
positive regulation of telomere maintenance via telomerase
positive regulation of chromosome organization
mitochondrial gene expression
mitochondrial gene expression
mitochondrial translation
translation
translation
chaperone−mediated protein folding
protein folding
cytoplasmic translational initiation
ribosomal subunit export from nucleus
ribosome localization
aerobic respiration

ME12

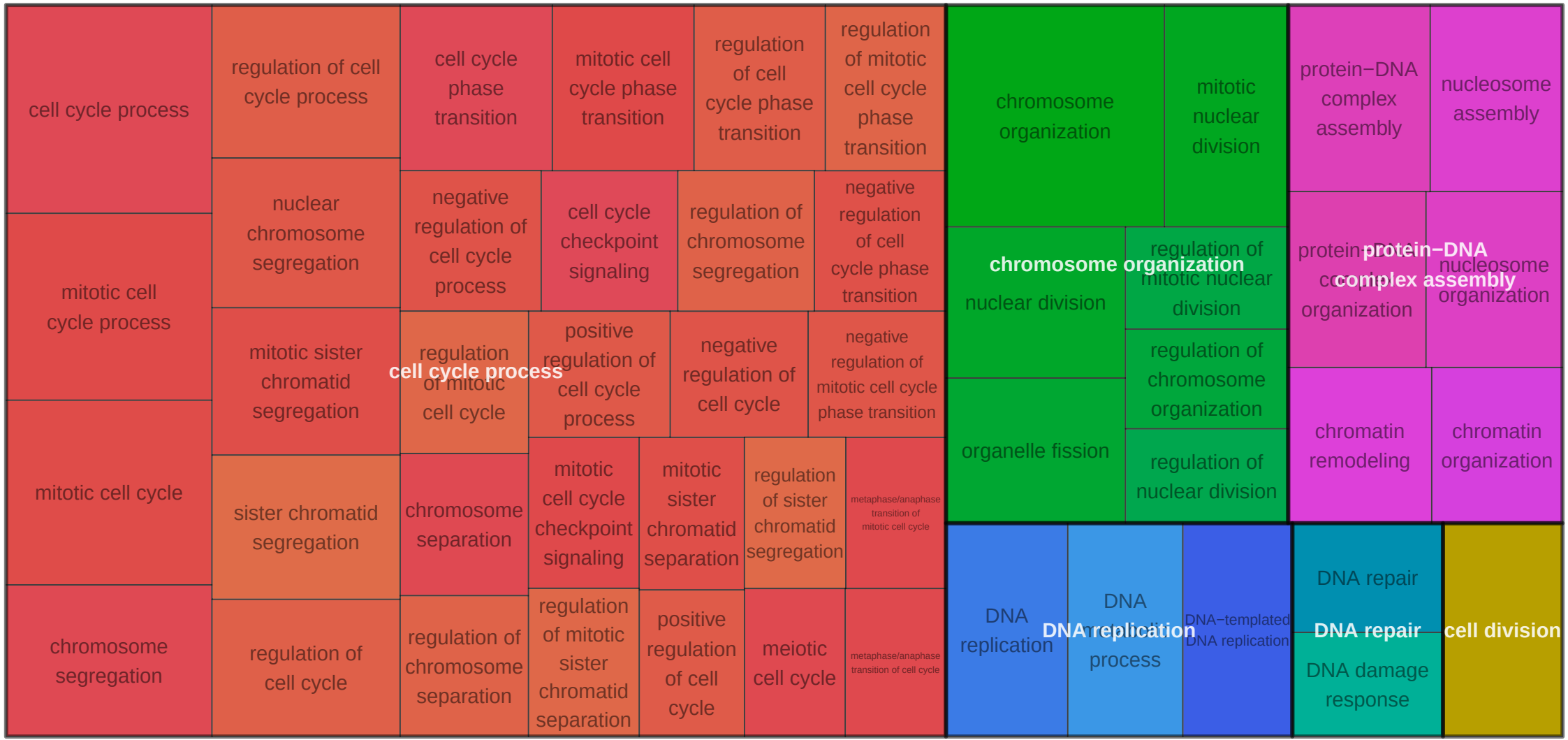
cell cycle process
regulation of cell cycle process
cell cycle phase transition
mitotic cell cycle phase transition
regulation of cell cycle phase transition
regulation of mitotic cell cycle phase transition
mitotic cell cycle process
nuclear chromosome segregation
negative regulation of cell cycle process
cell cycle checkpoint signaling
regulation of chromosome segregation
negative regulation of cell cycle phase transition
mitotic cell cycle
mitotic sister chromatid segregation
regulation of mitotic cell cycle
positive regulation of cell cycle process
negative regulation of cell cycle
negative regulation of mitotic cell cycle phase transition
cell cycle process
sister chromatid segregation
chromosome separation
mitotic cell cycle checkpoint signaling
mitotic sister chromatid separation
regulation of sister chromatid segregation
metaphase/anaphase transition of mitotic cell cycle
chromosome segregation
regulation of cell cycle
regulation of chromosome separation
regulation of mitotic sister chromatid separation
positive regulation of cell cycle
meiotic cell cycle
metaphase/anaphase transition of cell cycle
chromosome organization
mitotic nuclear division
chromosome organization
regulation of mitotic nuclear division
nuclear division
regulation of chromosome organization
organelle fission
regulation of nuclear division
protein−DNA complex assembly
nucleosome assembly
protein−DNA complex assembly
nucleosome organization
chromatin remodeling
chromatin organization
DNA replication
DNA replication
DNA-templated DNA replication
DNA repair
DNA repair
cell division
DNA damage response

ME13

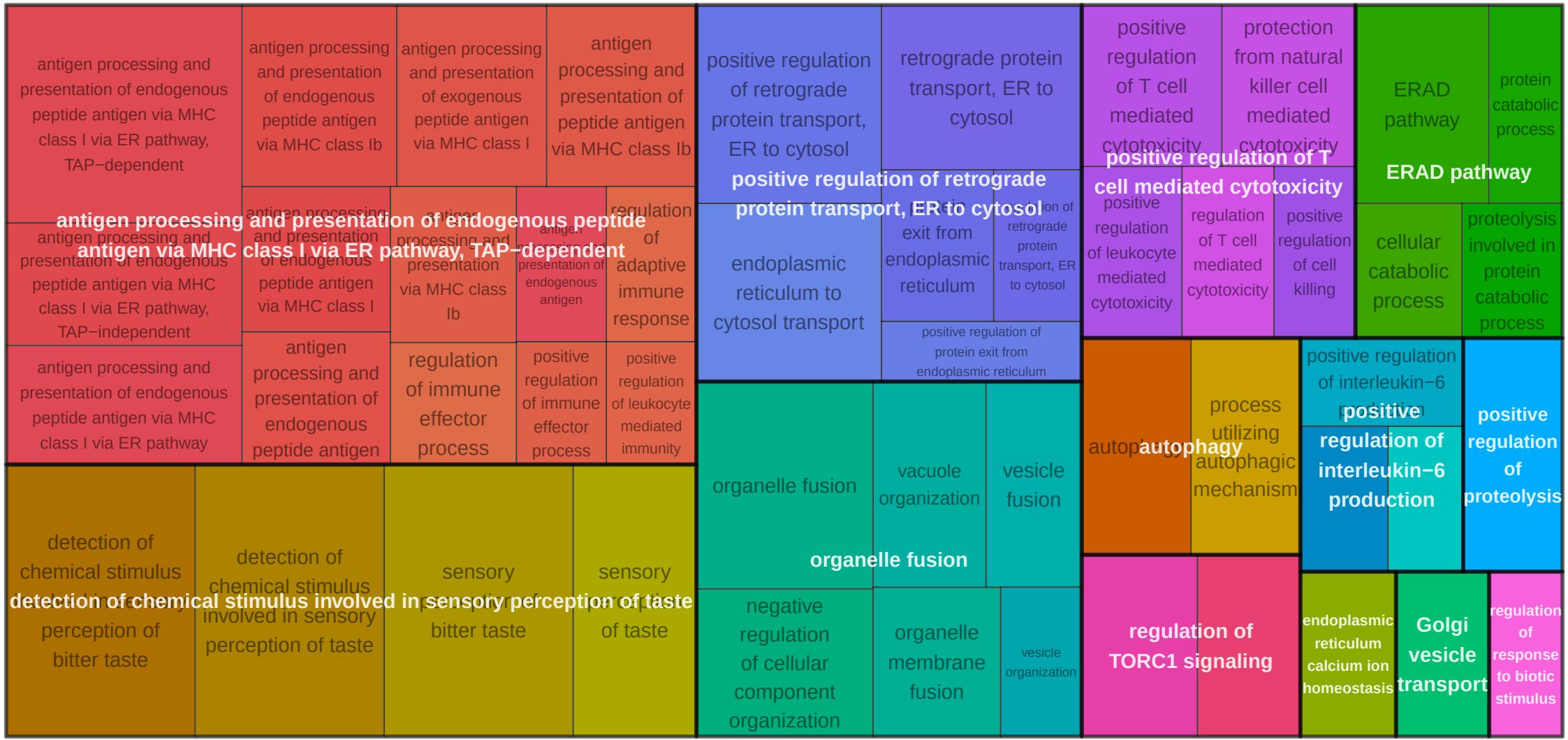
antigen processing and presentation of endogenous peptide antigen via MHC class I via ER pathway, TAP−dependent
antigen processing and presentation of endogenous peptide antigen via MHC class Ib
antigen processing and presentation of exogenous peptide antigen via MHC class I
antigen processing and presentation of peptide antigen via MHC class Ib
antigen processing and presentation of endogenous peptide antigen via MHC class I via ER pathway, TAP−independent
antigen processing and presentation of endogenous peptide antigen via MHC class I
antigen processing and presentation via MHC class Ib
antigen processing and presentation of endogenous antigen
regulation of adaptive immune response
antigen processing and presentation of endogenous peptide antigen via MHC class I via ER pathway
antigen processing and presentation of endogenous peptide antigen
regulation of immune effector process
positive regulation of immune effector process
positive regulation of leukocyte mediated immunity
antigen processing and presentation of endogenous peptide antigen
antigen processing and presentation of endogenous peptide antigen via MHC class I via ER pathway, TAP−dependent
positive regulation of retrograde protein transport, ER to cytosol
endoplasmic reticulum to cytosol transport
retrograde protein transport, ER to cytosol
positive regulation of protein exit from endoplasmic reticulum
regulation of protein exit from endoplasmic reticulum
retrograde protein transport, ER to cytosol
positive regulation of T cell mediated cytotoxicity
positive regulation of leukocyte mediated cytotoxicity
regulation of T cell mediated cytotoxicity
positive regulation of cell killing
protection from natural killer cell mediated cytotoxicity
ERAD pathway
protein catabolic process
cellular catabolic process
proteolysis involved in protein catabolic process
autophagy
process utilizing autophagic mechanism
positive regulation of interleukin−6 production
positive regulation of proteolysis
detection of chemical stimulus involved in sensory perception of bitter taste
detection of chemical stimulus involved in sensory perception of taste
sensory perception of bitter taste
sensory perception of taste
organelle fusion
vacuole organization
vesicle fusion
negative regulation of cellular component organization
organelle membrane fusion
vesicle organization
regulation of TORC1 signaling
endoplasmic reticulum calcium ion homeostasis
Golgi vesicle transport
regulation of response to biotic stimulus

ME14


defense response to symbiont
regulation of innate immune response
regulation of response to biotic stimulus
innate immune response
regulation of response to external stimulus
positive regulation of response to external stimulus
defense response to symbiont
defense response to other organism
activation of innate immune response
positive regulation of innate immune response
pattern recognition receptor signaling pathway
positive regulation of response to biotic stimulus
response to virus
innate immune response−activating signaling pathway
defense response to virus
positive regulation of pattern recognition receptor signaling pathway
positive regulation of immune system process
activation of immune response
immune response−activating signaling pathway
regulation of immune response
immune response−regulating signaling pathway
positive regulation of production of molecular mediator of immune response
positive regulation of cytokine production involved in immune response
positive regulation of immune system process
production of molecular mediator of immune response
positive regulation of immune effector process
regulation of immune effector process
positive regulation of immune response
immune effector process
cytokine production involved in immune response
regulation of defense response
regulation of defense response
inflammatory response
regulation of inflammatory response
positive regulation of inflammatory response
cytoplasmic pattern recognition receptor signaling pathway
positive regulation of intracellular signal transduction
regulation of canonical NF−kappaB signal transduction
cytoplasmic pattern recognition receptor signaling pathway
canonical NF−kappaB signal transduction
positive regulation of canonical NF−kappaB signal transduction
intracellular receptor signaling pathway
response to cytokine
response to peptide
response to cytokine
cellular response to cytokine stimulus
cytokine−mediated signaling pathway
response to type II interferon
cytokine production
regulation of cytokine production
cytokine production
positive regulation of cytokine production
leukocyte activation
cell activation
leukocyte activation

ME15


leukocyte activation
cell activation
lymphocyte activation
alpha−beta T cell activation
T cell activation
regulation of lymphocyte activation
alpha−beta T cell differentiation involved in immune response
lymphocyte activation involved in immune response
alpha−beta T cell activation involved in immune response
regulation of leukocyte activation
leukocyte activation involved in immune response
leukocyte activation
alpha−beta T cell differentiation
CD4−positive, alpha−beta T cell differentiation
T cell differentiation
CD4−positive, alpha−beta T cell activation
T cell differentiation involved in immune response
CD4−positive, alpha−beta T cell differentiation involved in immune response
regulation of natural killer cell activation
regulation of cell activation
cell activation involved in immune response
T cell activation involved in immune response
natural killer cell activation
adaptive immune response
lymphocyte mediated immunity
regulation of immune response
positive regulation of natural killer cell mediated cytotoxicity
negative regulation of immune system process
immune effector process
natural killer cell mediated cytotoxicity
positive regulation of natural killer cell mediated immunity
positive regulation of lymphocyte mediated immunity
positive regulation of immune system process
adaptive immune response
regulation of lymphocyte mediated immunity
regulation of leukocyte mediated immunity
T cell mediated immunity
leukocyte mediated immunity
natural killer cell mediated immunity
regulation of immune effector process
positive regulation of leukocyte mediated immunity
positive regulation of cell killing
positive regulation of cell killing
leukocyte mediated cytotoxicity
regulation of cell killing
positive regulation of leukocyte mediated cytotoxicity
defense response to other organism
defense response to other organism
innate immune response
regulation of response to external stimulus
granzyme−mediated programmed cell death signaling pathway
cellular defense response

ME16

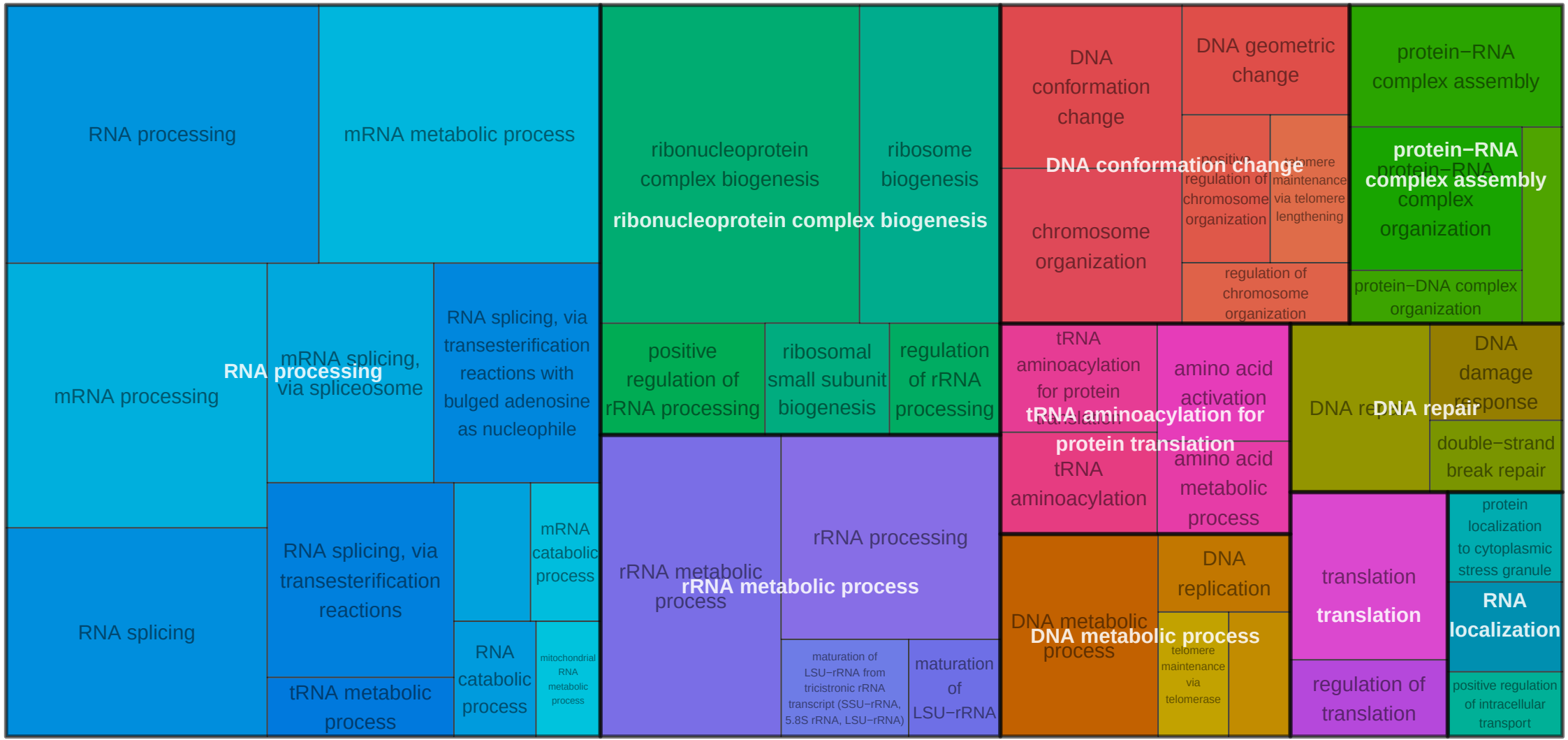
RNA processing
mRNA metabolic process
mRNA processing
RNA processing
mRNA splicing, via spliceosome
RNA splicing, via transesterification reactions with bulged adenosine as nucleophile
RNA splicing
RNA splicing, via transesterification reactions
mRNA catabolic process
RNA catabolic process
mitochondrial RNA metabolic process
tRNA metabolic process
ribonucleoprotein complex biogenesis
ribosome biogenesis
ribonucleoprotein complex biogenesis
positive regulation of rRNA processing
ribosomal small subunit biogenesis
regulation of rRNA processing
rRNA metabolic process
rRNA processing
rRNA metabolic process
maturation of LSU−rRNA from tricistronic rRNA transcript (SSU−rRNA, 5.8S rRNA, LSU−rRNA)
maturation of LSU−rRNA
DNA conformation change
DNA geometric change
DNA conformation change
chromosome organization
positive regulation of chromosome organization
telomere maintenance via telomere lengthening
regulation of chromosome organization
protein−RNA complex assembly
protein−RNA complex organization
protein−RNA complex assembly
protein−DNA complex organization
tRNA aminoacylation for protein translation
amino acid activation
tRNA aminoacylation for protein translation
tRNA aminoacylation
amino acid metabolic process
DNA repair
DNA damage response
DNA repair
double−strand break repair
DNA metabolic process
DNA replication
DNA metabolic process
telomere maintenance via telomerase
translation
translation
regulation of translation
protein localization to cytoplasmic stress granule
RNA localization
positive regulation of intracellular transport

ME18

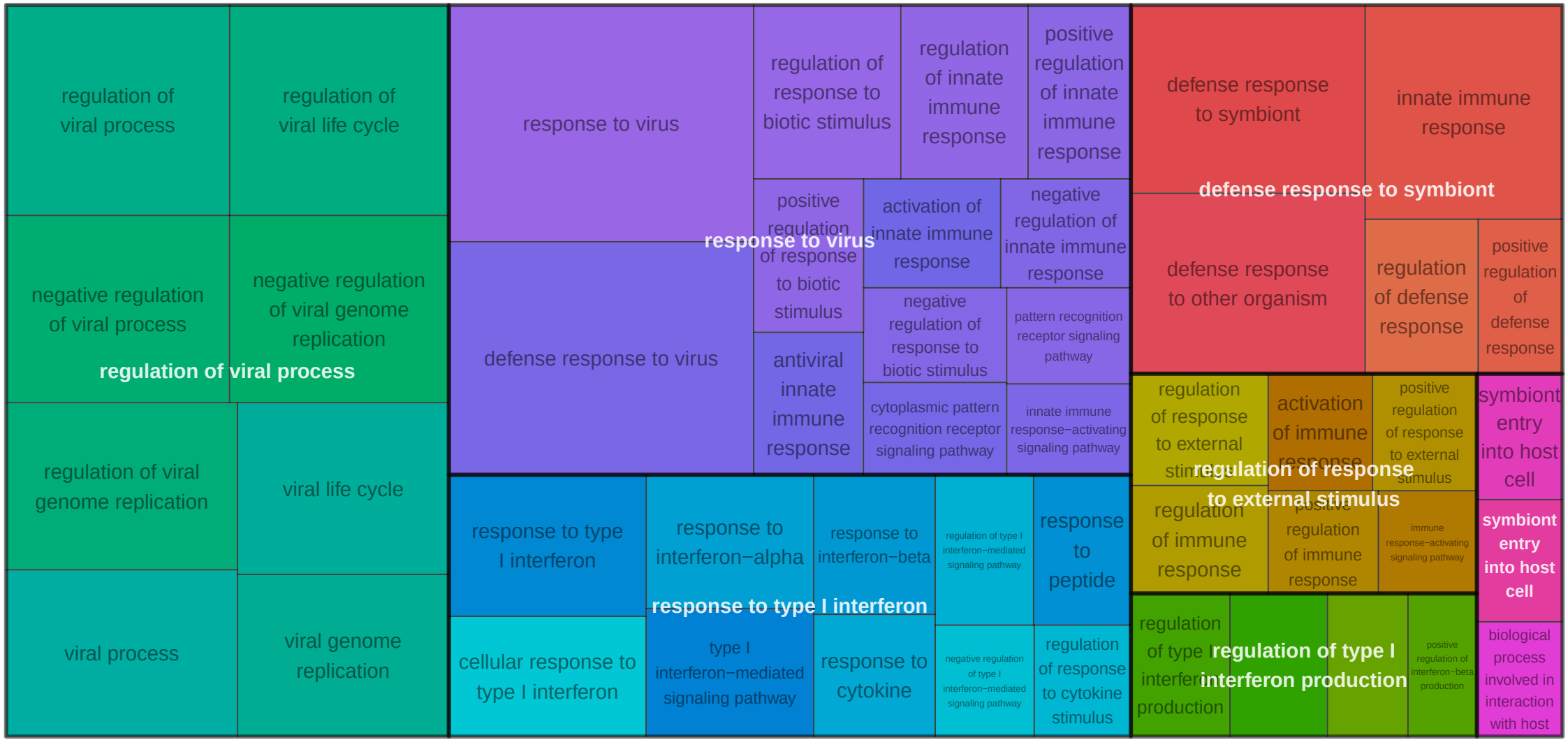
regulation of viral process
regulation of viral life cycle
negative regulation of viral process
negative regulation of viral genome replication
regulation of viral process
regulation of viral genome replication
viral life cycle
viral process
viral genome replication
response to virus
regulation of response to biotic stimulus
regulation of innate immune response
positive regulation of innate immune response
response to virus
positive regulation of response to biotic stimulus
activation of innate immune response
negative regulation of innate immune response
defense response to virus
antiviral innate immune response
negative regulation of response to biotic stimulus
pattern recognition receptor signaling pathway
cytoplasmic pattern recognition receptor signaling pathway
innate immune response−activating signaling pathway
response to type I interferon
response to interferon−alpha
response to interferon−beta
regulation of type I interferon−mediated signaling pathway
response to peptide
response to type I interferon
cellular response to type I interferon
type I interferon−mediated signaling pathway
response to cytokine
negative regulation of type I interferon−mediated signaling pathway
regulation of response to cytokine stimulus
defense response to symbiont
innate immune response
defense response to symbiont
defense response to other organism
regulation of defense response
positive regulation of defense response
regulation of response to external stimulus
activation of immune response
positive regulation of response to external stimulus
regulation of response to external stimulus
regulation of immune response
positive regulation of immune response
immune response−activating signaling pathway
symbiont entry into host cell
symbiont entry into host cell
regulation of type I interferon production
regulation of type I interferon production
positive regulation of interferon−beta production
biological process involved in interaction with host

ME2


homophilic cell adhesion via plasma membrane adhesion molecules
cell−cell adhesion via plasma−membrane adhesion molecules
import across plasma membrane
import across plasma membrane
inorganic ion import across plasma membrane
monoatomic ion transmembrane transport
cell junction organization
detection of stimulus

ME20

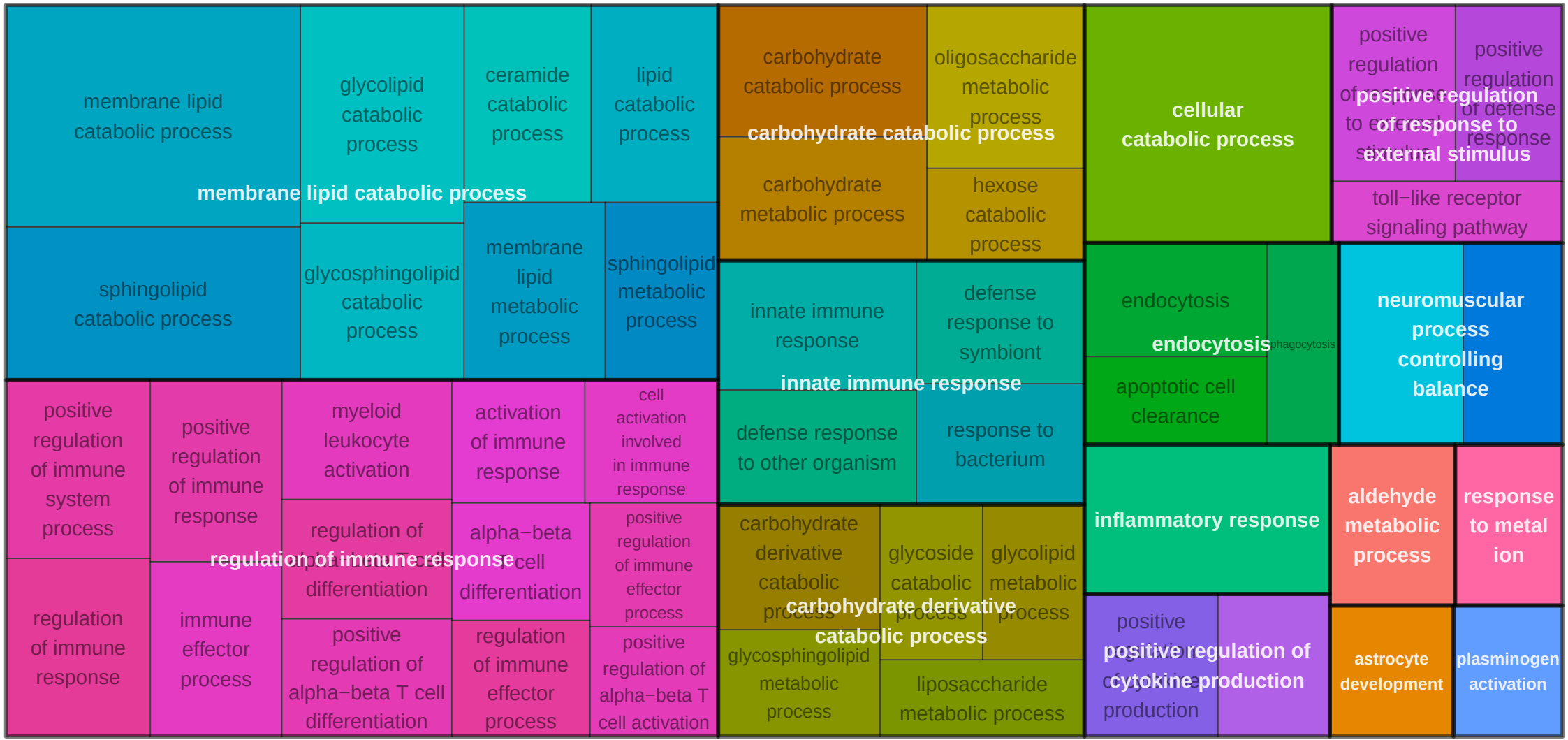
membrane lipid catabolic process
glycolipid catabolic process
ceramide catabolic process
lipid catabolic process
membrane lipid catabolic process
sphingolipid catabolic process
glycosphingolipid catabolic process
membrane lipid metabolic process
sphingolipid metabolic process
carbohydrate catabolic process
oligosaccharide metabolic process
carbohydrate catabolic process
carbohydrate metabolic process
hexose catabolic process
cellular catabolic process
positive regulation of response to external stimulus
positive regulation of defense response
positive regulation of response to external stimulus
toll−like receptor signaling pathway
innate immune response
defense response to symbiont
innate immune response
defense response to other organism
response to bacterium
endocytosis
endocytosis
phagocytosis
apoptotic cell clearance
neuromuscular process controlling balance
positive regulation of immune system process
positive regulation of immune response
myeloid leukocyte activation
activation of immune response
cell activation involved in immune response
regulation of immune response
regulation of alpha−beta T cell differentiation
alpha−beta T cell differentiation
positive regulation of immune effector process
regulation of immune response
immune effector process
positive regulation of alpha−beta T cell differentiation
regulation of immune effector process
positive regulation of alpha−beta T cell activation
carbohydrate derivative catabolic process
glycoside catabolic process
glycolipid metabolic process
carbohydrate derivative catabolic process
glycosphingolipid metabolic process
liposaccharide metabolic process
inflammatory response
aldehyde metabolic process
response to metal ion
positive regulation of cytokine production
positive regulation of cytokine production
astrocyte development
plasminogen activation

ME21

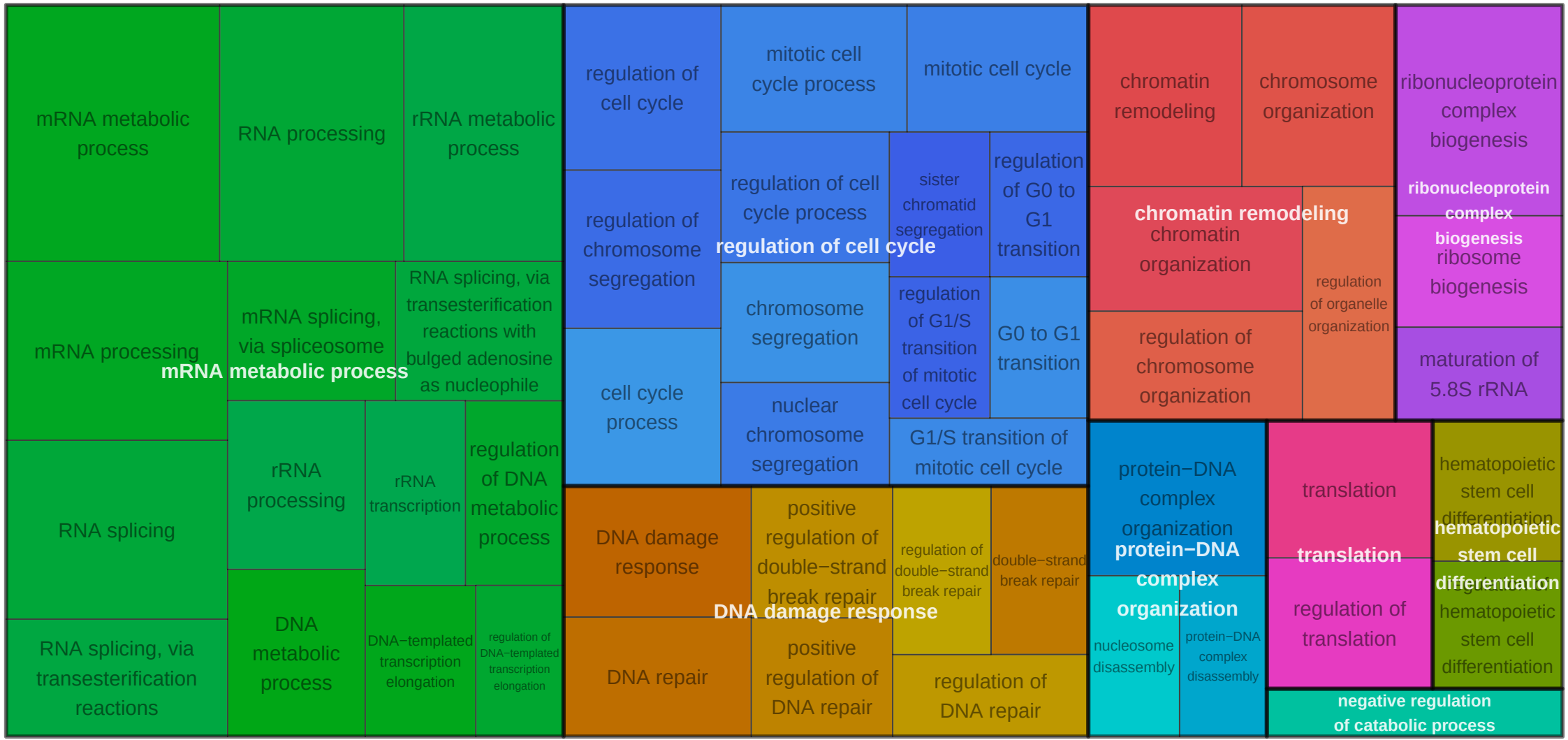
mRNA metabolic process
RNA processing
rRNA metabolic process
mRNA processing
mRNA splicing, via spliceosome
RNA splicing, via transesterification reactions with bulged adenosine as nucleophile
mRNA metabolic process
RNA splicing
rRNA processing
rRNA transcription
regulation of DNA metabolic process
RNA splicing, via transesterification reactions
DNA metabolic process
DNA-templated transcription elongation
regulation of DNA-templated transcription elongation
regulation of cell cycle
mitotic cell cycle process
mitotic cell cycle
regulation of chromosome segregation
regulation of cell cycle process
regulation of cell cycle
sister chromatid segregation
regulation of G0 to G1 transition
cell cycle process
chromosome segregation
regulation of G1/S transition of mitotic cell cycle
G0 to G1 transition
nuclear chromosome segregation
G1/S transition of mitotic cell cycle
DNA damage response
positive regulation of double-strand break repair
regulation of double-strand break repair
double-strand break repair
DNA repair
positive regulation of DNA repair
regulation of DNA repair
chromatin remodeling
chromosome organization
chromatin remodeling
chromatin organization
regulation of organelle organization
regulation of chromosome organization
ribonucleoprotein complex biogenesis
ribonucleoprotein complex biogenesis
ribosome biogenesis
maturation of 5.8S rRNA
protein-DNA complex organization
protein-DNA complex organization
nucleosome disassembly
protein-DNA complex disassembly
translation
translation
regulation of translation
hematopoietic stem cell differentiation
hematopoietic stem cell differentiation
hematopoietic stem cell differentiation
negative regulation of catabolic process

ME22

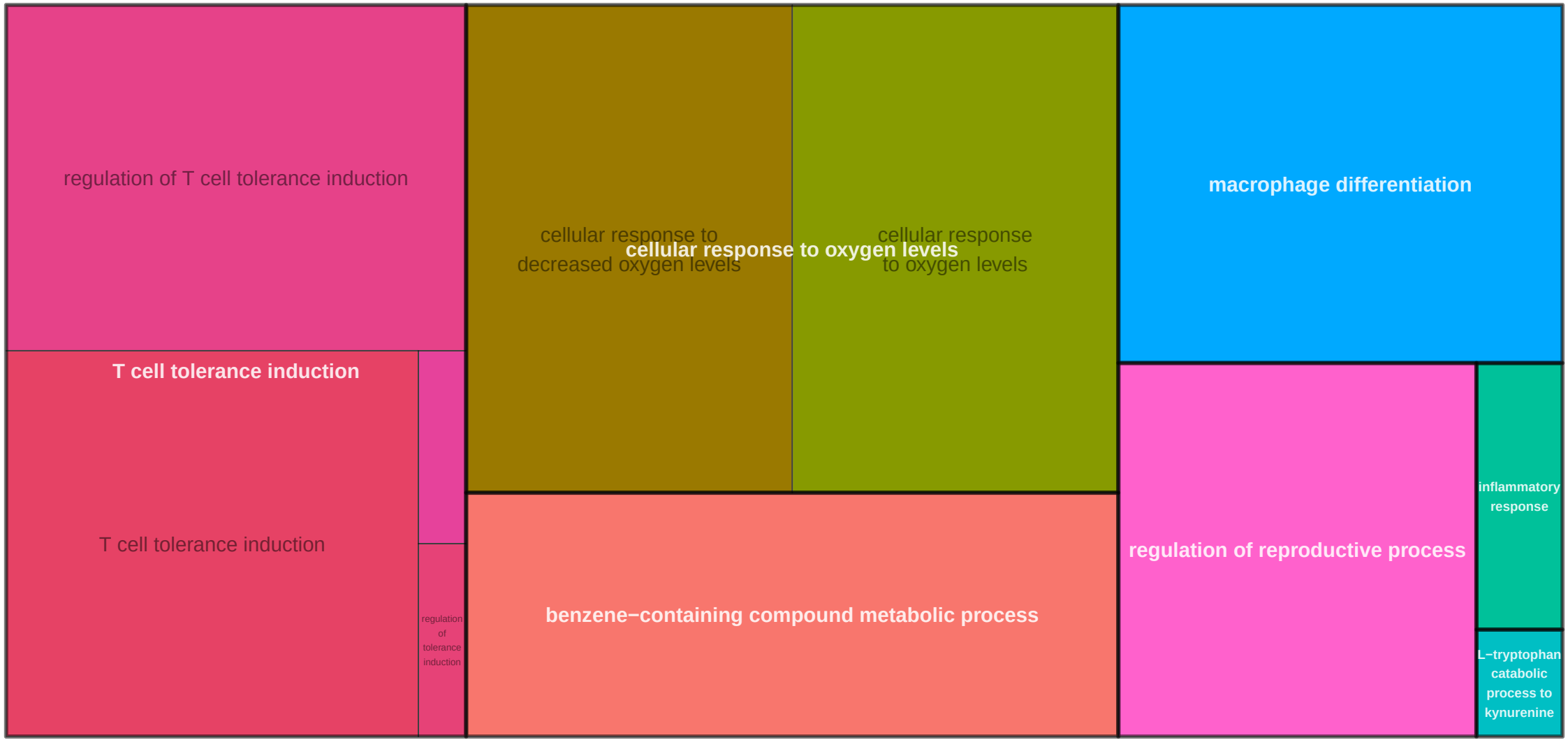
regulation of T cell tolerance induction
T cell tolerance induction
T cell tolerance induction
regulation of tolerance induction
cellular response to decreased oxygen levels
cellular response to oxygen levels
cellular response to oxygen levels
benzene−containing compound metabolic process
macrophage differentiation
regulation of reproductive process
inflammatory response
L−tryptophan catabolic process to kynurenine

ME24


adaptive immune response
B cell mediated immunity
adaptive immune response based on somatic recombination of immune receptors built from immunoglobulin superfamily domains
production of molecular mediator of immune response
positive regulation of type I hypersensitivity
regulation of type I hypersensitivity
positive regulation of type II hypersensitivity
positive regulation of type IIa hypersensitivity
type I hypersensitivity
type II hypersensitivity
regulation of type II hypersensitivity
type IIa hypersensitivity
regulation of hypersensitivity
regulation of type IIa hypersensitivity
positive regulation of acute inflammatory response to antigenic stimulus
hypersensitivity
adaptive immune response
lymphocyte mediated immunity
immune effector process
protein folding
protein maturation
protein folding
response to endoplasmic reticulum stress
ERAD pathway
response to endoplasmic reticulum stress
chaperone−mediated protein folding
protein folding in endoplasmic reticulum
response to topologically incorrect protein
response to topologically incorrect protein
regulation of response to endoplasmic reticulum stress
immunoglobulin mediated immune response
immunoglobulin production
leukocyte mediated immunity
B cell receptor signaling pathway
complement activation, classical pathway
complement activation
antimicrobial humoral response
antibacterial humoral response
antigen receptor−mediated signaling pathway
protein exit from endoplasmic reticulum
protein localization to endoplasmic reticulum
vesicle−mediated transport between endosomal compartments
protein exit from endoplasmic reticulum
protein targeting to ER
reticulum to cytosol transport

ME25

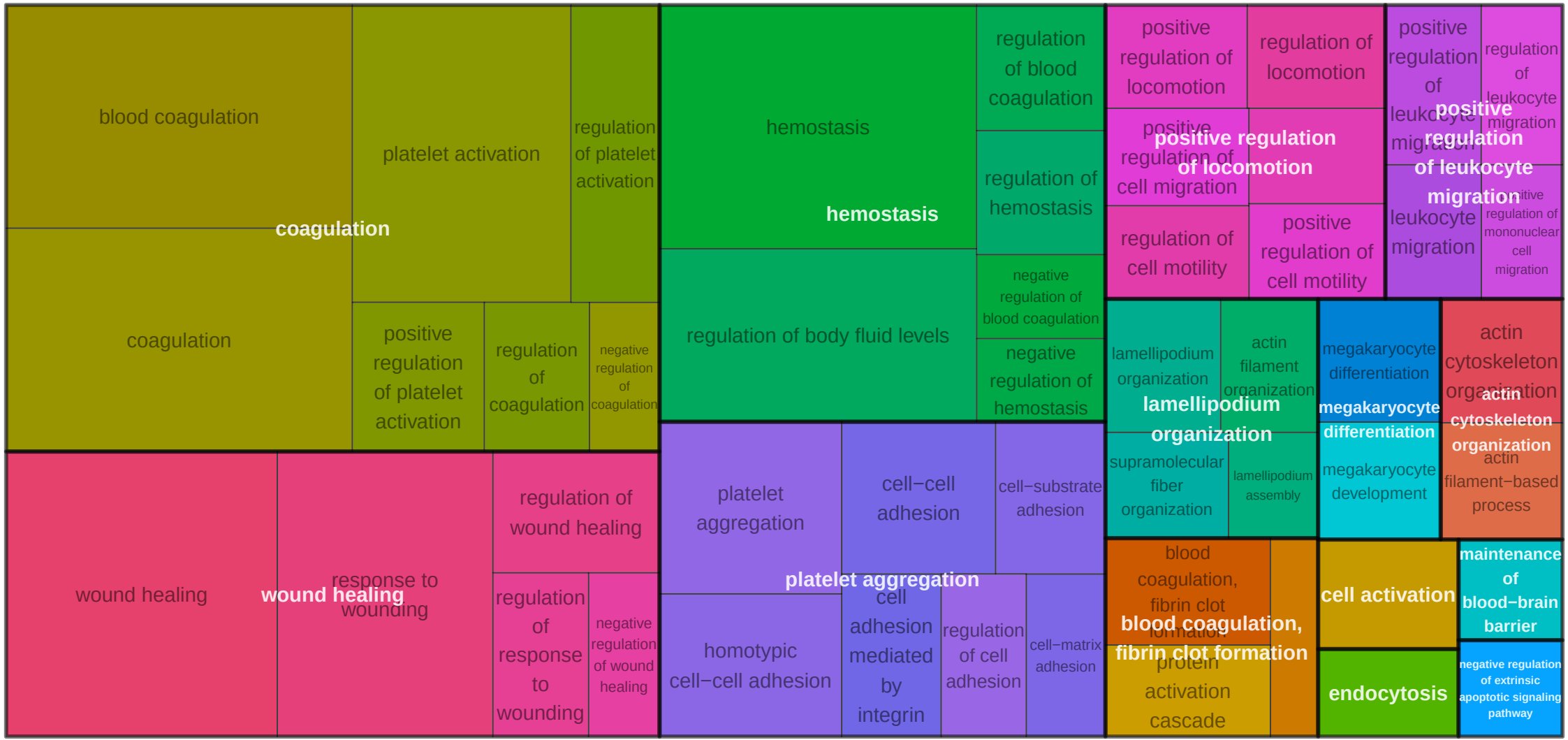
blood coagulation
platelet activation
regulation of platelet activation
coagulation
coagulation
positive regulation of platelet activation
regulation of coagulation
negative regulation of coagulation
hemostasis
hemostasis
regulation of blood coagulation
regulation of hemostasis
regulation of body fluid levels
negative regulation of blood coagulation
negative regulation of hemostasis
positive regulation of locomotion
regulation of locomotion
positive regulation of cell migration
positive regulation of locomotion
regulation of cell motility
positive regulation of cell motility
positive regulation of leukocyte migration
regulation of leukocyte migration
positive regulation of leukocyte migration
leukocyte migration
positive regulation of mononuclear cell migration
lamellipodium organization
actin filament organization
lamellipodium organization
supramolecular fiber organization
lamellipodium assembly
megakaryocyte differentiation
megakaryocyte differentiation
megakaryocyte development
actin cytoskeleton organization
actin cytoskeleton organization
actin filament−based process
wound healing
response to wounding
wound healing
regulation of wound healing
regulation of response to wounding
negative regulation of wound healing
platelet aggregation
cell−cell adhesion
cell−substrate adhesion
platelet aggregation
homotypic cell−cell adhesion
cell adhesion mediated by integrin
regulation of cell adhesion
cell−matrix adhesion
blood coagulation, fibrin clot formation
blood coagulation, fibrin clot formation
protein activation cascade
cell activation
maintenance of blood−brain barrier
endocytosis
negative regulation of extrinsic apoptotic signaling pathway

ME26


defense response to other organism
regulation of response to biotic stimulus
innate immune response
defense response to symbiont
negative regulation of response to biotic stimulus
negative regulation of innate immune response
xenophagy
defense response to Gram−positive bacterium
defense response to bacterium
defense response to protozoan
regulation of response to external stimulus
response to bacterium
response to protozoan
response to virus
regulation of innate immune response
defense response to virus
regulation of defense response to virus
response to molecule of bacterial origin
negative regulation of response to external stimulus
regulation of immune response
positive regulation of immune response
positive regulation of immune system process
antigen processing and presentation
negative regulation of immune system process
activation of immune response
negative regulation of immune response
immune response−activating signaling pathway
response to cytokine
response to peptide
response to type II interferon
cellular response to cytokine stimulus
cellular response to interferon−beta
cellular response to type II interferon
cytokine−mediated signaling pathway
response to interferon−beta
regulation of defense response
pyroptotic inflammatory response
positive regulation of defense response
negative regulation of defense response
cytolysis in another organism
cytolysis
cell killing
killing of cells of another organism
adhesion of symbiont to host

ME28

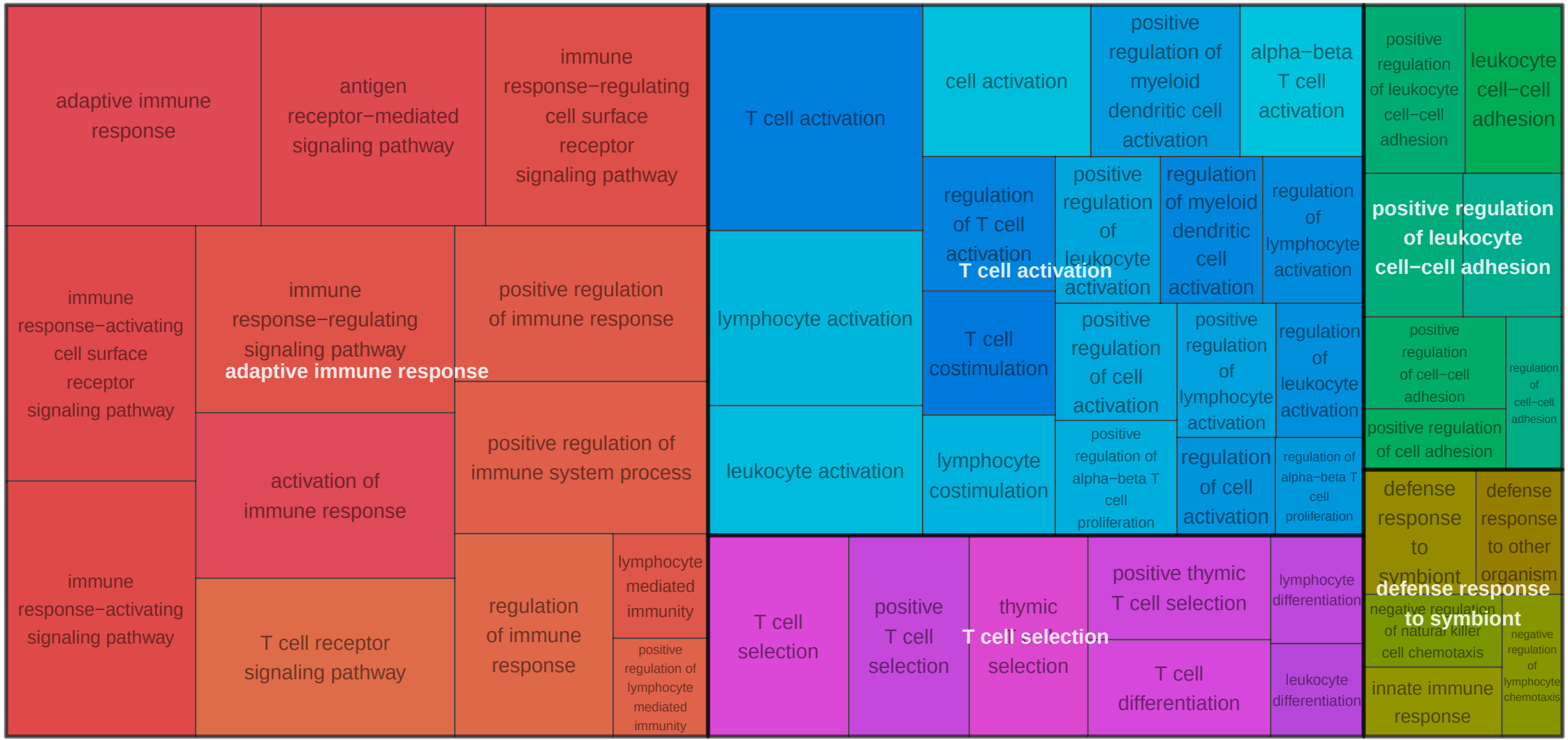
adaptive immune response
antigen receptor−mediated signaling pathway
immune response−regulating cell surface receptor signaling pathway
immune response−activating cell surface receptor signaling pathway
immune response−regulating signaling pathway
positive regulation of immune response
adaptive immune response
activation of immune response
positive regulation of immune system process
immune response−activating signaling pathway
T cell receptor signaling pathway
regulation of immune response
lymphocyte mediated immunity
positive regulation of lymphocyte mediated immunity
T cell activation
cell activation
positive regulation of myeloid dendritic cell activation
alpha−beta T cell activation
regulation of T cell activation
positive regulation of leukocyte activation
regulation of myeloid dendritic cell activation
regulation of lymphocyte activation
T cell activation
lymphocyte activation
T cell costimulation
positive regulation of cell activation
positive regulation of lymphocyte activation
regulation of leukocyte activation
leukocyte activation
lymphocyte costimulation
positive regulation of alpha−beta T cell proliferation
regulation of cell activation
regulation of alpha−beta T cell proliferation
positive regulation of leukocyte cell−cell adhesion
leukocyte cell−cell adhesion
positive regulation of leukocyte cell−cell adhesion
positive regulation of cell−cell adhesion
regulation of cell−cell adhesion
positive regulation of cell adhesion
T cell selection
positive T cell selection
thymic selection
T cell selection
positive thymic T cell selection
lymphocyte differentiation
T cell differentiation
leukocyte differentiation
defense response to symbiont
defense response to other organism
defense response to symbiont
negative regulation of natural killer cell chemotaxis
negative regulation of lymphocyte chemotaxis
innate immune response

ME3

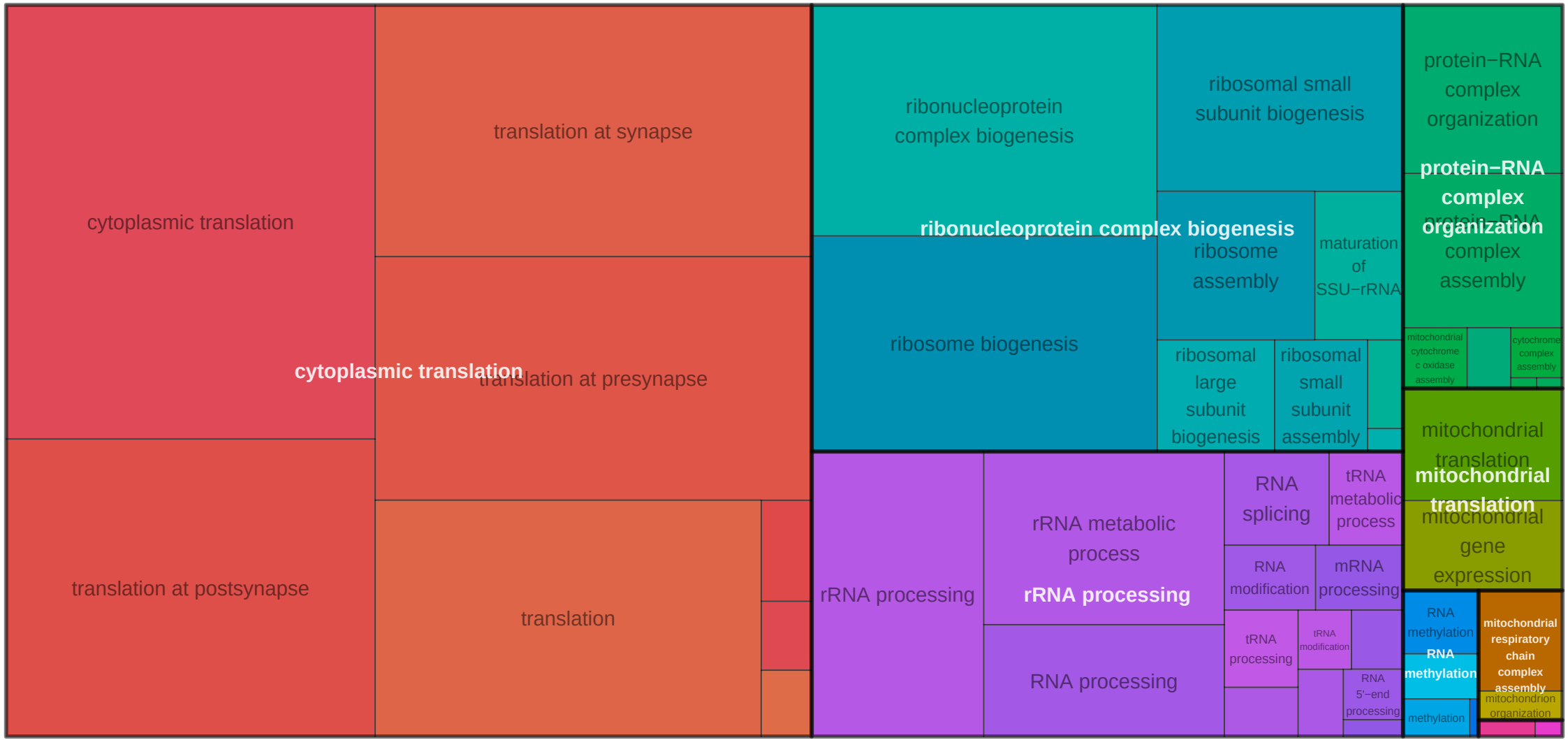
cytoplasmic translation
translation at synapse
cytoplasmic translation
translation at presynapse
translation at postsynapse
translation
ribonucleoprotein complex biogenesis
ribosomal small subunit biogenesis
ribonucleoprotein complex biogenesis
ribosome assembly
maturation of SSU−rRNA
ribosome biogenesis
ribosomal large subunit biogenesis
ribosomal small subunit assembly
protein−RNA complex organization
protein−RNA complex organization
protein−RNA complex assembly
mitochondrial cytochrome c oxidase assembly
cytochrome complex assembly
mitochondrial translation
mitochondrial translation
mitochondrial gene expression
rRNA processing
rRNA metabolic process
rRNA processing
RNA processing
RNA splicing
tRNA metabolic process
RNA modification
mRNA processing
tRNA processing
tRNA modification
RNA 5'−end processing
RNA methylation
RNA methylation
methylation
mitochondrial respiratory chain complex assembly
mitochondrion organization

ME32


nuclear transport
nucleocytoplasmic transport
nucleocytoplasmic transport

ME33

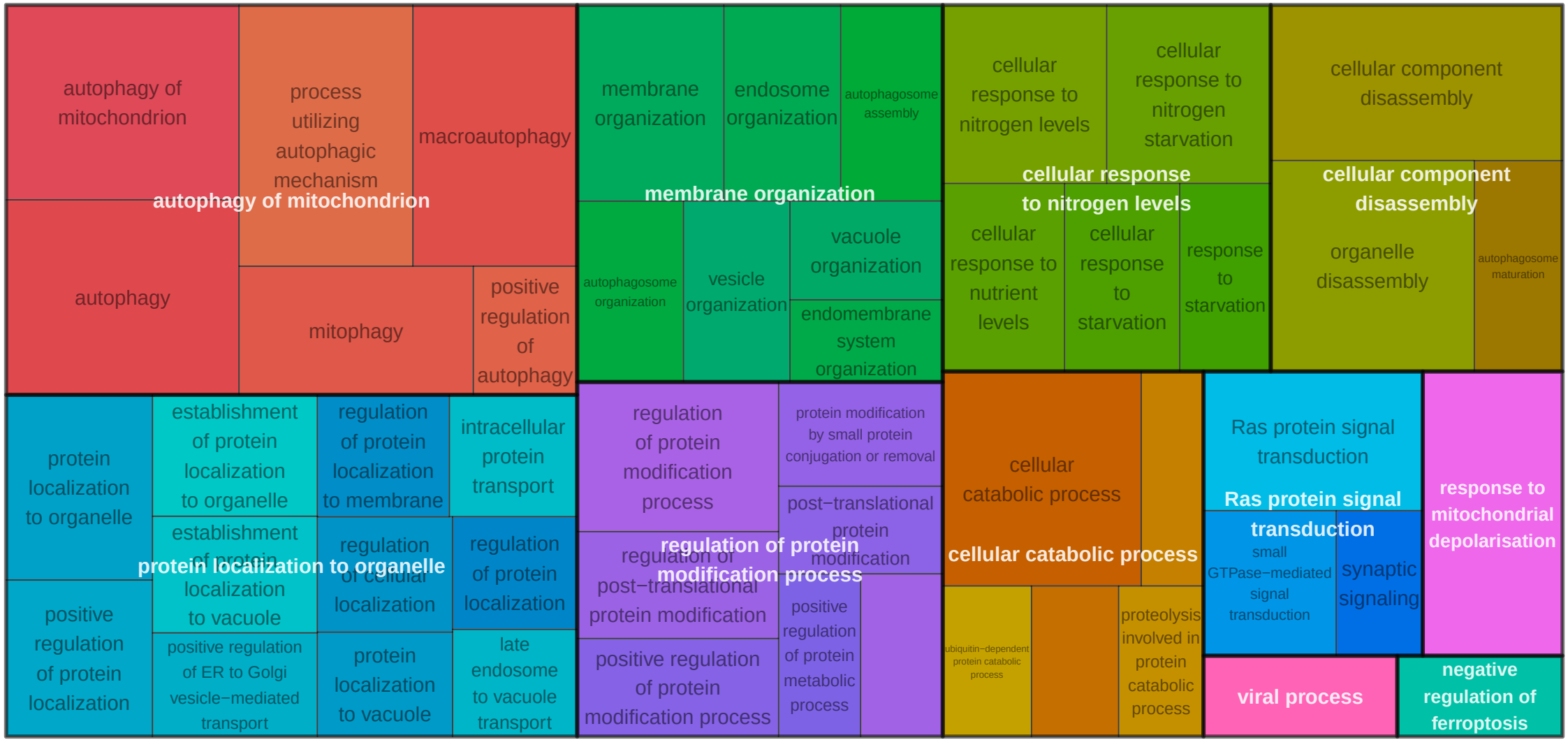
autophagy of mitochondrion
process utilizing autophagic mechanism
macroautophagy
autophagy
mitophagy
positive regulation of autophagy
autophagy of mitochondrion
membrane organization
endosome organization
autophagosome assembly
autophagosome organization
vesicle organization
vacuole organization
endomembrane system organization
membrane organization
cellular response to nitrogen levels
cellular response to nitrogen starvation
cellular response to nutrient levels
cellular response to starvation
response to starvation
cellular response to nitrogen levels
cellular component disassembly
organelle disassembly
autophagosome maturation
cellular component disassembly
protein localization to organelle
establishment of protein localization to organelle
regulation of protein localization to membrane
intracellular protein transport
establishment of protein localization to vacuole
regulation of cellular localization
regulation of protein localization
positive regulation of protein localization
positive regulation of ER to Golgi vesicle−mediated transport
protein localization to vacuole
late endosome to vacuole transport
protein localization to organelle
regulation of protein modification process
protein modification by small protein conjugation or removal
regulation of post−translational protein modification
post−translational protein modification
positive regulation of protein modification process
positive regulation of protein metabolic process
regulation of protein modification process
cellular catabolic process
ubiquitin−dependent protein catabolic process
proteolysis involved in protein catabolic process
cellular catabolic process
Ras protein signal transduction
small GTPase−mediated signal transduction
synaptic signaling
Ras protein signal transduction
response to mitochondrial depolarisation
viral process
negative regulation of ferroptosis

ME34

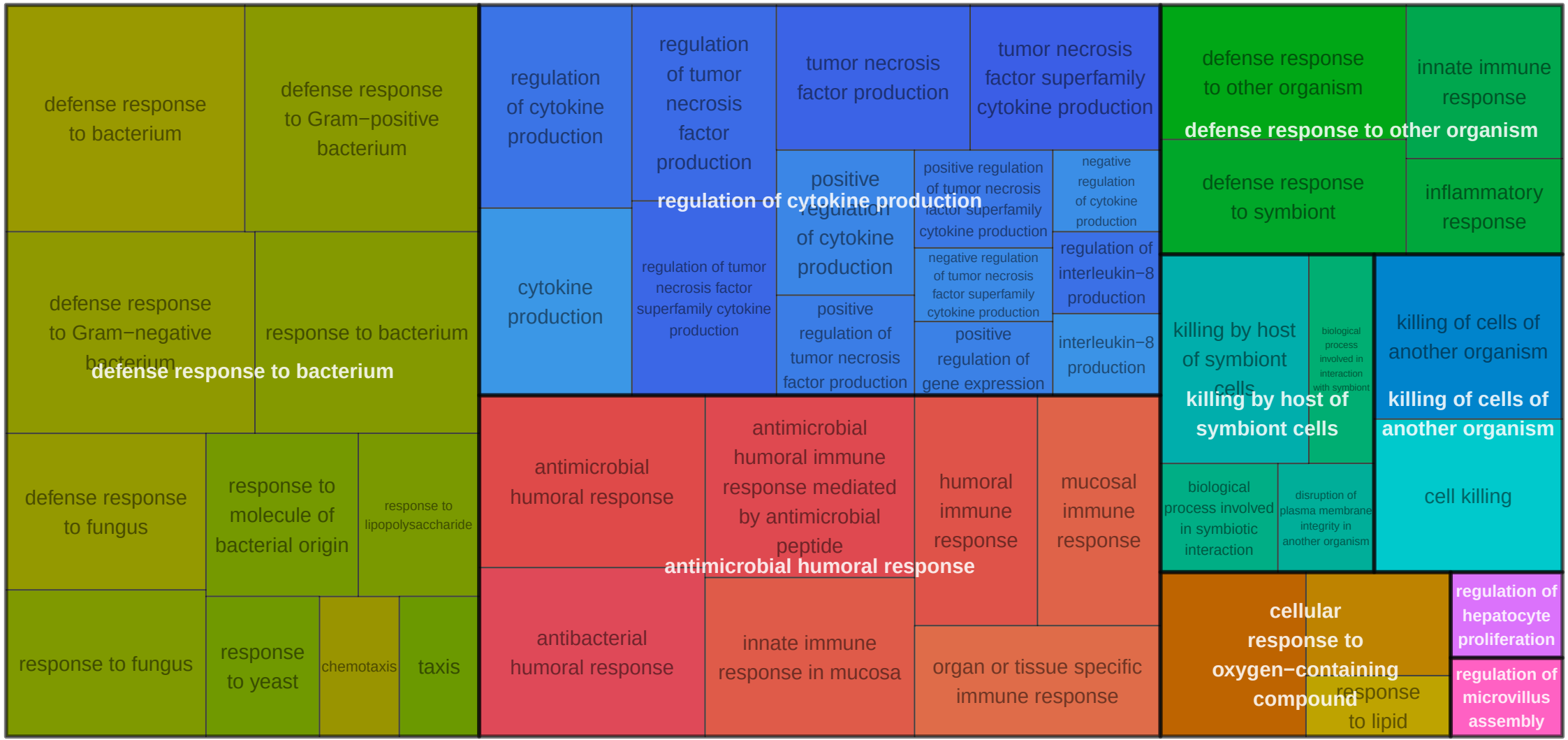
defense response to bacterium
defense response to Gram−positive bacterium
defense response to Gram−negative bacterium
response to bacterium
defense response to bacterium
defense response to fungus
response to molecule of bacterial origin
response to lipopolysaccharide
response to fungus
response to yeast
chemotaxis
taxis
regulation of cytokine production
regulation of tumor necrosis factor production
tumor necrosis factor production
tumor necrosis factor superfamily cytokine production
cytokine production
regulation of tumor necrosis factor superfamily cytokine production
positive regulation of cytokine production
positive regulation of tumor necrosis factor superfamily cytokine production
negative regulation of cytokine production
regulation of cytokine production
negative regulation of tumor necrosis factor superfamily cytokine production
regulation of interleukin−8 production
positive regulation of tumor necrosis factor production
positive regulation of gene expression
interleukin−8 production
antimicrobial humoral response
antimicrobial humoral immune response mediated by antimicrobial peptide
humoral immune response
mucosal immune response
antimicrobial humoral response
antibacterial humoral response
innate immune response in mucosa
organ or tissue specific immune response
defense response to other organism
innate immune response
defense response to other organism
defense response to symbiont
inflammatory response
killing by host of symbiont cells
biological process involved in interaction with symbiont
killing by host of symbiont cells
killing of cells of another organism
killing of cells of another organism
biological process involved in symbiotic interaction
disruption of plasma membrane integrity in another organism
cell killing
cellular response to oxygen−containing compound
response to lipid
regulation of hepatocyte proliferation
regulation of microvillus assembly

ME38

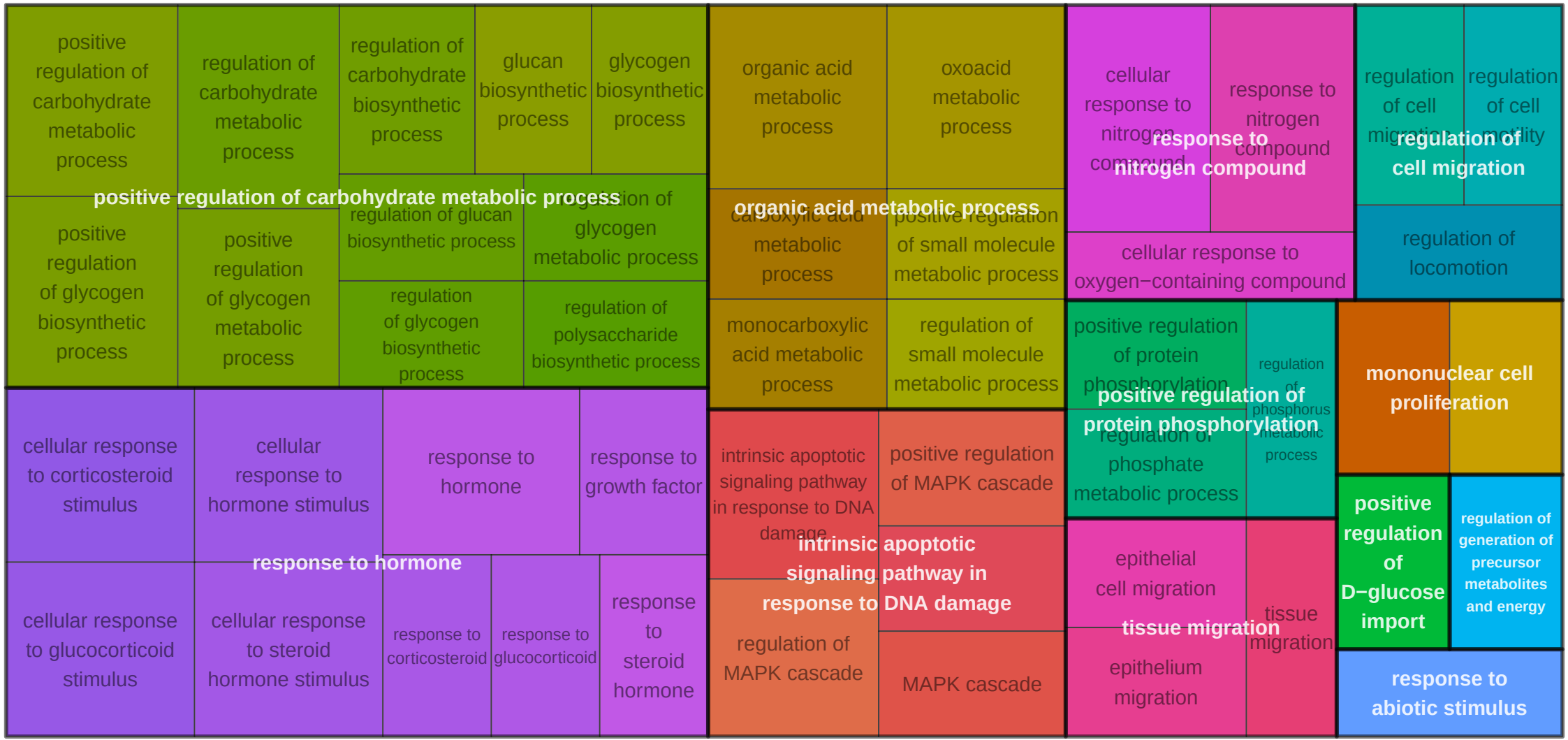
positive regulation of carbohydrate metabolic process
regulation of carbohydrate metabolic process
regulation of carbohydrate biosynthetic process
glucan biosynthetic process
glycogen biosynthetic process
positive regulation of glycogen biosynthetic process
positive regulation of glycogen metabolic process
regulation of glucan biosynthetic process
regulation of glycogen metabolic process
regulation of glycogen biosynthetic process
regulation of polysaccharide biosynthetic process
organic acid metabolic process
oxoacid metabolic process
carboxylic acid metabolic process
positive regulation of small molecule metabolic process
monocarboxylic acid metabolic process
regulation of small molecule metabolic process
cellular response to nitrogen compound
response to nitrogen compound
cellular response to oxygen−containing compound
regulation of cell migration
regulation of cell motility
regulation of locomotion
positive regulation of protein phosphorylation
regulation of phosphate metabolic process
mononuclear cell proliferation
cellular response to corticosteroid stimulus
cellular response to hormone stimulus
response to hormone
response to growth factor
cellular response to glucocorticoid stimulus
cellular response to steroid hormone stimulus
response to corticosteroid
response to glucocorticoid
response to steroid hormone
intrinsic apoptotic signaling pathway in response to DNA damage
positive regulation of MAPK cascade
regulation of MAPK cascade
MAPK cascade
epithelial cell migration
tissue migration
epithelium migration
positive regulation of D−glucose import
regulation of generation of precursor metabolites and energy
response to abiotic stimulus

ME4

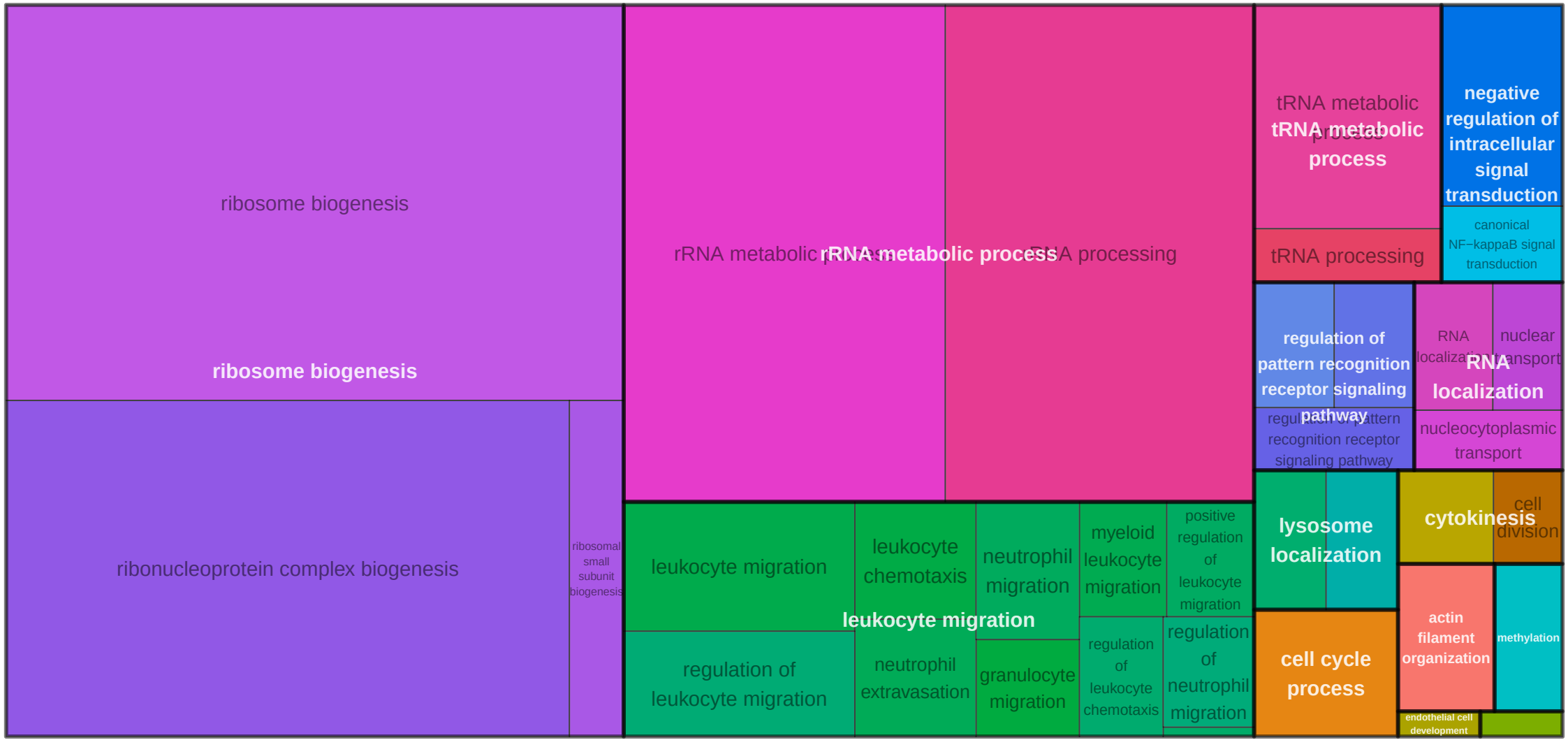
ribosome biogenesis
ribosome biogenesis
ribonucleoprotein complex biogenesis
ribosomal small subunit biogenesis
rRNA metabolic process
rRNA metabolic process
RNA processing
tRNA metabolic process
tRNA metabolic process
tRNA processing
negative regulation of intracellular signal transduction
canonical NF−kappaB signal transduction
regulation of pattern recognition receptor signaling pathway
regulation of pattern recognition receptor signaling pathway
RNA localization
nuclear transport
RNA localization
nucleocytoplasmic transport
leukocyte migration
leukocyte chemotaxis
neutrophil migration
myeloid leukocyte migration
positive regulation of leukocyte migration
leukocyte migration
regulation of leukocyte migration
neutrophil extravasation
granulocyte migration
regulation of leukocyte chemotaxis
regulation of neutrophil migration
lysosome localization
cytokinesis
cell division
cell cycle process
actin filament organization
methylation
endothelial cell development

ME40

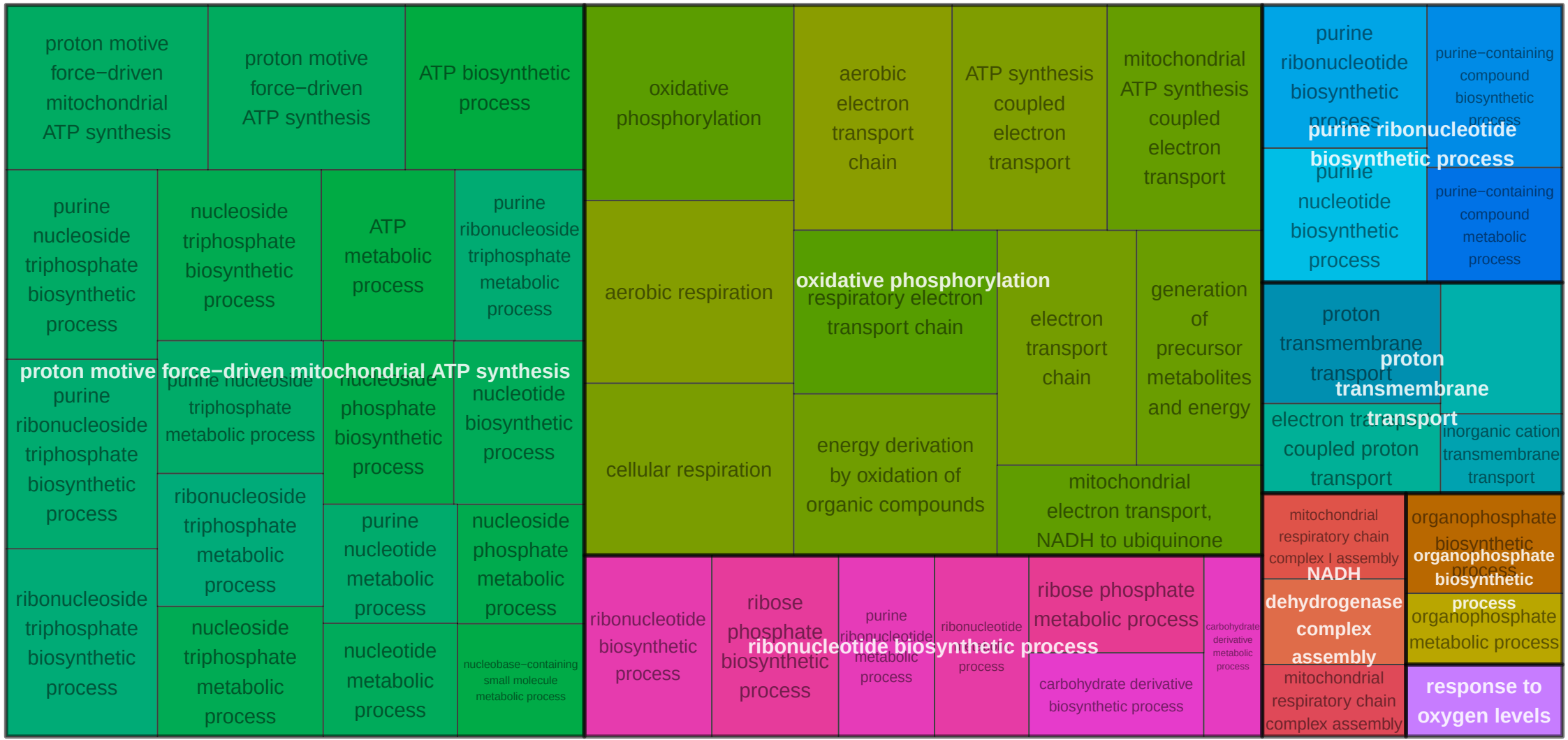
proton motive force−driven mitochondrial ATP synthesis
proton motive force−driven ATP synthesis
ATP biosynthetic process
purine nucleoside triphosphate biosynthetic process
nucleoside triphosphate biosynthetic process
ATP metabolic process
purine ribonucleoside triphosphate metabolic process
purine ribonucleoside triphosphate biosynthetic process
purine nucleoside triphosphate metabolic process
nucleoside phosphate biosynthetic process
nucleotide biosynthetic process
ribonucleoside triphosphate biosynthetic process
ribonucleoside triphosphate metabolic process
purine nucleotide metabolic process
nucleoside phosphate metabolic process
nucleoside triphosphate metabolic process
nucleotide metabolic process
nucleobase−containing small molecule metabolic process
oxidative phosphorylation
aerobic electron transport chain
ATP synthesis coupled electron transport
mitochondrial ATP synthesis coupled electron transport
aerobic respiration
oxidative phosphorylation
respiratory electron transport chain
electron transport chain
generation of precursor metabolites and energy
cellular respiration
energy derivation by oxidation of organic compounds
mitochondrial electron transport, NADH to ubiquinone
ribonucleotide biosynthetic process
ribose phosphate biosynthetic process
purine ribonucleotide metabolic process
ribonucleotide metabolic process
ribose phosphate metabolic process
carbohydrate derivative metabolic process
carbohydrate derivative biosynthetic process
ribonucleotide biosynthetic process
purine ribonucleotide biosynthetic process
purine−containing compound biosynthetic process
purine nucleotide biosynthetic process
purine−containing compound metabolic process
proton transmembrane transport
proton transmembrane transport
inorganic cation transmembrane transport
mitochondrial respiratory chain complex I assembly
organophosphate biosynthetic process
NADH dehydrogenase complex assembly
organophosphate biosynthetic process
organophosphate metabolic process
mitochondrial respiratory chain complex assembly
response to oxygen levels

ME7

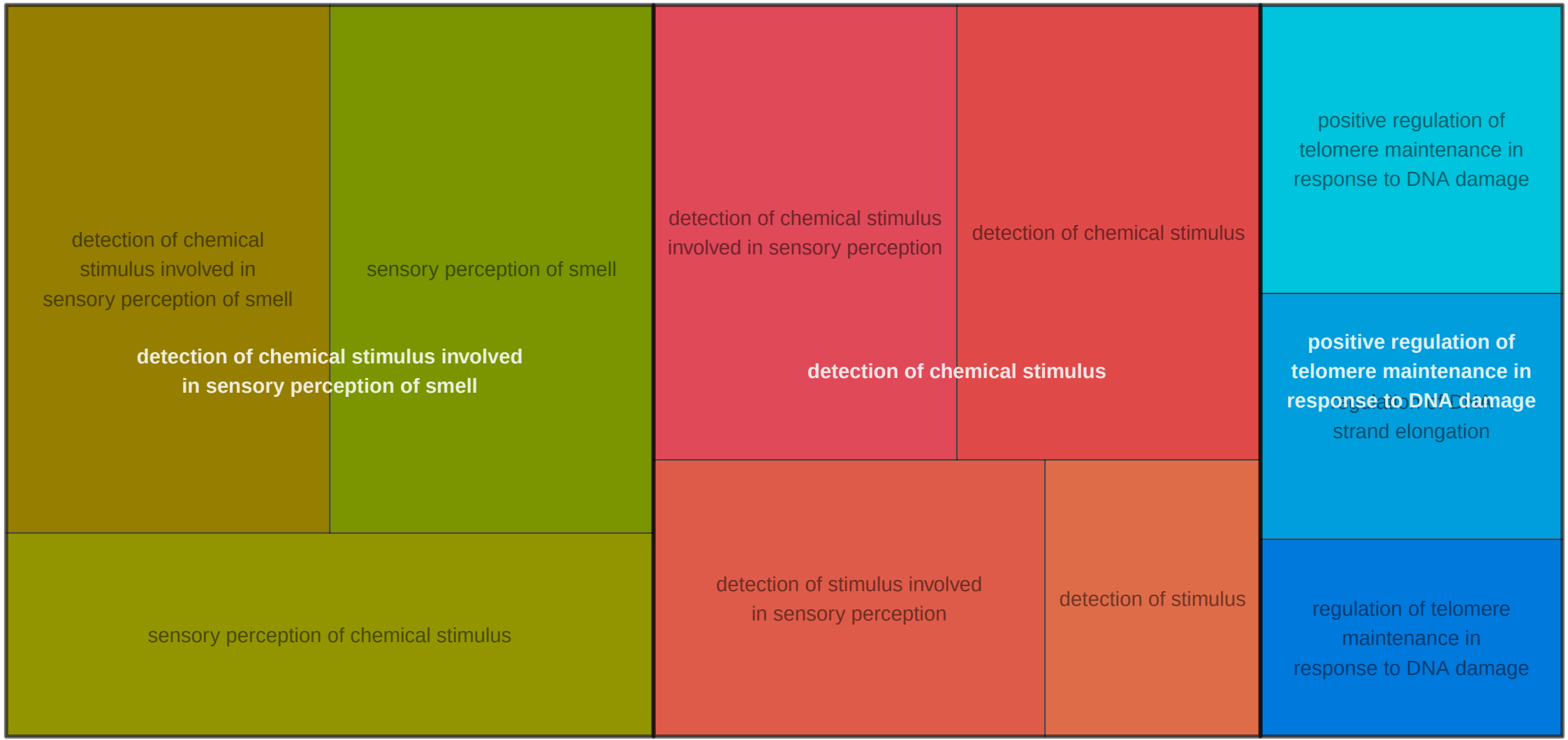
detection of chemical stimulus involved in sensory perception of smell
sensory perception of smell
detection of chemical stimulus involved in sensory perception of smell
sensory perception of chemical stimulus
detection of chemical stimulus involved in sensory perception
detection of chemical stimulus
detection of chemical stimulus
detection of stimulus involved in sensory perception
detection of stimulus
positive regulation of telomere maintenance in response to DNA damage
positive regulation of telomere maintenance in response to DNA damage
strand elongation
regulation of telomere maintenance in response to DNA damage

ME8

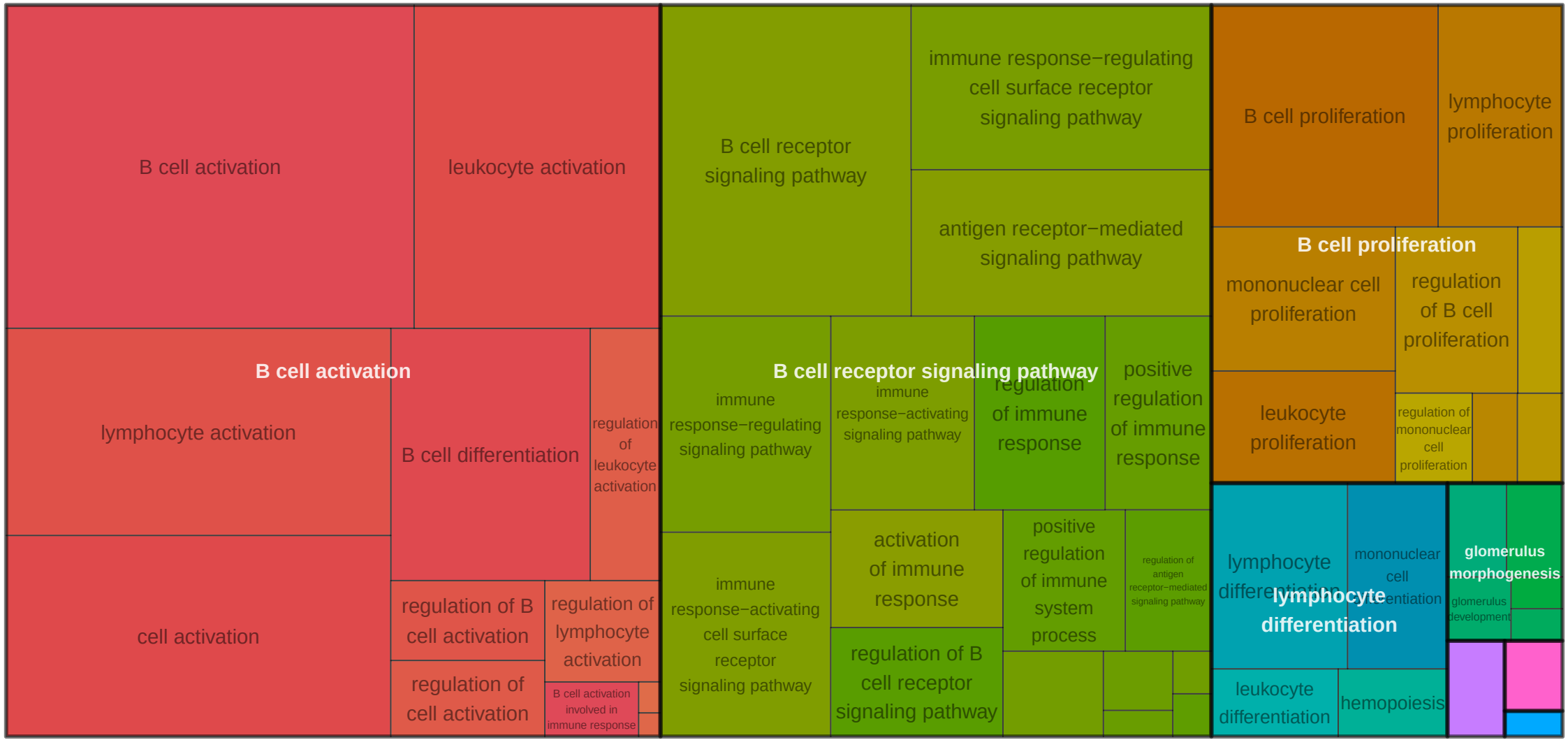
B cell activation
leukocyte activation
B cell receptor signaling pathway
immune response−regulating cell surface receptor signaling pathway
antigen receptor−mediated signaling pathway
B cell proliferation
lymphocyte proliferation
B cell proliferation
mononuclear cell proliferation
regulation of B cell proliferation
leukocyte proliferation
regulation of mononuclear cell proliferation
B cell activation
lymphocyte activation
B cell differentiation
regulation of leukocyte activation
B cell receptor signaling pathway
immune response−regulating signaling pathway
immune response−activating signaling pathway
regulation of immune response
positive regulation of immune response
cell activation
regulation of B cell activation
regulation of lymphocyte activation
regulation of cell activation
B cell activation involved in immune response
immune response−activating cell surface receptor signaling pathway
activation of immune response
positive regulation of immune system process
regulation of antigen receptor−mediated signaling pathway
regulation of B cell receptor signaling pathway
lymphocyte differentiation
mononuclear cell differentiation
lymphocyte differentiation
glomerulus morphogenesis
glomerulus development
leukocyte differentiation
hemopoiesis

ME9

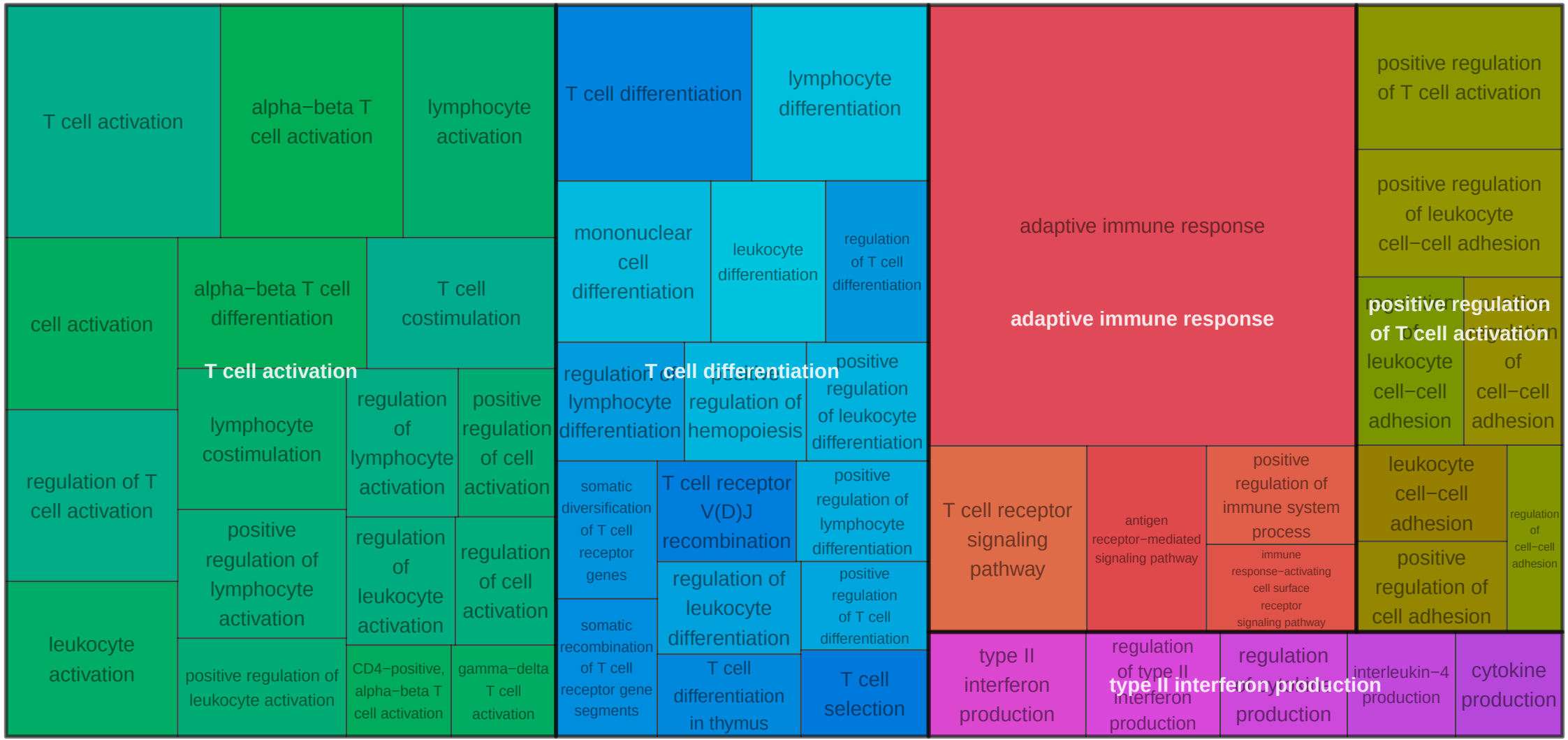
T cell activation
alpha−beta T cell activation
lymphocyte activation
cell activation
alpha−beta T cell differentiation
T cell costimulation
T cell activation
regulation of T cell activation
lymphocyte costimulation
regulation of lymphocyte activation
positive regulation of cell activation
positive regulation of lymphocyte activation
regulation of leukocyte activation
regulation of cell activation
leukocyte activation
positive regulation of leukocyte activation
CD4−positive, alpha−beta T cell activation
gamma−delta T cell activation
T cell differentiation
lymphocyte differentiation
mononuclear cell differentiation
leukocyte differentiation
regulation of T cell differentiation
regulation of lymphocyte differentiation
positive regulation of hemopoiesis
positive regulation of leukocyte differentiation
T cell differentiation
somatic diversification of T cell receptor genes
T cell receptor V(D)J recombination
positive regulation of lymphocyte differentiation
somatic recombination of T cell receptor gene segments
regulation of leukocyte differentiation
positive regulation of T cell differentiation
T cell differentiation in thymus
T cell selection
adaptive immune response
adaptive immune response
T cell receptor signaling pathway
antigen receptor−mediated signaling pathway
positive regulation of immune system process
immune response−activating cell surface receptor signaling pathway
positive regulation of T cell activation
positive regulation of leukocyte cell−cell adhesion
positive regulation of T cell activation
leukocyte cell−cell adhesion
regulation of cell−cell adhesion
leukocyte cell−cell adhesion
positive regulation of cell adhesion
regulation of cell−cell adhesion
type II interferon production
regulation of type II interferon production
regulation of type II interferon production
type II interferon production
interleukin−4 production
cytokine production

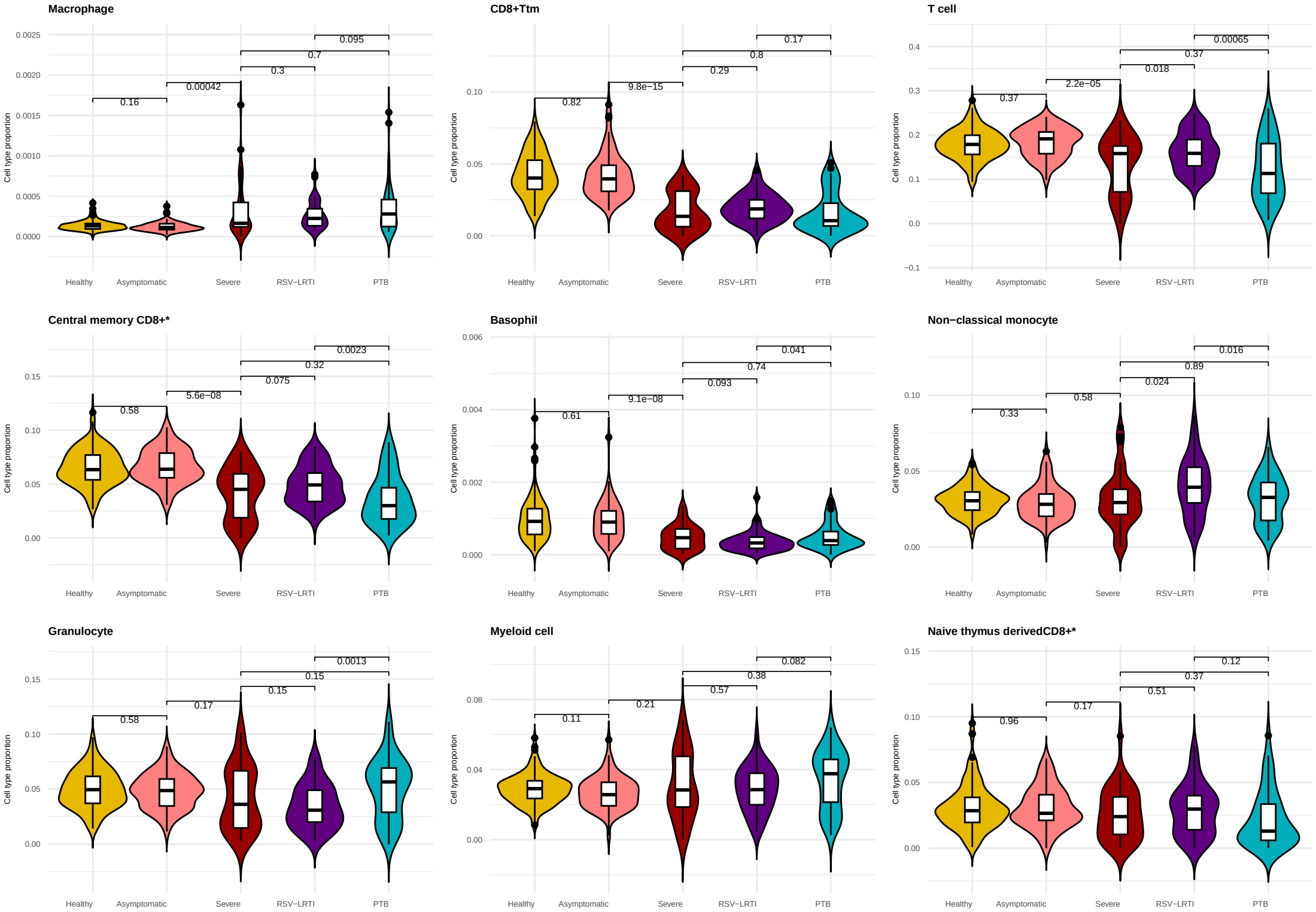
Macrophage
Cell type proportion
0.0025
0.0020
0.0015
0.0010
0.0005
0.0000
0.16
0.00042
0.3
0.7
0.095
Healthy
Asymptomatic
Severe
RSV−LRTI
PTB
CD8+Ttm
Cell type proportion
0.10
0.05
0.00
0.82
9.8e−15
0.29
0.8
0.17
Healthy
Asymptomatic
Severe
RSV−LRTI
PTB
T cell
Cell type proportion
0.4
0.3
0.2
0.1
0.0
−0.1
0.37
2.2e−05
0.018
0.37
0.00065
Healthy
Asymptomatic
Severe
RSV−LRTI
PTB
Central memory CD8+*
Cell type proportion
0.15
0.10
0.05
0.00
0.58
5.6e−08
0.075
0.32
0.0023
Healthy
Asymptomatic
Severe
RSV−LRTI
PTB
Basophil
Cell type proportion
0.006
0.004
0.002
0.000
0.61
9.1e−08
0.093
0.74
0.041
Healthy
Asymptomatic
Severe
RSV−LRTI
PTB
Non−classical monocyte
Cell type proportion
0.10
0.05
0.00
0.33
0.58
0.024
0.89
0.016
Healthy
Asymptomatic
Severe
RSV−LRTI
PTB
Granulocyte
Cell type proportion
0.15
0.10
0.05
0.00
0.58
0.17
0.15
0.15
0.0013
Healthy
Asymptomatic
Severe
RSV−LRTI
PTB
Myeloid cell
Cell type proportion
0.08
0.04
0.00
0.11
0.21
0.57
0.38
0.082
Healthy
Asymptomatic
Severe
RSV−LRTI
PTB
Naive thymus derivedCD8+*
Cell type proportion
0.15
0.10
0.05
0.00
0.96
0.17
0.51
0.37
0.12
Healthy
Asymptomatic
Severe
RSV−LRTI
PTB

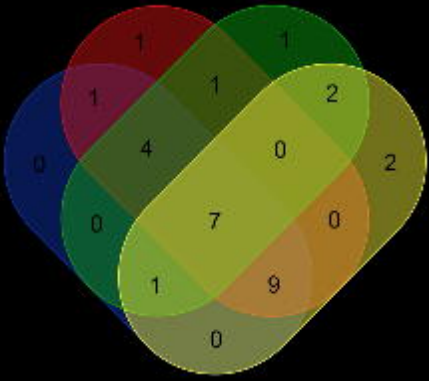
1
1
1
2
0
4
0
2
0
7
0
1
9
0

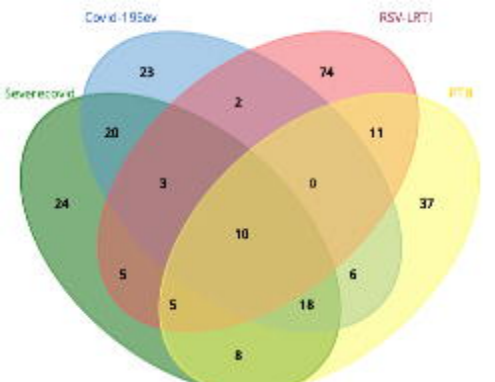
Covid-19Sev
RSV-LRTI
Severecovid
23
74
2
20
11
3
0
24
37
10
5
6
5
18
8